



<https://theses.gla.ac.uk/>

Theses Digitisation:

<https://www.gla.ac.uk/myglasgow/research/enlighten/theses/digitisation/>

This is a digitised version of the original print thesis.

Copyright and moral rights for this work are retained by the author

A copy can be downloaded for personal non-commercial research or study,
without prior permission or charge

This work cannot be reproduced or quoted extensively from without first
obtaining permission in writing from the author

The content must not be changed in any way or sold commercially in any
format or medium without the formal permission of the author

When referring to this work, full bibliographic details including the author,
title, awarding institution and date of the thesis must be given

Enlighten: Theses

<https://theses.gla.ac.uk/>
research-enlighten@glasgow.ac.uk

THE PHOTODEGRADATION OF SOME
POLYACRYLATES

Submitted by:

MRS. SHAGUFTA ZULFIQAR, M.Sc.

in part fulfillment of the requirements for

The Degree of DOCTOR OF PHILOSOPHY

Supervisor:

DR. I.C. McNEILL

Chemistry Dept.,
University of Glasgow,
November, 1979.

ProQuest Number: 10984308

All rights reserved

INFORMATION TO ALL USERS

The quality of this reproduction is dependent upon the quality of the copy submitted.

In the unlikely event that the author did not send a complete manuscript and there are missing pages, these will be noted. Also, if material had to be removed, a note will indicate the deletion.



ProQuest 10984308

Published by ProQuest LLC (2018). Copyright of the Dissertation is held by the Author.

All rights reserved.

This work is protected against unauthorized copying under Title 17, United States Code
Microform Edition © ProQuest LLC.

ProQuest LLC.
789 East Eisenhower Parkway
P.O. Box 1346
Ann Arbor, MI 48106 – 1346

PREFACE

I wish to express my gratitude to the technical staff of the Chemistry Department, to the staff and students of the Polymer Group for their friendship and helpful advice, with special thanks to my supervisor throughout the long period of this work, Dr. I.C. McNeill, for his constructive comments and criticisms on this thesis and his friendly guidance during the course of the work.

CONTENTS

	<u>Page</u>
SUMMARY	
<u>CHAPTER ONE</u> INTRODUCTION	vi
1.1 General Aspects of Polymer Degradation 	1
1.2 Photodegradation , 	2
1.3 Theoretical Considerations ..	2
1.4 Practical Considerations in Polymer Photolysis 	9
1.5 Preview of the Photolysis of Polyacrylates 	11
1.6 Polymethacrylates 	17
1.7 Acrylate - Methacrylate Copolymers	20
1.8 Photosensitizers 	21
1.9 Aim of this Work 	25
 <u>CHAPTER TWO</u> EXPERIMENTAL PROCEDURE AND ANALYTICAL TECHNIQUES	
2.1 Preparation of Polymers 	26
2.2 Photodegradation Techniques ..	32
2.3 Analysis of Degradation Products	36
2.4 Spectroscopic Techniques . ..	47
2.5 Determination of Extent of Crosslinking in Polyacrylates ..	48
 <u>CHAPTER THREE</u> PRELIMINARY INVESTIGATIONS	
3.1 Introduction 	61
3.2 Preparation of the Polymer Film	61
3.3 Effect of Lamp-to-Sample Distance on Photodegradation Products	62

	<u>Page</u>
3.4 Film Thickness	66
3.5 Effect of Time	66
 <u>CHAPTER FOUR</u> PHOTODEGRADATION STUDIES ON POLY(METHYL ACRYLATE)	
4.1 Introduction	72
4.2 Product Analysis	73
4.3 Molecular Mass Changes ..	94
4.4 Spectral Changes Occurring During Degradation	101
 <u>CHAPTER FIVE</u> PHOTODEGRADATION OF POLY (2-ETHYLHEXYL ACRYLATE)	
5.1 Introduction	105
5.2 Product Analysis . ..	108
5.3 Dependence of Products Evolution on Film Thickness	116
5.4 Molecular Mass Changes . ..	123
5.5 Spectral Changes During Photo- degradation	131
5.6 Mechanism of Degradation ..	131
 <u>CHAPTER SIX</u> EFFECT OF PHOTSENSITIZERS ON THE PHOTODEGRADATION OF POLYACRYLATES	
6.1 Introduction	141
6.2 Experimental Results	143
6.3 Molecular Mass Changes ..	159
6.4 Spectral Changes	180
6.5 Discussion	190
REFERENCES	197

SUMMARY

Thin films of poly(methyl acrylate) and poly (2-ethylhexyl acrylate) were photodegraded with a medium pressure mercury lamp in vacuum at 30°C. Degradation yielded volatile low molecular mass products and a solid high molecular mass residue. Qualitative and quantitative analysis of volatile products was carried out by employing the subambient thermal volatilisation analysis technique, recently developed in this laboratory. Subambient TVA was also used in combination with infrared spectroscopy mass spectrometry and gas-liquid chromatographic techniques for the identification of products. Spectral changes in the residual polymer films were examined by ultra-violet and infrared spectroscopy. The molecular mass changes, which occur during photodegradation of polyacrylates were observed by using a sorption technique developed by the author. This technique is used to observe the extent of crosslinking in systems with high crosslink density.

Volatile products formed during the photodegradation of poly(methyl acrylate) were carbon dioxide, formaldehyde, methanol and methyl formate. Mechanisms for the formation of all the condensable volatiles are suggested and discussed.

Photolysis of Poly(2-ethylhexyl acrylate) in vacuum produced a similar spectrum of products to that found for poly(methyl acrylate) viz. carbon dioxide, 3-methylheptane,, 2-ethyl-1-hexene, 2-ethyl-1-hexanal, 2-ethylhexyl formate, 2-ethyl-1-hexanol together with short chain fragments.

Molecular mass changes indicated that the extent of crosslinking is more profound in the case of poly(methyl acrylate) than for poly(2-ethylhexyl acrylate) as explained in Chapter Five.

The effects of the photosensitizers, benzoin, fluorenone and 2-chlorothioxanthone on the photodegradation behaviour of poly(methyl acrylate) have been studied. However, in the case of poly(2-ethylhexyl acrylate), benzoin was the only photosensitizer used. The nature of the degradation products remains unchanged. Comparisons are drawn with studies on polymer systems with and without photosensitizers. Photosensitizers seem to affect the degradation process by decreasing the amounts of volatile products formed, and by retarding the crosslinking process in the initial stages of degradation.

CHAPTER ONE

INTRODUCTION

1.1 General Aspects of Polymer Degradation

Ever since synthetic polymers became commercially important materials, attempts have been made to understand the processes which lead to the deterioration of their useful properties. Although the polymer may become unserviceable in severe conditions, it could last indefinitely in a less arduous environment. It is in the interests of both the manufacturer and consumer to be aware of the degradative effects of commonly encountered conditions such as sunlight and high temperatures. Much research has been devoted to the causes and effects of degradation in polymers since the development of the plastics industry. At first progress was hindered by an imperfect understanding of the true nature and complexity of macromolecular structure and a lack of suitable analytical techniques. The expansion of the market for polymers in the late 1940's together with a more profound conception of polymer chemistry and new techniques rekindled interest in the study of degradation. In recent years this has been stimulated by the development of new applications for polymeric materials in which they must be stable to a wide variety of chemicals, physical, mechanical and even biological agencies. The whole field of degradation has been reviewed by Grassie (1).

1.2 Photodegradation

As very few polymers spend their entire existence in darkness, it is not surprising that photolytic degradative processes have received considerable attention. Detailed mechanisms began to be described in the early 1950's. Among the first was the study by Cowley and Melville (2) of photo degradation of poly(methyl methacrylate) at elevated temperature under vacuum conditions. Since then systematic studies have appeared on many polymers either in vacuo or in gaseous atmosphere. These have been reviewed by Fox (3) and more recently by Ranby and Rabek (4).

Historically, prevention of degradation by the incorporation of stabilizers was the main interest of industry but with increasing concern about the disposal of plastic waste, its attention has been focussed on the control of degradation.

1.3 Theoretical Considerations

Photolytic degradation is brought about by the absorption of energy in the form of photons. This causes the formation of free radicals which ultimately lead to changes such as main chain scission, crosslinking, unsaturation and the formation of small molecules.

Most organic molecules lie in a singlet ground state. After absorption of a photon to give an excited singlet state, the molecule may revert to the ground state by emission of a photon (fluorescence) or by radiationless transitions and the generation of heat. In some instances, intersystem crossing can take place, and the molecule will shift to an excited triplet level of lower energy. Again the reversion to the ground state may be accompanied by photon emission (phosphorescence) or heat. If the molecule has sufficient energy in the excited state, either the singlet or the triplet, dissociation or rearrangement may take place. Reversion to the ground state may also be accompanied by transfer of energy between the excited molecule and a second molecule. These processes are illustrated in fig. 1.1. Radiationless transitions are favoured in complex molecules (5) and processes involving such intermolecular energy transfer are the most likely route to photodissociation.

In view of the possibilities for energy transfer within a polymer system, the site of initial bond break may be distant from that of the absorbing chromophore. Dissociation of the bond may occur from an excited singlet or triplet state and results when sufficient energy accumulates at the fracture point. The energy of radiation is dependent on the wavelength of the resonance line employed. As most organic polymers contain

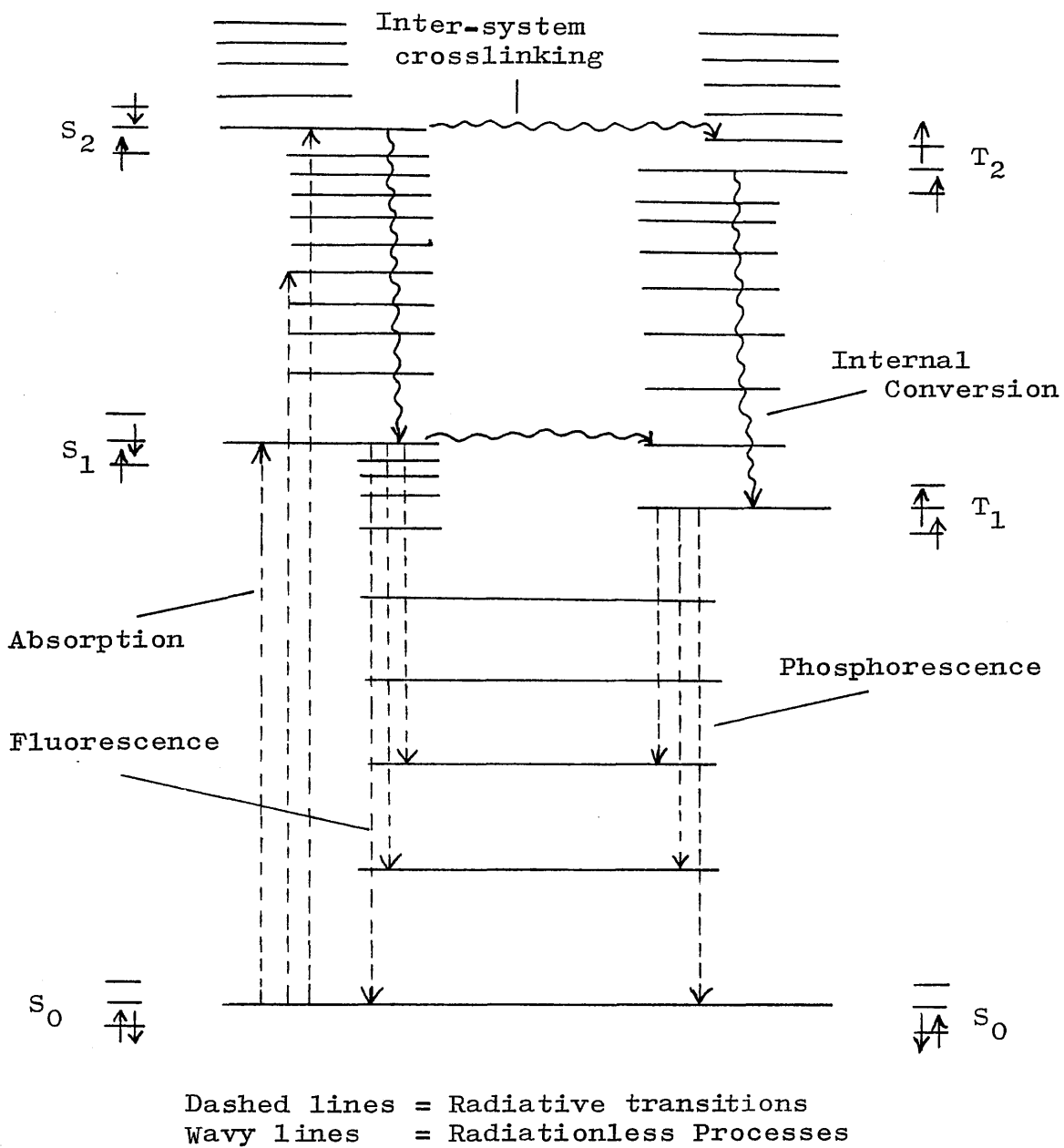


Fig.1.1: Electronic transitions and photophysical processes in an organic molecule.

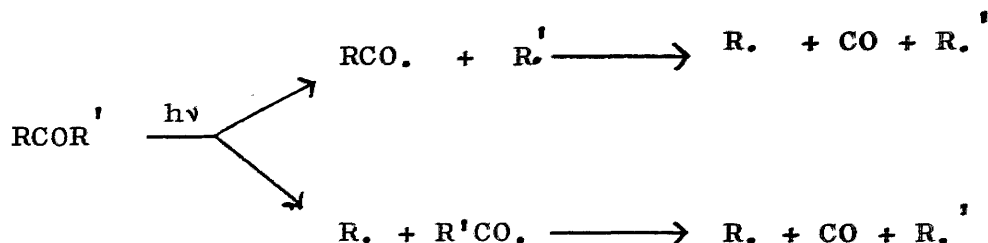
only carbon-carbon, carbon-hydrogen, carbon-nitrogen, carbon-oxygen, and carbon-halogen bonds, the magnitude for energy required for bond scission, based on the bond dissociation energies (6) is such that single bonds in a polymer molecule should be susceptible to cleavage when exposed to ultraviolet radiation. In practice a chromophore is required in order to first absorb energy before scissioning can occur. Further the process may be subject to kinetic restraints, or energy dissipation processes may outweigh scissioning processes.

1.3.1 Chromophoric Groups

The chromophores which can form by the thermal oxidation of the polymer during fabrication, processing or storage absorb in the ultraviolet range. The section of light decomposes the hydroperoxides to yield hydroxy and alkoxy radicals. The former can abstract hydrogen leaving centres for crosslinking, the latter are capable of undergoing isomerisation and fragmentation reactions as has been discovered in studies on polypropylene(7,8). The aliphatic aldehydes and ketones are not less harmful. By a forbidden transition ultra-violet light is absorbed and a variety of cleavage reactions becomes possible. Their major photochemical reactions are known as Norrish Type I and Type II reactions, as follows:-

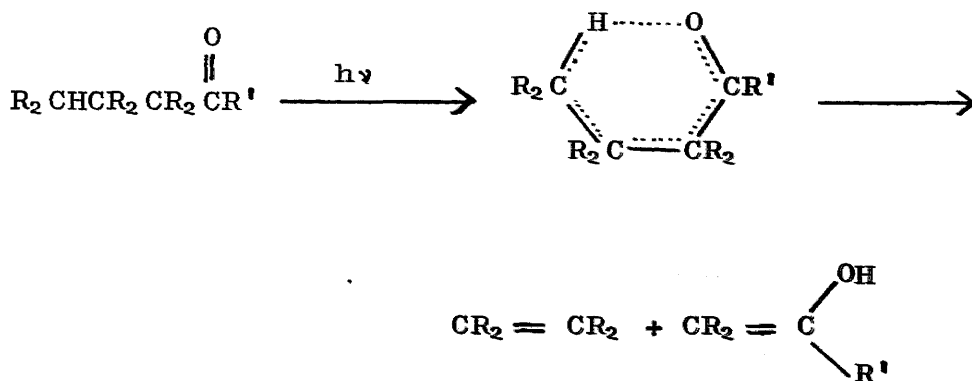
(i) Type I Norrish Reaction

In the primary process, the bond between the carbonyl group and adjacent α -carbon is homolytically cleaved. Two possible primary reactions can occur:



(ii) Type II Norrish Reaction

A nonradical intramolecular process which occurs with the formation of six-membered cyclic intermediate. Abstraction of a hydrogen atom from the γ -carbon results in its subsequent decomposition into an olefin and an alcohol or an aldehyde:



The importance of carbonyl groups as irregular bonds in the photodegradation of polymer such as polyethylene was first suggested by Burgess (9) and has been confirmed by many workers. Metal impurities are more recent discoveries and are of particular importance in photo-oxidation studies. Transition metal ions have been used recently in the development of photo-degradable polymers (10).

Oxygen in molecular form exists in the ground state as the triplet $^3\text{O}_2$ and singlet oxygen, $^1\text{O}_2$ in the excited state. Singlet oxygen can react with vinyl groups to form hydroperoxides. Decomposition of these may lead to disproportionation and further degradation (4). Under vacuum conditions the risk of oxygen being trapped in the film as an impurity is minimised.

1.3.2 Classification of Degradation Reaction Type

Degradation processes have been broadly classified as chain scission, crosslinking and functional group reactions. These processes have been discussed at length in many authoritative texts (11,12,13,14).

Chain scission is characterised by the breakdown of the polymer backbone into chain fragments. After the initial cleavage step which may occur at random along the length of the chain or at specific sites such as unsaturated chain ends, two extremes of

8

behaviour may be observed. In one case, a rapid decrease in molecular weight occurs without evolution of monomer. Volatiles other than monomer may be observed resulting from functional group cleavage. This type of behaviour is common in photodegradation reactions at ambient temperatures. Alternatively, degradation may proceed by an unzipping process resulting in the evolution of large quantities of monomer. In this case the molecular weight remains essentially constant during the early stages of reaction. The thermal degradation of poly(methyl methacrylate) is thought to occur in this fashion.

The process of crosslinking results ultimately in a three-dimensional network of polymer which renders it insoluble. Crosslinking and chain scissioning reactions can occur consecutively in the same polymer system, e.g. poly(methyl acrylate). Crosslinking induced by ultra-violet radiation results from cleavage of functional groups leaving radicals on the main chain. In poly(methyl acrylate) and polystyrene these radicals are produced by cleavage of tertiary hydrogen atoms. These radical centres can migrate (4) and combine with other radicals on adjacent chains or may add to unsaturated sites on the chains. The build-up of these crosslinks quickly leads to insolubility. When crosslinking does occur it has a considerable effect on the interpretation of photodegradation

results, making molecular weight determinations impossible, although sedimentation pattern and gel fraction studies can be made. Crosslinking also interferes with the determination of the rate of evolution of volatiles since the rigid structure has a much higher bulk viscosity which slows down the rate of diffusion of small product molecules.

Side group reactions or functional group reactions involve alteration to the polymer structure but may include chain scission or crosslinking as a secondary step. Examples of these are the elimination of HCl from irradiation of PVC (15) and the formation of conjugated carbon-nitrogen sequences during thermal degradation of nitrile polymers (16,17).

1.4 Practical Considerations in Polymer Photolysis

1.4.1 Analytical Techniques

The investigation of polymer photodegradation requires the application of complicated and highly sensitive analytical methods. The cost involved places severe limitations on the average laboratory and, consequently most workers tend to concentrate on particular aspects of the degradation process. Many techniques have provided valuable information. Amongst those commonly employed are: viscometry, osmometry, ultra centrifuge, and gel permeation chromatography for the analysis of molecular mass and

distribution of polymers; infrared, visible and ultra-violet spectroscopy, nuclear magnetic resonance spectroscopy and electron microscopy for the determination of structural changes and product analysis. Gas chromatography and mass spectrometry are also used for product analysis, while analysis of the short-lived intermediates is done by electron spin resonance spectroscopy and flash photolysis. A brief description of these techniques and the instruments involved may be obtained in many polymer text books (4,18).

1.4.2 Radiation Sources

A variety of sources are listed in the literature which will produce emission spectra ranging from single resonance lines to continuous bands. The preferential selection of wavelengths by the interposition of filters is discussed by Calvert and Pitts (8). Low pressure mercury discharge lamps are usually employed where monochromatic ultra-violet light is required. Medium pressure mercury lamps operating below 1 atm. are more extensively used in laboratories and in industry. The application of monochromators or filter combinations permits the use of a medium pressure lamp for a few narrow monochromatic bands in the visible and ultraviolet region. These lamps are cooled by air circulation. A high pressure mercury arc is the source of most intense ultra-violet and visible radiations.

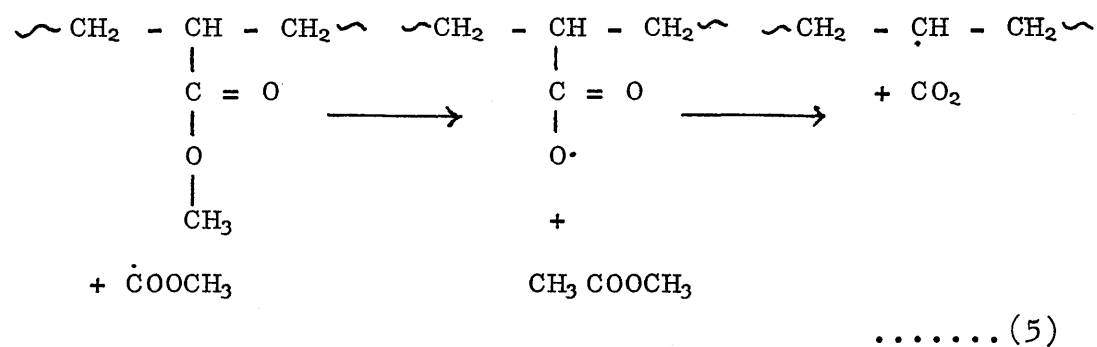
In weathering studies the sun's emission spectrum has been simulated in the laboratory by a xenon discharge lamp with appropriate filters. Irrespective of the nature of the source, it is essential that the apparatus constructed for photolysis studies should transmit at the required wavelength. For this reason when the ultra-violet region of the spectrum is being studied all the optical material must be made from silica.

1.5 Preview of the Photolysis of Polyacrylates

The photochemical degradation of polyacrylates has been much neglected when compared to the large volume of work that has been published on the corresponding polymethylacrylates. This might be due to the fact that both crosslinking and chain scission take place on irradiation and molecular mass changes are thus more difficult to evaluate than in case of the methacrylates.

Fox et al (19) reported on the volatile products formation and molecular mass changes observed on vacuum photolysis of poly(methyl acrylate). Thin films photolysed in vacuum at 22°C, gave formaldehyde, methanol, methyl formate and carbon dioxide as major products. Carbon monoxide, hydrogen and methane constituted minor reaction products.

with H₂, CH₄, and CO as permanent gases. The products were essentially similar to those found by Fox et al (19) but obtained in different ratios. Methyl acetate had not been reported previously and the following reaction for its formation was proposed.



It was pointed out that the amount of CO₂ evolved was generally slightly less than the amount of CH₃COOCH₃ produced.

The filtering effect of the upper layers of polymer in screening the lower layers from irradiation was found to influence product formation markedly. Only traces of products other than CH₃OH were found at film thicknesses greater than 300 μm and it was concluded that two reaction mechanisms for the formation of methoxy radical were operative.

Molecular mass changes and gel formation on photolysis of PMA in nitrogen and air atmospheres was studied by the same authors (21) and the results evaluated using the Charlesby Pinner equation (22) to

calculate the number of chain scissions and crosslinking events. Chain scission and crosslinking were found for both nitrogen and air exposures, and only slightly less crosslinking was found in air than in nitrogen. In contrast, Fox et al (19) obtained a marked decrease in crosslinking in an air atmosphere.

McGill and Ackerman (23) also investigated the photolysis of poly(ethyl acrylate) (PEA) and poly(butyl acrylate) (PBA) in vacuum. The main gaseous products found were CO, CO₂ and the alcohol, aldehyde, alkane and formate derived from the various ester groups. In addition, PEA evolved acetal CH₃CH(OC₂H₅)₂ as well as ethyl propionate, while n-butyl valerate was evolved from PBA only after prolonged exposure. Scission and crosslinking were observed to occur in both these polymers. The products could all be visualized as resulting from the three homolytic reactions proposed by Fox et al (19) above, together with CH₃OH production via the formation of lactones in the chains, as proposed by Cameron and Kane (24) for PMA.

Jacob and Steele (25) studied the effect of ultra-violet radiation on PEA in thin films in vacuum. Gaseous products were CO, C₂H₆, CO₂ and H₂ and both crosslinking and scission of the polymer were found above the glass transition temperature (T_g) of the polymer. Below T_g,

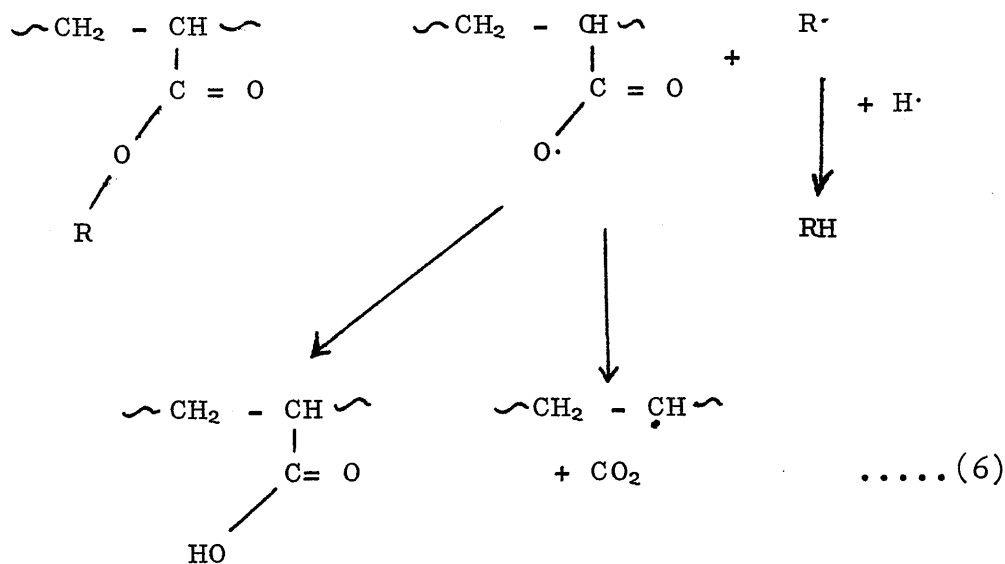
11

scission was the major reaction and crosslinking was virtually non-existent. It was suggested that the polymer radicals involved in crosslinking were those found by homolysis of the ester side chain, and crosslinking increased with the degradation time.

1.5.1 Radiolysis in Vacuum

Radiation induced crosslinking of the polyacrylates has been reported by Schultz and Bovey (26) and also by Burlant et al (27). From the observed increase of crosslinking efficiency with increasing length of the alkylester group, the latter authors concluded that crosslinking should take place predominantly on the hydrocarbon side chains. Todd (28) however, argued that side chain removal is not essential for the crosslinking reaction in PMA.

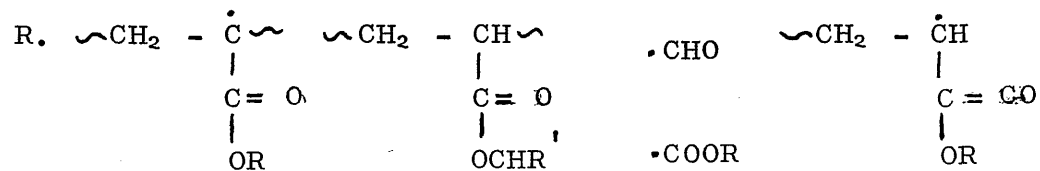
Rosenberg and Heusinger (29) reported on the radiation induced crosslinking, main chain scission, and product formation observed on radiolysis of PEA. Decomposition products found were H_2 , CO , CO_2 , C_2H_6 , C_2H_4 , CH_3CHO and C_2H_5OH . The formation of C_2H_6 was formed to exceed that of C_2H_4 throughout the decomposition. Formation of CO_2 was considered to proceed via the following reaction sequence:-



Incomplete decarboxylation of the polymer carboxylate radical was believed to be responsible for the low $\text{CO}_2 : \text{C}_2\text{H}_6$ ratio. Hydrogen abstraction by the carboxylate radical would lead to carboxylic acid formation. Infrared spectroscopic changes supported, but did not prove this assumption.

Ethoxy radicals and polymer carbonyl radicals were formed on homolysis of the ester C-O bond. Hydrogen abstraction by these radicals led to the formation of C_2H_6 , while decarbonylation of the carbonyl radical gave CO and a new polymer radical. When C-O homolysis was preceded by loss of an ester α -hydrogen atom, CH_3CHO and CO were formed. The H_2 , CO and aldehyde production as well as the extent of crosslinking decreased with α -deuteration of the ester group and this was considered proof that α -hydrogen loss was important.

Electron-spin resonance (ESR) investigations (30) to identify the radical formed on radiolysis of the polyacrylates have shown the following radicals to be present on radiolysis of PMA and PEA, viz.



1.6 Polymethacrylates

Polymethacrylates have a molecular structure very similar to that of polyacrylates and it is instructive to compare the behaviour of these two types of polymer on degradation.

More attention has perhaps been paid to the quantitative aspects of radiolytic, photolytic and thermal degradation of poly(methyl methacrylate) (PMMA) than any other polymer. This polymer is of interest not only because of its practical applications, but also due to the well defined degradation reactions. It is also unusual in that the mechanisms for photo-degradation at room temperature and for thermal degradation are entirely different. The latter feature is due to the polymer having $T_g = 106^\circ\text{C}$, which means that the polymer molecules are entirely rigid at

room temperature, whereas in photodegradation at elevated temperatures the chains are highly mobile and degradation products can easily escape from the polymer.

1.6.1 Photolysis

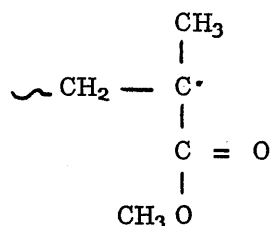
Photolysis of PMMA in vacuo caused rapid decreases in molecular mass concomitant with the formation of small amounts of volatile material. The main products found by Fox et al (31) were methyl formate, methanol and monomer. In photolysis in air, minor amounts of methane, hydrogen, carbon monoxide and carbon dioxide were formed in addition. Photolysis of PMMA results in a random scission of the polymer backbone by a radical process. Three major reactions are reported to occur at the same time:

- (i) Random homolytic scission of main-chain carbon-carbon bonds.
- (ii) Photolysis of the ester side groups.
- (iii) Photo-dissociation of the methyl side groups.

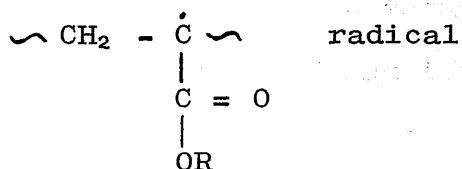
Monomer was formed during irradiation mainly due to chain depolymerization after photolytic scission of main chains. No tendency to crosslink was found when PMMA was irradiated in the form of films.

Campbell (32) reviewed Electron Spin Resonance

(ESR) studies done on PMMA and showed that the initiating radical is



as opposed to the



in acrylate polymers.

Both oxygen and nitrogen act as inhibitors to photodegradation of PMMA (33). As the temperature of the irradiation was increased, an increased yield of monomer was found by Cowley and Melville (34). Grassie and MacCallum (35) made a comparison of the thermal and photoinitiated degradation of poly(n-butyl methacrylate) and poly(t-butyl methacrylate) in vacuum. The n-butyl methacrylate polymer was completely converted to monomer by photolysis at 170°C, while only 40% of the volatile products in the thermal degradation consisted of monomer. The t-butyl ester yielded mostly olefin by thermal degradation whereas it yielded 100% monomer on photolysis at 170°C. Isaacs and Fox (36) showed that

the latter polymer yielded monomer, 1-butene and n-butyl formate on photolysis.

1.7 Acrylate - Methacrylate Copolymers

The investigations of thermal and photodegradation of these copolymers have played an important part in elucidating the mechanism of degradation of the homopolymers.

Grassie, Torrance and Colford (37) investigated the photolysis of methyl methacrylate - methylacrylate copolymers in vacuum at between 150°C and 170°C chain scission was found to be a predominant reaction under these conditions and no crosslinking could be found, even in 50 mole % MA copolymers. The rate of scission was not dependent on monomer sequences and scission occurred in a random manner. The rate of volatilization was progressively retarded by increasing the acrylate content and it was concluded that the MA units block the MMA depolymerization reaction. The thermal degradation behaviour of these polymers (38) followed much the same pattern as the photodegradation, although increased depolymerization was found in the former case.

Photodecomposition at elevated temperature (165°C) of methyl methacrylate - butyl acrylate copolymers has also been reported (39). The observed decomposition products were n-butyraldehyde, n-butanol, methyl methacrylate, n-butylacrylate, hydrogen, methane and

carbon monoxide. n-Butyraldehyde was only observed on photodegradation and appeared from copolymers containing only 3.9 mole% of acrylate. This was seen as evidence that n-butyraldehyde formation was a function of isolated acrylate units. Carbon dioxide and butene were the major products of thermal degradation (40). However, in photothermal studies neither of these was detected. Butoxy radical formation was believed to proceed in a manner identical to that proposed for the thermal decomposition.

The photolysis of copolymers of methyl methacrylate and methyl acrylate was studied by Grassie, Scotney and Davis (41) both for film samples and in solution, under vacuum and in an oxygen atmosphere. Crosslinking was not found with poly(methyl methacrylate) while it is a very important reaction in poly(methyl acrylate). The rate of crosslinking decreased with decreasing methyl acrylate content in the copolymers. It seemed that crosslinking was not to be associated with isolated methyl acrylate units in polymer chains, but with sequences of two or more.

1.8 Photosensitizers

The photochemical reactions of polymers can be induced and promoted by different inorganic and organic compounds which can react in the following ways:-

(i) Photo-initiators

Compounds which are excited by absorbed light and subsequently decompose into free radicals which may initiate degradation and oxidation of a polymer.

(ii) Photosensitizers

Compounds which are excited by light and transfer their excitation energy to polymer molecules or to oxygen molecules forming singlet oxygen. In this way degradation and oxidation of polymers may occur.

(iii) Photo-Optical sensitizers

Compounds which extend the optical sensitivity of polymers to radiation of a longer wavelength. Increased photodegradation and photocrosslinking are observed.

In many cases a chemical compound may depending upon the conditions of the experiment, behave either as a photo-initiator or as a photosensitizer. The positive influence on the rate of photochemical reaction is described as 'sensitization' of the reaction.

Aromatic carbonyl compounds may, under appropriate circumstances, function as photosensitizers or photochemically active initiators for free radical vinyl polymerization. There are many reported examples of technological applications of photo-initiated vinyl polymerization in which these compounds are active ingredients, although in many cases details of the

photoinduced processes and the nature of the actual initiating radical fragments are not known. Such processes are important in the development of photochemical curing techniques for the manufacture of printed circuits, relief printing plates, and the more recent development of 100 per cent reactive systems in the coatings and printing ink industries (42,43).

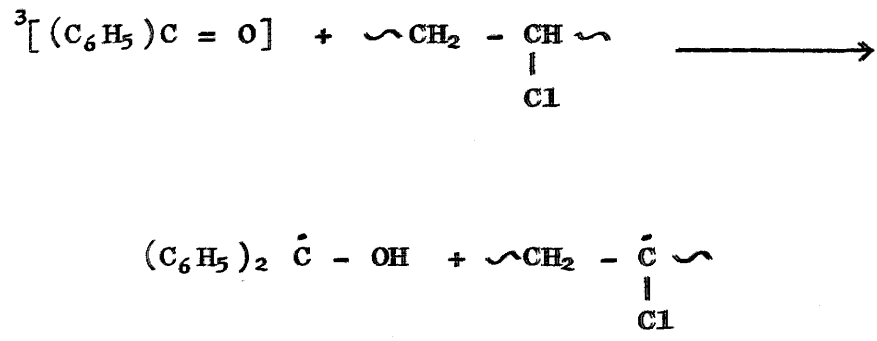
Photopolymerization might be defined as the process whereby light is used to induce an increase in molecular mass. Photopolymerization involves the chain reaction polymerization of a vinyl monomer. Another type of photopolymerization is concerned with the crosslinking of pre-existing high polymers. The distinction between these two processes is not always clear cut. For example, the photochemically induced copolymerization of a vinyl monomer with a pre-existing polymer containing unsaturated groups results in a crosslinked polymer. Photodegradation also involves photocrosslinking, which if carried out excessively, results in an embrittlement and hence a 'degradation' of the elastic properties of the polymeric material.

1.8.1 Photosensitized Reactions of Polymers

Aromatic ketones have been widely investigated as sensitizers in photoreactions of polymers.

Owen and Bailey (44) reported the benzophenone-photosensitized degradation of poly(vinyl chloride)

under vacuum and in the presence of oxygen. The initial rapid increase in absorption in the 340 nm region strongly implies the formation of ketyl radicals in the initiation process, involving hydrogen abstraction from poly(vinyl chloride) by excited benzophenone in triplet state.



The formation of unsaturated bonds in vacuum and oxidative degradation of the polymer then occur.

Trudelle and Neel (45) observed oxidative degradation of poly(vinylalcohol) in the presence of benzophenone. Hydrogen abstraction from polymer by the sensitizer in its triplet state was proposed as the initial step in degradation.

Oster et al (46) reported an extensive crosslinking of polyethylene containing benzophenone, when irradiated with 254 nm light.

Benzoin ($C_6H_5COCH(OH)C_6H_5$), which has a similar structure to benzophenone, and benzoin alkyl ethers have been most widely used as photo-initiators for vinyl polymerization (42). Benzoin has been investigated as a photosensitizer for accelerating the formation of free radicals under ultra-violet light in poly(vinyl pyrrolidone), poly(vinyl butyral) and poly(oxyethylene) (47).

1.9 Aim of This Work

During the past few years cure of coatings by exposure to ultra-violet radiation has received a great deal of attention commercially. The main advantages of UV curing are speed, economy, convenience and improved environmental conditions. It naturally stimulated further interest in the problems of improving the properties and stability of photocuring system.

The main purpose of our work is to study the effect of ultra-violet radiation on crosslinked polymers of the type produced in photocurable systems. But as this is a complex system, the initial interest is in studying the photodegradation of polymers of the individual components of a typical UV curing system.

CHAPTER 2

EXPERIMENTAL PROCEDURE AND ANALYTICAL TECHNIQUES

2.1 Preparation of Polymers

2.1.1 Purification of Monomers

Methyl acrylate (B.D.H. Ltd) and 2-ethylhexyl (Union Carbide Ltd.) were supplied, stabilized by inhibitors of the hydroquinone type. Before polymerization all the monomers were allowed to stand for 24 hours over dried calcium chloride followed by treatment overnight with ground calcium hydride, to remove any traces of water. For methyl acrylate, the inhibitor was removed by distilling twice under vacuum, each time the first and last 10% of the liquid was discarded. The second distillation was into a graduated reservoir. The monomer was then thoroughly degassed three times. It was thereafter ready for distillation into the polymerization vessel.

2-Ethylhexyl acrylate was purified in a different manner because its low volatility at room temperature made normal distillation under vacuum impracticable. A conventional vacuum distillation apparatus with an oxygen free nitrogen leak was used. The collecting vessel was a graduated reservoir which was connected to the polymerization dilatometer by a glass tube. The monomer distilled over at 85-86°C under a pressure of 0.8 mm mercury into the reservoir which was cooled

at -80°C . 100 ml of monomer was used, the first 10 ml of which was allowed to pump away, the next 44 ml was collected. The distillation apparatus was then removed and the reservoir closed at the top with a ground glass stopper. The monomer was then thoroughly degassed as described above.

2.1.2 Purification and Introduction of Initiator

In all the polymerizations $\alpha\alpha'$ -azobisisobutyronitrile (AZBN) (Kodak Ltd) was used as initiator. It was recrystallised from methanol, and added to the dilatometer as a standard benzene solution. The benzene was removed under vacuum.

2.1.3 Purification of Solvents

Methyl acetate was used as a solvent for methyl acrylate polymerization and analar benzene was used as solvent for 2-ethylhexyl acrylate polymerization.

Solvents were purified by treatment for 24 hours with dried calcium chloride, then overnight with ground calcium hydride to remove all traces of water. They were degassed by the freezing and thawing technique and distilled under vacuum into a graduated reservoir.

2.1.4 Introduction of Monomer and Solvent into Dilatometers

Purified monomer was distilled under vacuum into the dilatometers except in the case of 2-ethylhexyl acrylate. In this case, the monomer was transferred

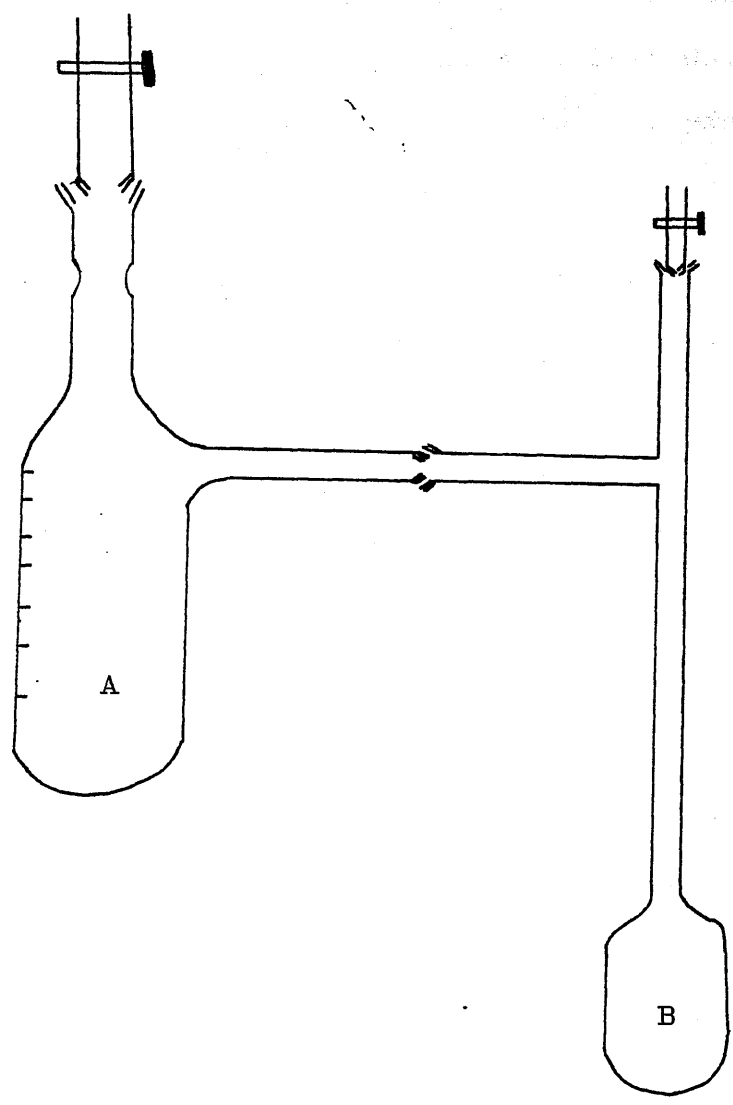


Fig. 2.1: Apparatus for the introduction of monomer into the dilatometer.

from the reservoir A, through the connecting tube into the dilatometer B with the system under vacuum (Fig. 2.1). The tube between reservoir A and dilatometer B was then sealed under vacuum and the reservoir removed. In all cases, once the monomer has been introduced into the dilatometer, it was kept at -196°C to prevent polymerization.

Solvent was introduced to the dilatometer by distillation under vacuum from a graduated reservoir. Once the polymerization mixture of initiator, monomer and solvent had been made up in the dilatometer it was frozen with liquid nitrogen, pumped to a pressure of less than 10^{-5} torr and the dilatometer sealed at the constriction.

2.1.5 Polymerization

Polymerizations were carried out at $40.0 \pm 0.1^{\circ}\text{C}$ in a stirred thermostat bath. Some monomer and polymer density data have been obtained for methyl acrylate (48) and the density of 2-ethylhexyl acrylate at 20°C (49) is also known. From these data, an approximate relationship between volume, concentration and percentage conversion at the polymerization temperature could be derived. The polymerizations were followed dilatometrically and taken to no further than 20% conversion, then stopped by pouring the contents of the dilatometer into 3 litres of analar methanol in the case of poly(2-ethylhexyl acrylate) or ^a methanol/water mixture

for poly(2-ethylhexyl acrylate). For the latter polymer, a methanol/water mixture was used because the polymer is sparingly soluble in methanol.

2.1.6 Purification of the Polymer

The precipitated polymer was removed by filtration, dried under vacuum, redissolved in the solvent and reprecipitated by slowly dripping the polymer solution into well stirred precipitant. This process was repeated twice. Finally the polymer was dissolved in benzene and freeze dried until a vapour pressure of less than 10^{-5} torr was obtained at room temperature. Thermal volatilization analysis and thermogravimetric analysis of the polymers revealed no significant amount of solvent after this treatment.

Table 2.1 summarises the polymerization data.

TABLE 2.1: POLYMERIZATION DATA

Polymerization done at 40°C

Poly- acrylates	Initiator concentration	Monomer concentration	% conversion	Molecular weight
2-Ethyl Hexyl	0.11	30%	16%	77,000
Methyl	0.55	40%	6%	51,000
Methyl	0.35	40%	6%	65,700
Methyl	0.05	40%	10%	352,000
Methyl	0.08	40%	10%	429,700
Methyl	0.3	40%	6%	71,000
Methyl	0.02	40%	10%	297,000
Methyl	0.21	40%	7%	160,000

2.2 Photodegradation Techniques

2.2.1 Source of Radiation

A medium pressure mercury lamp (Hanovia Lamps Ltd) was used as the source of ultra-violet radiation in this work. The characteristics of the spectrum of the lamp are shown in table 2.2. The lamp has a spectral output of 52.2% in the ultraviolet region with the remainder at longer wavelengths and took five minutes to reach its full intensity. It was connected to the intensity stabilizer which is provided to maintain the output of the tube at a reasonably constant intensity for an operating life of 1000 hours. The intensity was monitored by Blak-Ray Ultra-violet meter J225 (Ultra-violet Products Ltd) sensitive to light in the region 230-270 nm, and the deviation was $\pm 8\%$. The lamp output below 400 nm at 30 cm distance was of the order of $2400 \mu\text{W}/\text{cm}^2$.

2.2.2 Photolysis Cell

The main requirement of any photolysis cell is its transparency to the wavelength of radiation employed. The transmission of fused silica is shown in fig. 2.2 and is seen to be transparent to the wavelengths used for photolysis. The photolysis cell is shown in fig. 2.3. The cell was made up of lower part of pyrex glass together with a replaceable silica top. The stainless steel support plate (used for casting film described in Chapter 3)

TABLE 2.2: Spectral characteristics of medium pressure mercury arc tube (Hanovia Lamps Ltd., Slough, Bucks., England)

<u>Region</u>	<u>Spectral Line (nanometres)</u>	<u>Watts per centimetre of arc length</u>		
Infrared	1367.3	0.35		
	1128.7	0.94		
	1014	3.27		
	Total infrared	4.56	9.34%
Visible	578/579	5.51		
	546.1	6.06		
	435.8	4.80		
	404.5	2.40		
	Total visible	18.77	38.46%
Ultra-violet	365/366.3	4.76		
	334.1	0.55		
	313	2.17		
	302.5	1.26		
	296.7	0.79		
	289.4	0.28		
	280.4	0.55		
	275.2	0.16		
	270	0.28		
	265.2	0.59		
	257.2	0.83		
	253.7	0.47		
	248	0.51		
	240	0.47		
	below 240	11.81		
Total ultraviolet	25.48	52.2%	
Total Radiated	46.81	100%	

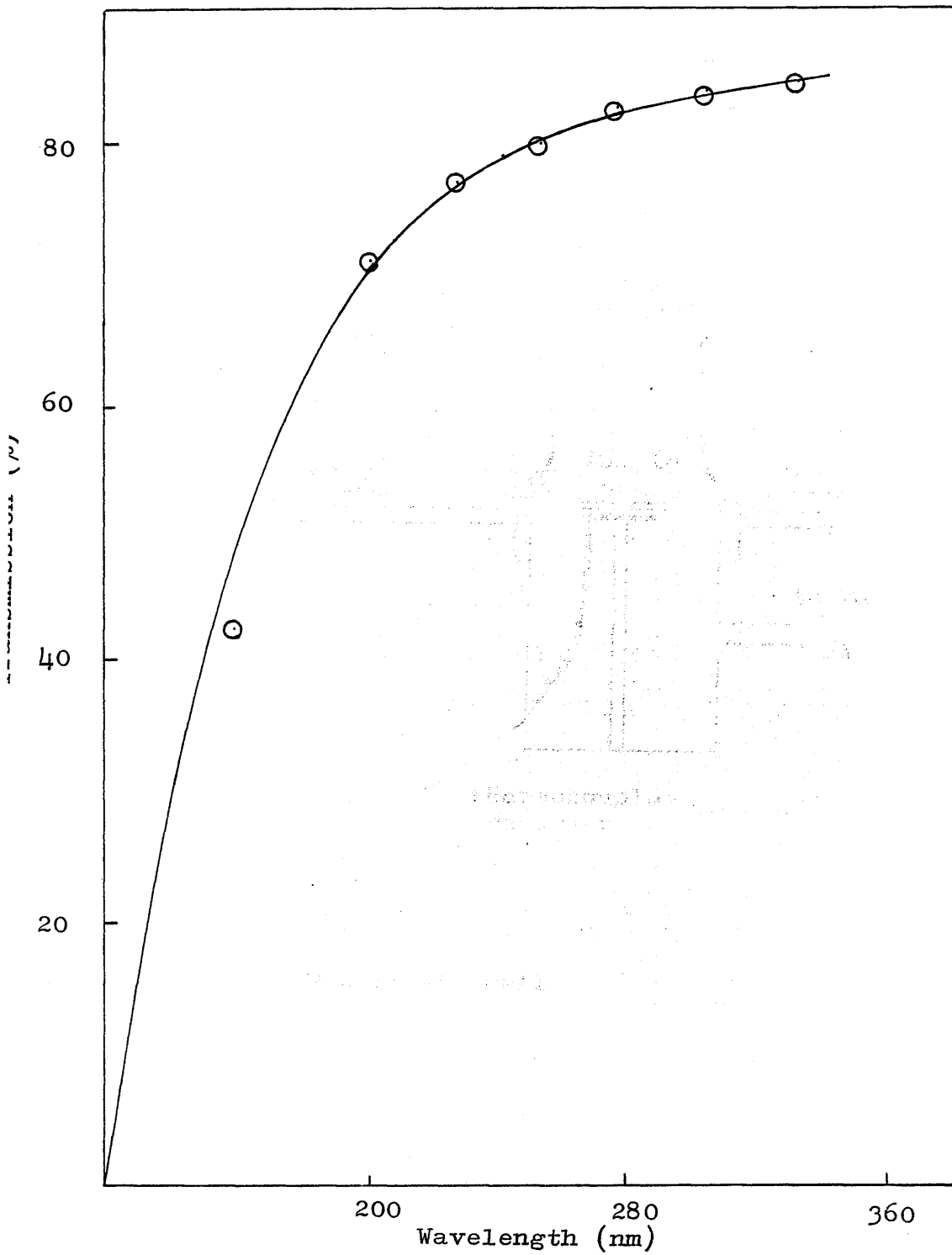


Fig. 2.2: Transmission spectrum of fused silica (2mm)

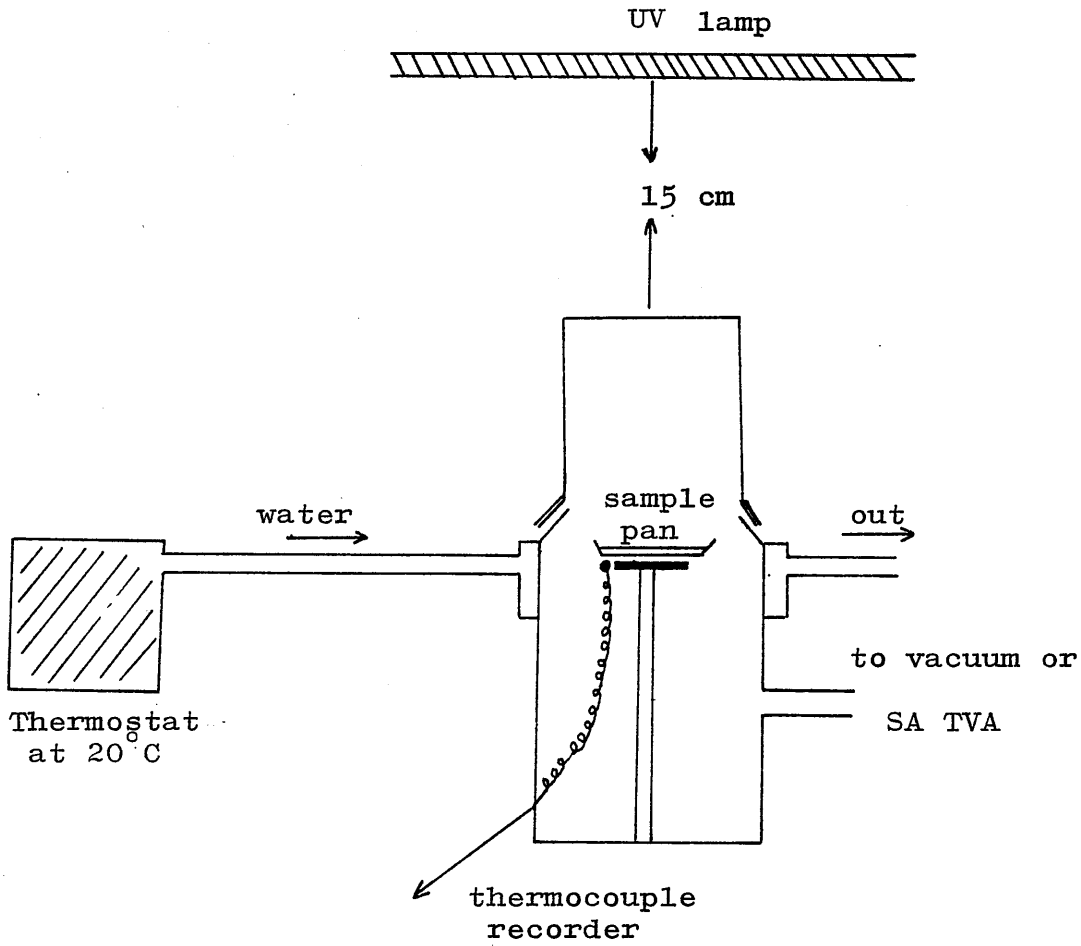


Fig.2.3: The Photolysis Cell

was mounted on a specially designed T-shaped holder connected at the lower part of the cell. A chromel-alumel thermocouple was attached to the sample holder to determine the temperature of photolysis.

2.3 Analysis of Degradation Products

2.3.1 Introduction

During photolysis the quantity of the volatile material produced is very small, hence its analysis requires sensitive techniques. Such a technique was employed by Ackerman and McGill (20) in their study of poly(methyl acrylate) and proved to be more sensitive than conventional gas chromatography. A similar technique was independently developed in our laboratories (50). A fractionation system has been devised which differs from the above workers' procedure and more satisfactory control of the rate of warming up of the sample trap has been achieved. In view of the importance of the results obtained from this method the principle and procedure are outlined below.

2.3.2 Separation Technique

Degradation products which exist in the vapour phase under low pressure conditions can be condensed at liquid nitrogen temperature (-196°C) at a specific point in the system. These condensable volatiles are readily separated from the permanent

gases which are pumped through the system without condensing.

The apparatus used in our laboratory, connected directly to the thermal or photodegradation system, is illustrated in fig.2.4.

The method is nondestructive, so that unless the products interact, repeat experiments are feasible from the same starting material. The separation which can be achieved by the technique depends ultimately on how much the materials present differ in volatility, and strong hydrogen bonding effects may also hinder separation. The efficiency of separation will depend mainly on the rate at which the sample trap warms to ambient temperature. Control of this rate is therefore very important. Ideally one product should transfer completely without the concurrent transfer of another. The rate of transfer was controlled by the introduction of a jacket containing a liquid initially frozen to -196°C by surrounding it with liquid nitrogen in a Dewar vessel. Removal of the latter allowed the inner jacket containing frozen liquid to warm up at a rate dependent on heat transfer from the surroundings. Ackerman and McGill (20) used petroleum ether (b.p. $40-60^{\circ}\text{C}$) for this purpose; for this material, however, there is a discontinuity in the rate of heating at the point when the substance

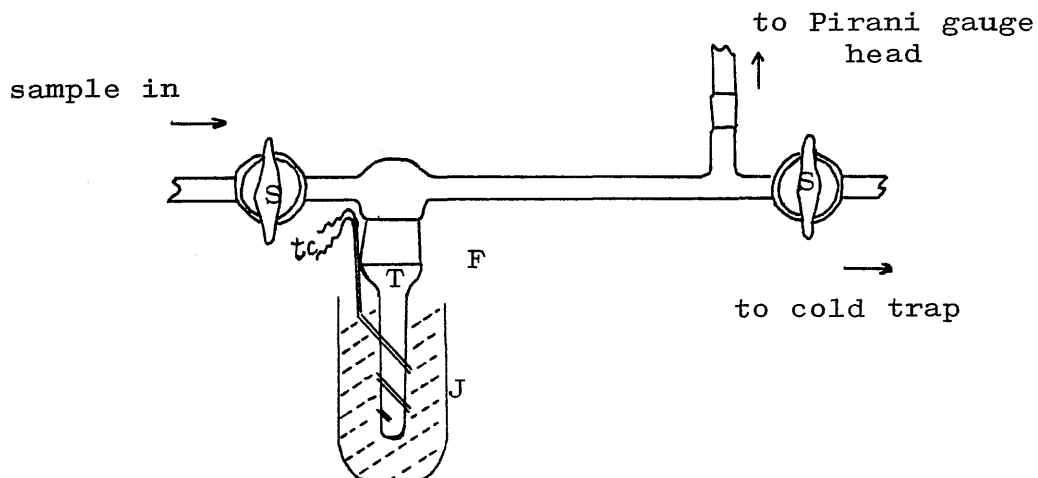


Fig.2.4: Apparatus for subambient TVA: (S) stopcock; (T) sample tube (with B34 joint); (tc) Chromel-Alumel thermocouple leads; (J) jacket containing jacket liquid; (F) filler port. Pirani gauge and thermocouple outputs are fed to a 10 mV recorder.

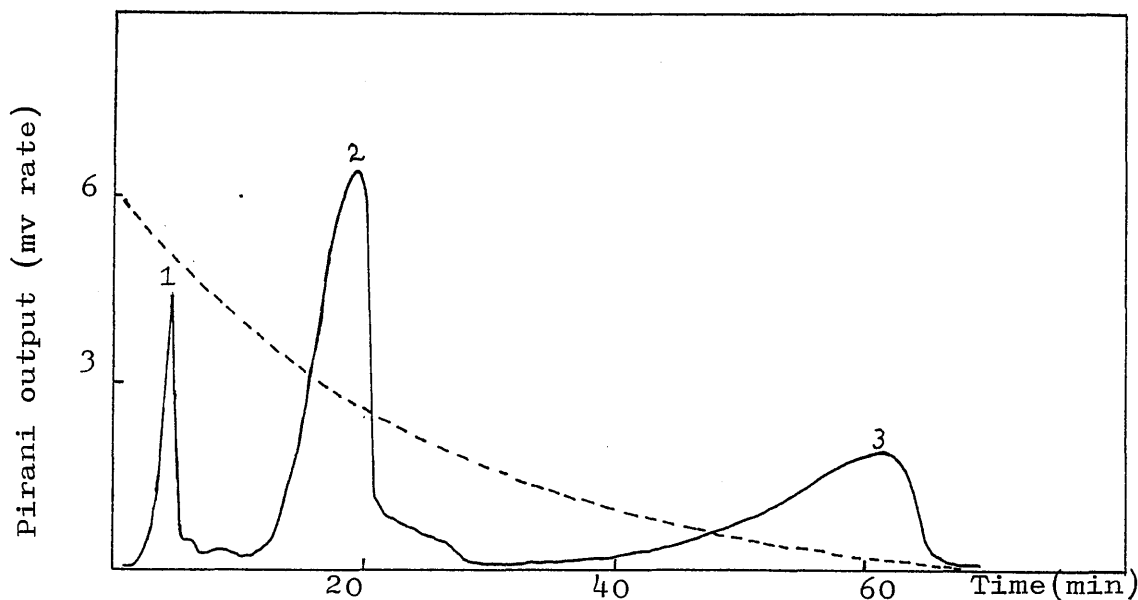


Fig.2.5: Subambient TVA curve for degradation products of poly(methyl acrylate) (from programmed degradation under vacuum to 500°C at 10°C/min, 2mg sample): (1) carbon dioxide; (2) methanol and some monomer; (3) short-chains fragments.

melts, which can give rise to confusing effects in the Pirani response curve if any products are volatilizing in this temperature region. p-Xylene, which melts very near to ambient temperature, was used as jacket liquid in the present study. The temperature of the laboratory should remain constant for complete reproducibility in the heating programme, but for most purposes, day-to-day variations are unimportant.

The method of use of the apparatus (fig.2.4) is to evacuate the system, surround the bottom 5 cm of the liquid in jacket J around the sample tube T, with liquid nitrogen, and when the lower part of the tube has reached -196°C as indicated by chromel-alumel thermocouple tc, allow the products from the degradation experiment to distil into the sample tube. The degradation section of the apparatus is then isolated. The liquid nitrogen level is then raised to the level of the jacket liquid. This condensation procedure of the sample gives better reproducibility in the subsequent procedure than simply freezing the entire jacket liquid in one stage, possibly because some separation of the sample takes place on the walls of the sample tube. The cold trap for the collection of products is

prepared at -196°C and the Dewar vessel with liquid nitrogen is removed from the jacket sample tube. The output from the Pirani gauge, between sample tube and cold trap, and the thermocouple are

recorded simultaneously as a function of time. Originally this technique was employed to separate the thermal degradation products of poly(methyl acrylate) and poly(2-ethylhexyl acrylate) but later extended to photodegradation studies. Typical traces for thermal degradation products of poly(methyl acrylate) and poly(2-ethylhexyl acrylate) are shown in fig.2.5, 2.6.

A G 5 C-2 gauge head and Pirani model 14 thermo-conductivity vacuum gauge (Edward High vacuum) were used to monitor pressure. The temperature at the sample tube was measured by a chromel-alumel thermocouple. Both the pressure gauge and thermocouple were linked to a Leeds and Northrup multichannel recorder with a full scale deflection of 2.5 mv.

It is possible to collect the material evolved at each stage of volatilization by changing the distillation route in an apparatus such as that of fig.2.7.

The fraction may then be analyzed separately to identify the substance or substances present. The gases and volatile liquids were examined using minimum volume infrared cells; while high boiling materials were identified by infra red spectroscopy of a solution in carbon tetrachloride. Mass spectrometry and GLC were also employed to identify the products.

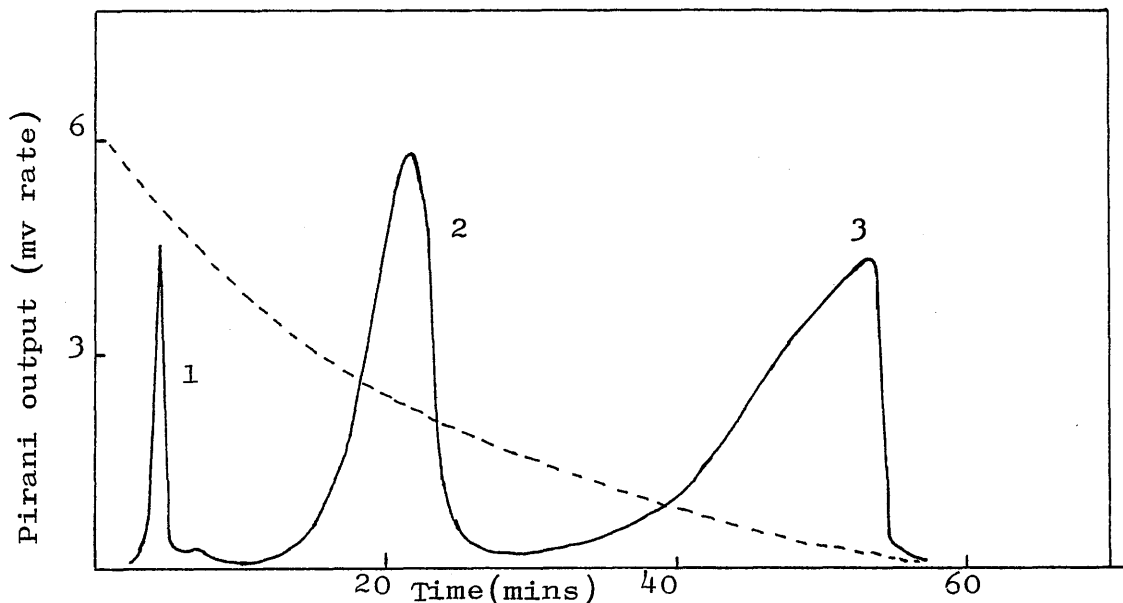


Fig.2.6: Subambient TVA curve for degradation products of poly(2-ethylhexyl acrylate) (from programmed degradation under vacuum to 500°C at 10°C/min, 20 mg sample): (1) carbon dioxide; (2) 2-ethylhexene-1; (3) 2-ethylhexanol-1 and monomer.

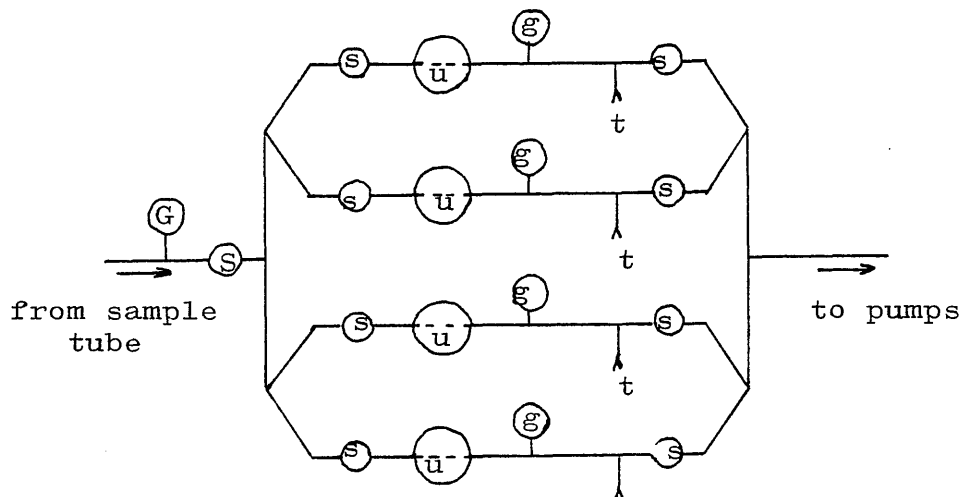


Fig.2.7: Arrangement for collection of fractions in subambient TVA: (G) main Pirani gauge with recorded output; (U) U-tube trap at -196°C; (s) stopcock; (t) take-off point for connection of infrared gas cell or sample collection tube; (g) Pirani gauge to monitor distillation from U to t (not recorded). Routes AB, AC, AD, AE are geometrically equivalent, each line being used in turn to collect products corresponding to four successive TVA peaks. The high-volatility products initially collected may be transferred from U to t (both stopcocks closed) while higher-boiling fractions are being collected in other lines.

2.3.3 Quantitative Analysis

The output from the Pirani gauge, between sample tube and cold trap, and the thermocouple were recorded simultaneously as a function of time on the chart recorder, giving a trace of all the condensable volatiles as shown in figs. 2.5, 2.6. Although the Pirani output is a measure of the rate of volatilization, the relationship between rate and output in millivolts was non-linear above about 1-2 mv. In photo-degradation studies, the amount of degradation products was very small and a recorder range of 2.5 mv was used. Observed peak heights were within the 0-1.5 mv range, so that peak area could be used as a direct measure of the quantity of products, as commonly applied in gas chromatography.

Calibration curves were constructed for standard known compounds as shown in fig. 2.8-2.15 from which the number of moles of each product formed were calculated.

2-Ethylhexyl formate was not available commercially so it was prepared in the laboratory and identified by mass spectroscopy, NMR and IR spectroscopy.

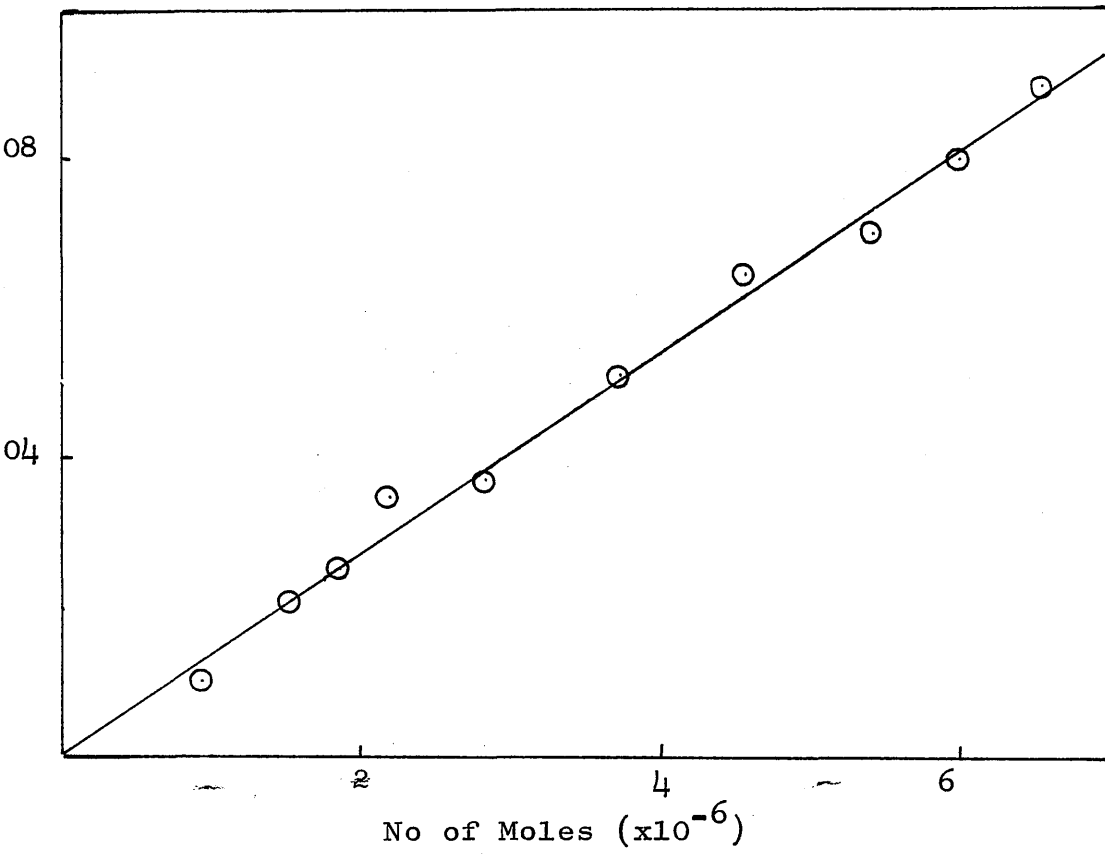


Fig.2.8: Calibration plot for carbon dioxide

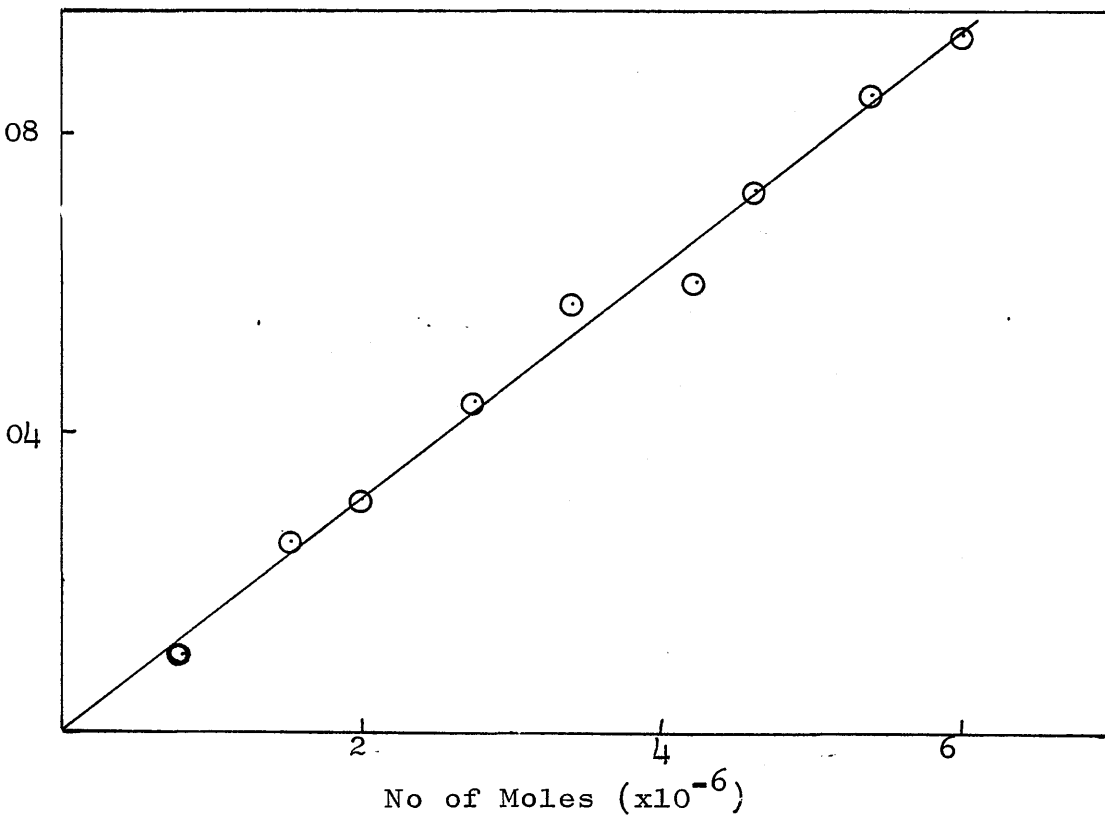


Fig. 2.9: Calibration plot for formaldehyde

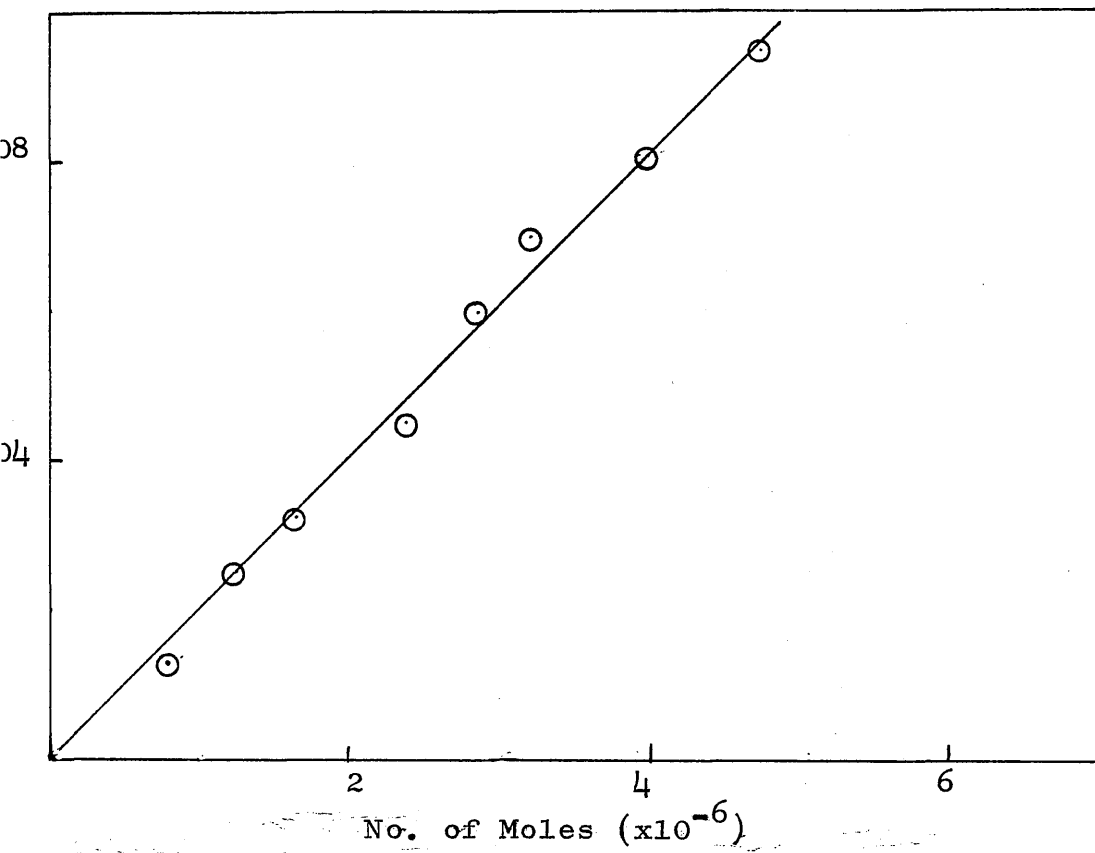


Fig.2.10: Calibration plot for methyl formate

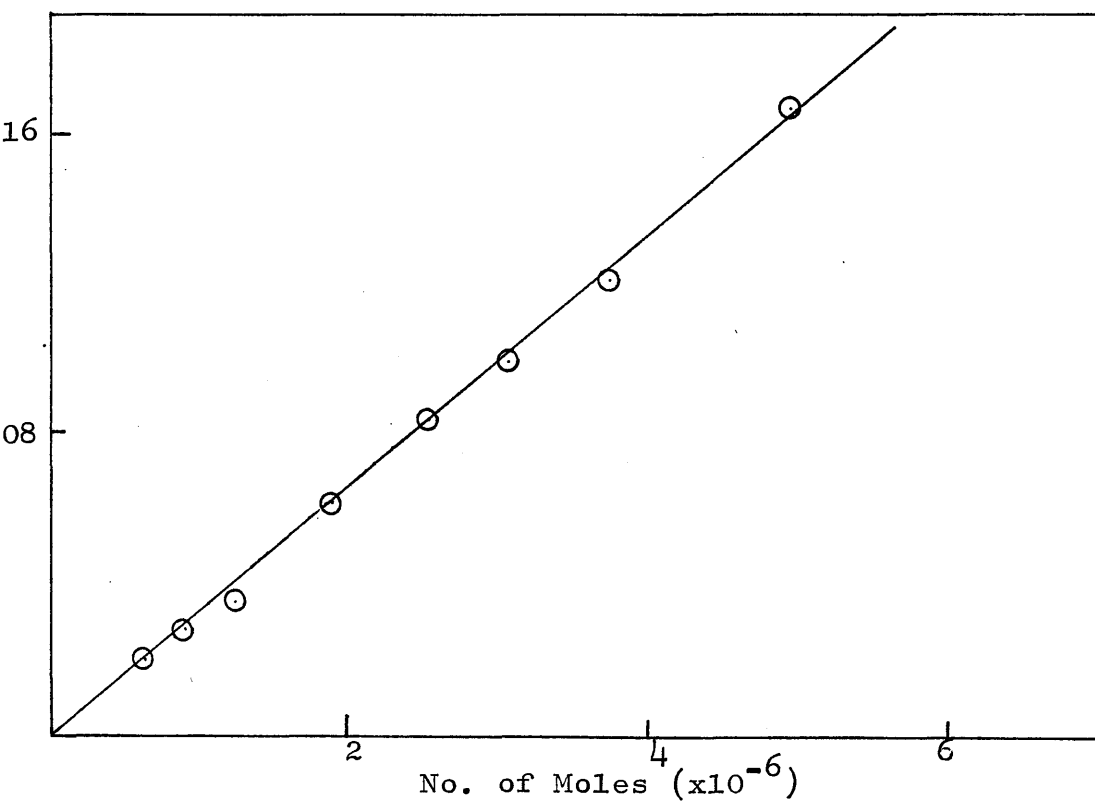


Fig. 2.11: Calibration plot for methanol

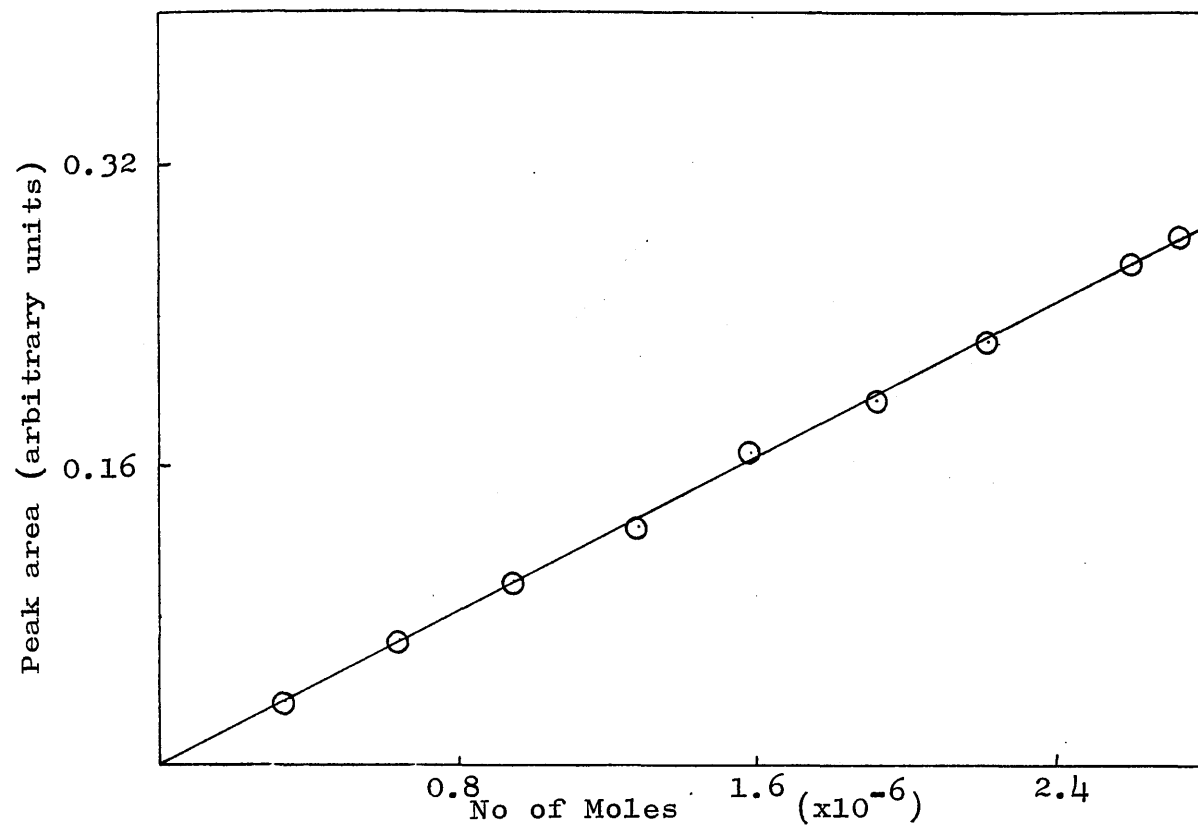


Fig.2.12: Calibration plot for 1:2 molar ratio of 3-methyl heptane: 2-ethyl-1-hexene.

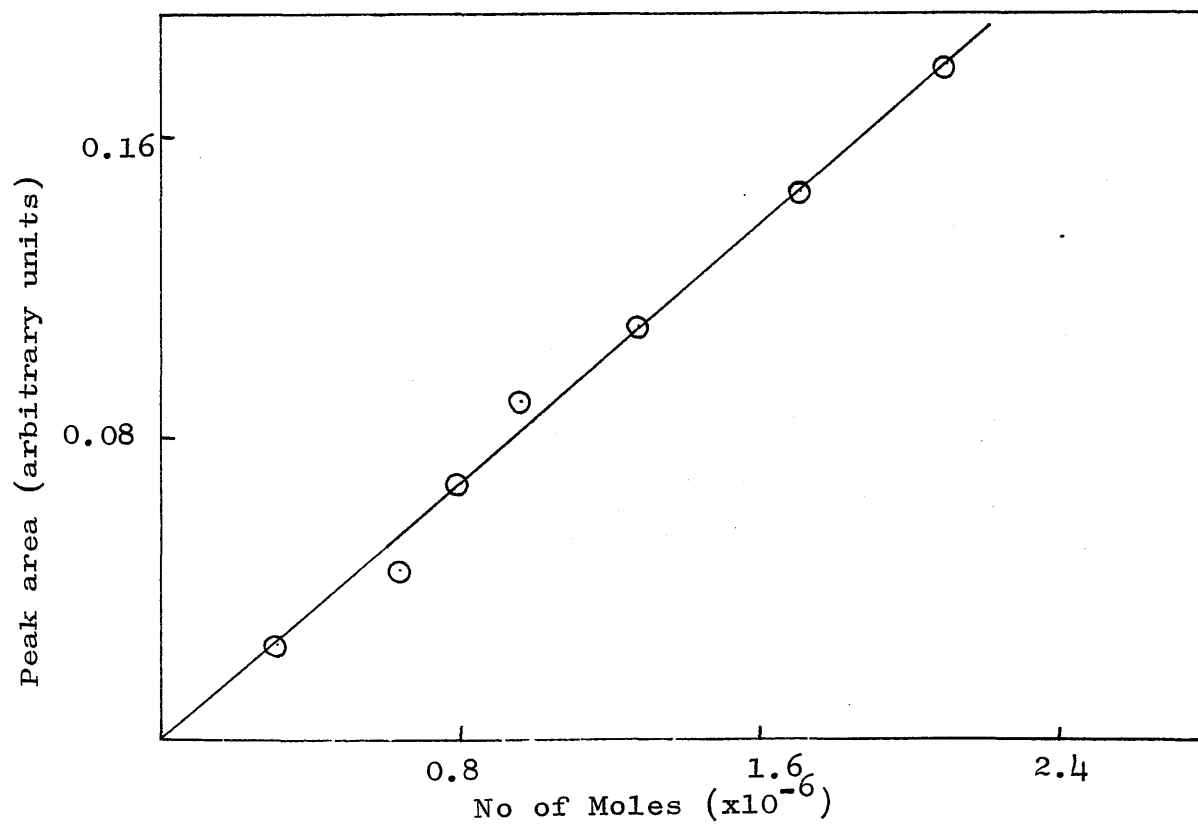


Fig. 2.13: Calibration plot for 2-ethyl-1-hexanal

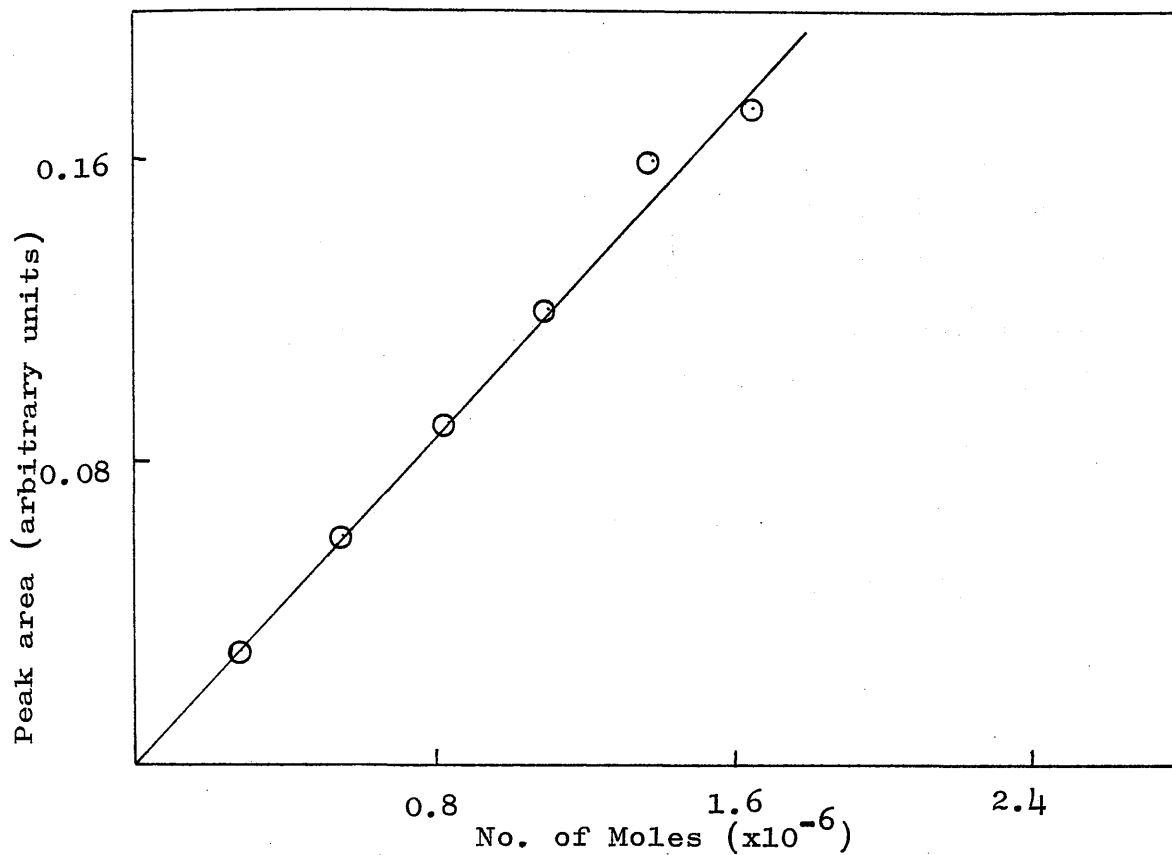


Fig.2.14: Calibration plot for 2-ethylhexyl formate

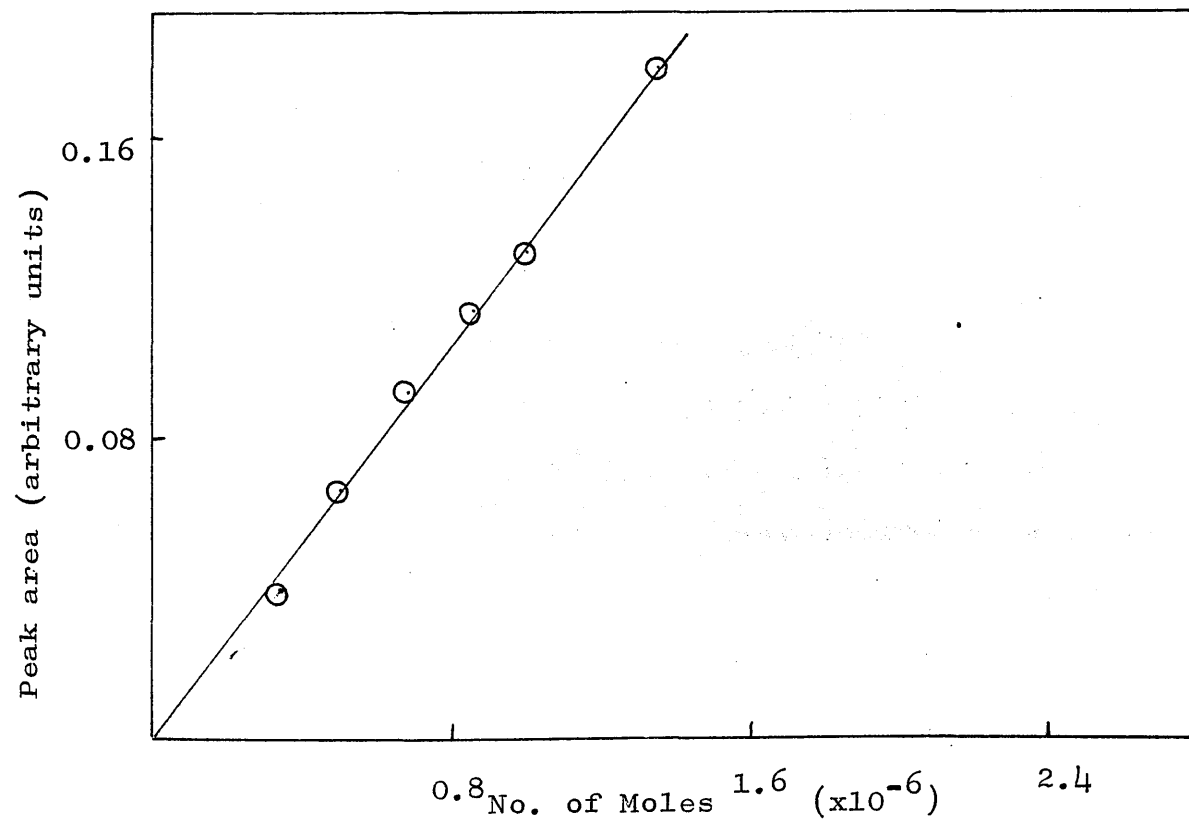


Fig.2.15: Calibration plot for 2-ethyl-1-hexanol

2.4 Spectroscopic Techniques

2.4.1 Infrared Spectroscopy

A minimum volume gas cell of 20 mm path length was employed in the analysis of gaseous products. The volatiles were condensed in a capillary tube at the base of the cell which was sealed under vacuum. On warming, the products expanded into the main chamber which was orientated to allow the infrared beam to pass through via the sodium chloride plates at either end. To enable the infrared spectrum of a thin film to be recorded, 0.3 ml of a polymer solution (2% w/v) was spotted on to a salt plate surrounded by a rubber ring. The solvent (methylene chloride) was allowed to evaporate at room temperature in air for 2 hours and the plate was then vacuum dried for 2 hours. Absorption changes were monitored by clamping the salt plate at a specific point in a magnetic holder ensuring that the same portion of the film was exposed each time. All spectra were recorded on a Perkin Elmer 257 infrared spectrophotometer.

2.4.2 Ultra-Violet Spectroscopy

Thin films were cast on silica plates, (using the same technique as detailed above in infrared spectroscopy) which were secured to a carrier plate by a magnet and all spectra were recorded on a Unicam SP800 spectrophotometer.

2.4.3 Mass Spectrometry

Samples were analysed on an A.E.I. MS12 Mass Spectrometer with gold inlet system for gases and gallium inlet system for liquids.

2.4.5 Gas Liquid Chromatography (GLC)

Products were identified by using a Perkin-Elmer F.11 gas chromatograph with flame ionization detector and a 6 feet long column containing 10% microwax (SGP. 317 Microcrystalline wax bottoms) on Chromsorb P, 80-100 mesh.

The high boiling liquid products from poly (2-ethylhexyl acrylate) were separated by dissolving them in methyl acetate and using the above column at 80°C isothermally.

2.5 Determination of Extent of Photocrosslinking in Polyacrylate

2.5.1 Introduction

During irradiation of polyacrylates both scission and crosslinking reactions occur simulatneously(19,21,25,41,51). Crosslinking is indicated by the formation of benzene insoluble material. These previous workers studied the extent of crosslinking and chain scission through the swelling, viscosity or solubility changes which occur in the polymer during irradiation. The above mentioned methods are applicable to systems with a low crosslink density(25).

A considerable portion of the polymer remains soluble due to chain scission and molecular mass changes could be observed by Viscosity measurements or sol-gel separation data.

A crosslinked polymer cannot dissolve in a solvent because the crosslinks prevent the complete separation of the chains required to disperse the polymer in solution.

But the absorption of solvent by the network (formed during crosslinking) causes the chains to expand, so that swelling of the polymer is observed. The expansion is counterbalanced by the tendency for the chains to coil up and an equilibrium degree of swelling is established, which depends upon the solvent and the crosslink density, i.e. the higher the crosslink density the lower the swelling. (Crosslink density will be defined as the fraction of the units which are crosslinked). Hence the Flory-Rehner equation (given below) for swelling is applicable only to polymers with a low crosslink density (52).

$$\begin{aligned} & - \left[\ln(1 - v_{2m}) + v_{2m} + \chi_1 v_{2m}^2 \right] \\ & = v_1 (v_e/v_0) (v_{2m}^{1/3} - v_{2m}/2) \end{aligned}$$

v_e/v_0 is moles of effective network chains per unit volume.

$$v_{2m} = \frac{1}{q_{2m}} \quad \text{where} \quad q_{2m} = \text{swelling ratio} = (W_0/W)(l/l_0)^3$$

(where W and W_0 represent the weight in grams before irradiation, and after irradiation and extraction respectively; and l_0 and l , are a dimension of the film before and after swelling, respectively).

v_1 = molar volume of the solvent and

χ_1 is thermodynamic interaction constant calculated from osmotic pressure data. In the case of photocuring systems, it is not possible to measure the extent of crosslinking with the help of existing methods, because under ultraviolet irradiation, such systems do not give a small number of random crosslinks but form an infinite network with high crosslink density and there is little or no soluble fraction.

A new sorption technique has been established in this investigation, for the purpose of extending studies of crosslinking to higher crosslink densities, such as are found in photocuring systems. The method is also applicable at low crosslink densities.

2.5.2 What is Sorption?

The surface of a liquid is in a state of strain or unsaturation (surface tension) and similarly the solid surface has a residual field of force. The free energy of any surface has a tendency to decrease and this tendency is ultimately responsible for the phenomenon of adsorption.

Adsorption is the existence of a higher concentration of a component at the surface of a solid or a liquid phase than is present in the bulk; while in case of absorption there is a more or less uniform penetration by the solid. It is not possible to separate the effects of adsorption from absorption, hence the term sorption is employed (53).

It is possible to measure the extent of absorption of a solvent by a polymer employing a counting technique if a labelled involatile solvent is used. The radioactivity of the latter should be high enough to give appreciable counts even with the highly crosslinked material.

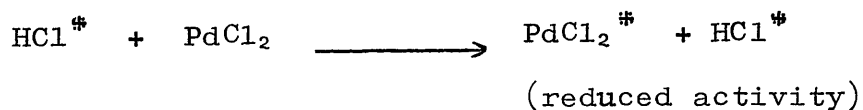
Polymer films were immersed for a standard time in a solvent/nonsolvent mixture consisting of petroleum ether (boiling point 40° - 60°C as non-solvent) containing a small proportion of [^{36}Cl]-labelled styrene dichloride (solvent). The film absorbed the involatile, radioactive solvent to an extent which varied inversely

with the increase in molecular weight, due to crosslinking. The volatile non-solvent rapidly evaporated from the surface of the film after removal from the solvent/non-solvent mixture, so that counting was readily carried out, under controlled conditions on the supported film sample.

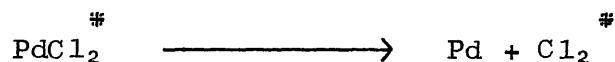
Preparation of radioactive styrene dichloride, counting technique and sorption technique are described below.

2.5.3 Preparation of Radioactive Styrene Dichloride

Preparation of radioactive chlorine from HCl has been described by McNeill (54). The hydrochloric acid HCl^{36} (The Radiochemical Centre, Ltd., Amersham) was diluted to 100 ml and a specific activity to $2.5 \mu\text{c/ml}$. 200 mg palladous chloride (Johnson Matthey Chemicals Ltd.) were placed in a specially designed silica glass round bottom flask A, and 25 ml of hydrochloric acid solution added. The mixture was heated gently until the palladium salt had dissolved. The acid was carefully distilled off leaving labelled palladous chloride in the flask.



Then the flask A was connected to a special assembly S having vessel B and a reservoir C (fig.2.16) connected to the vacuum line. The apparatus was evacuated and with stopcock T closed, the bulb A was heated gently to remove traces of moisture and acid. Greased joints and taps between decomposition flask and receiver were avoided, since chlorine attacks tap-grease. Vessel B was frozen at -196°C by liquid nitrogen and bulb A heated with a large luminous flame. The salt decomposed quantitatively to chlorine and palladium which formed a mirror-like deposit in the flask.

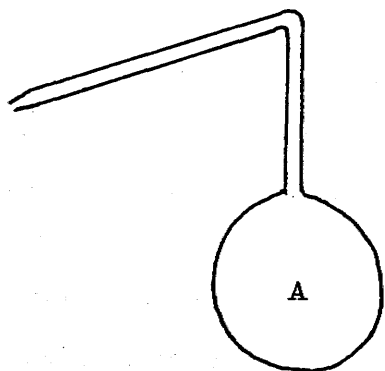


The liberated chlorine was condensed in vessel B.

Styrene along with styrene dichloride was placed in the reservoir C and degassed. Radiochlorine was transferred slowly into the reservoir C at -196°C , where it was allowed to react with styrene forming radioactive styrene dichloride. This labelled styrene dichloride was stored and used as 5% solution in a non-solvent for the polymer.

2.5.4 Counting Technique

Solutions were counted in an open Geiger-Muller counting tube (Mullard, MX124) in conjunction with a G.M. Scaling unit (type N529D, EKCO Electronics Ltd)



To vacuum

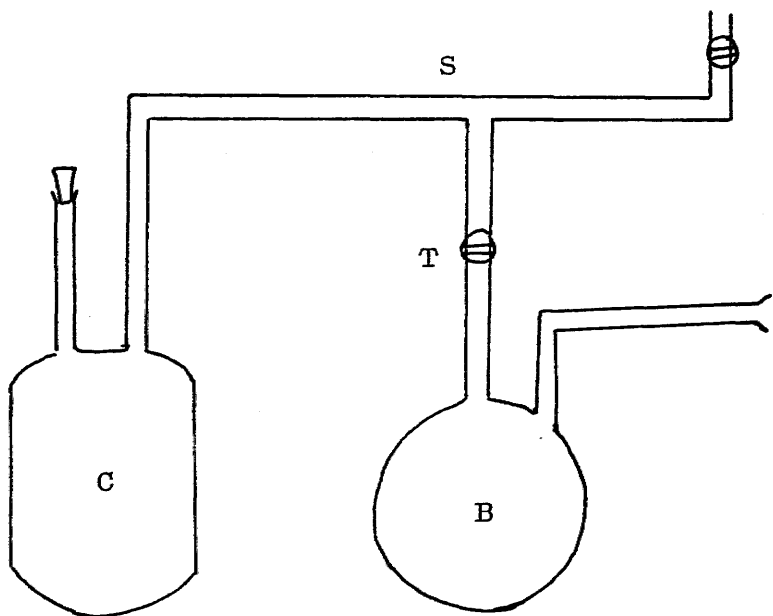


Fig.2.16: Apparatus for the preparation of labelled styrene dichloride..

and a probe unit (type 110A, Bendox-Ericsson Ltd.) Paralysis time was fixed at 400 μ s and correction for this dead time in the instrument were made from published table (55). Polymer films were counted using a Geiger Muller end window type counting tube (Mullard, Mx108).

Before a counting tube was used, its plateau region was determined by plotting the count-rate of a standard radioactive source against the applied voltage. A typical plot is shown in fig.2.17. For G.M. counting a voltage was selected corresponding to the mid-point of this plateau, i.e. 420-440V. All count rates were corrected for paralysis time of the counter and background which was measured experimentally. Only the corrected count-rates are recorded in this thesis. With the exception of very slow count-rates, count-rates were measured by counting until 10,000 pulses had been registered. Time was measured by a stopwatch. Since the standard deviation on the count-rate is equal to the square root of the total count (55) the standard deviation of count-rates was $\pm 1\%$.

2.5.5 Sorption Technique

A 5% solution of labelled styrene dichloride in a non-solvent for the polymer was prepared. The non-solvent used for poly(methyl acrylate) was petroleum ether (b.pt. 40°-60°C) and that for poly

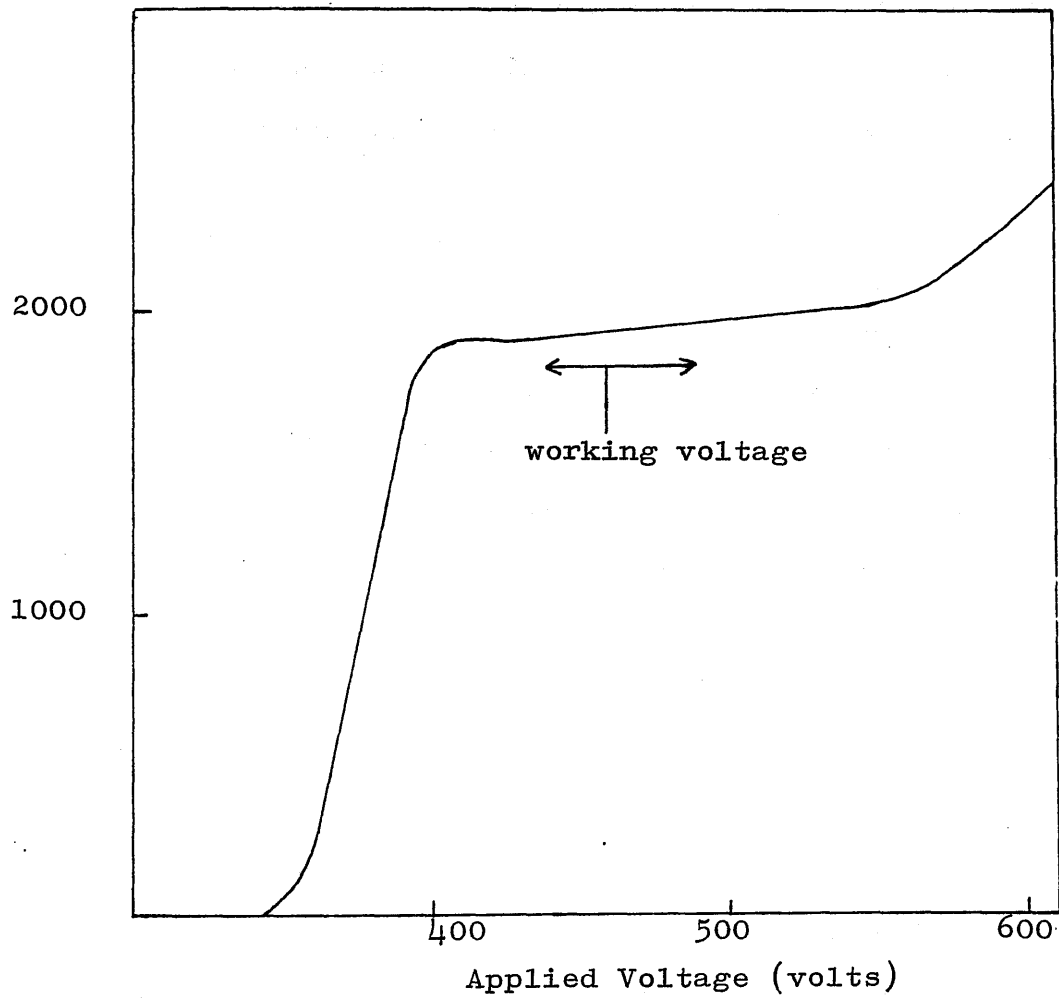


Fig. 2.17: Determination of working voltage for G.M. Counter.

(2-ethylhexyl acrylate) was a methanol/water mixture (5:1 ratio). A 5 ml portion of labelled styrene dichloride/non-solvent mixture was placed in a small jar with replaceable top and the polymer film was allowed to soak in this solution for two hours. The soaking time was kept constant for every experiment. After the soaking period the film was taken out and washed with non-solvent in order to remove the excess of solvent on the surface of the film and support plate which might give ambiguous results (details of support plate and film preparation are given in Chapter 3). The washing procedure was controlled by allowing the film to just dip in 5 ml of non-solvent, in a small dish and then washing it with another 5 ml of non-solvent. The film was then dried by simply allowing the non-solvent to evaporate in air for one minute and the count rate was measured. The deviation for the count rate was $\pm 6\%$.

When polymer films were photodegraded for different intervals of time and the count rates were measured after the standard sorption procedure, there was a decrease in count rate with the increase in irradiation time due to increased crosslinking. So that sorption technique provided a convenient means of assessing the extent of crosslinking process as could be seen in fig.2.18.

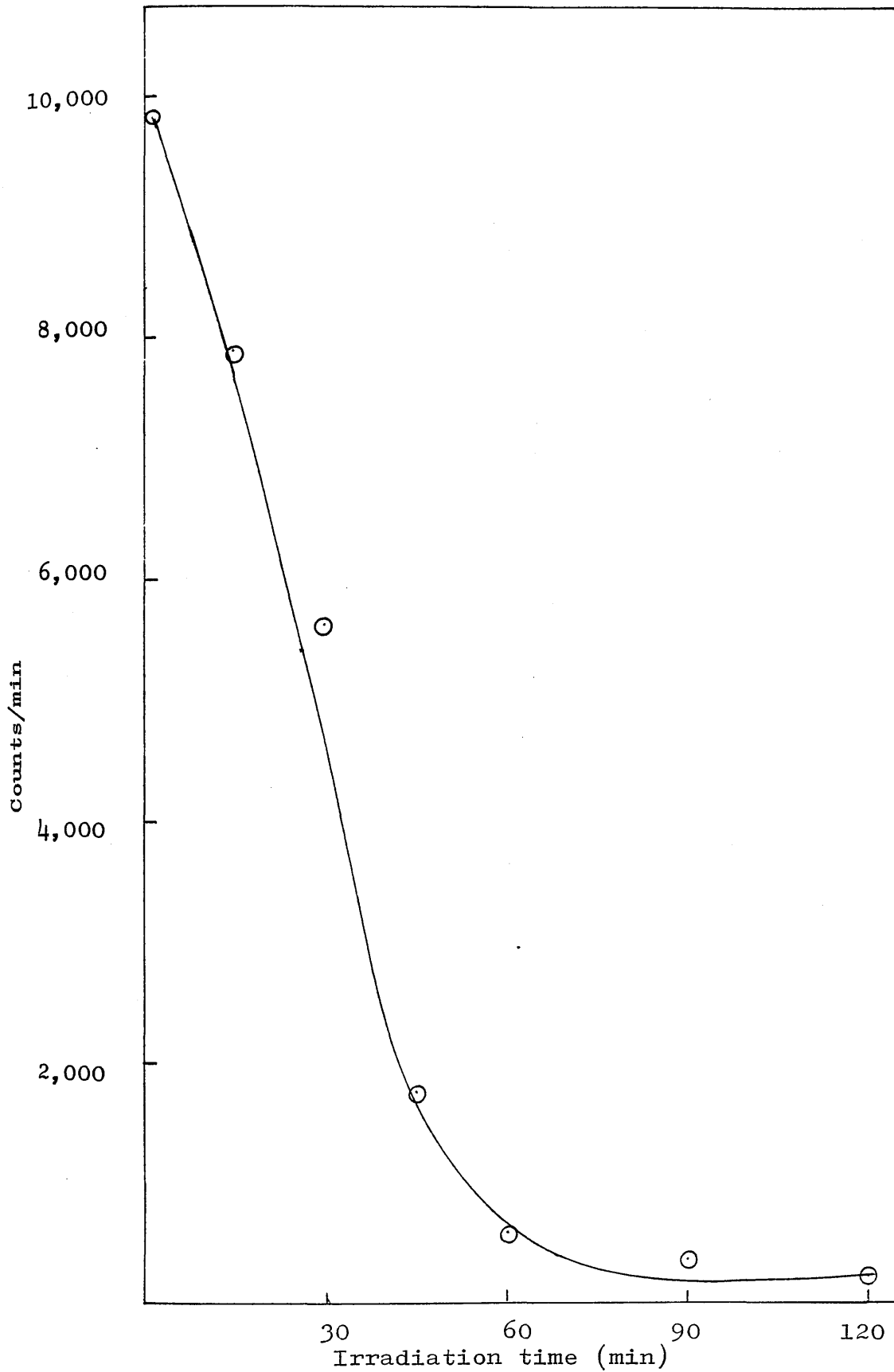


Fig. 2.18: Relationship between photodegradation time and count rate of PMA (molecular mass 352,000)

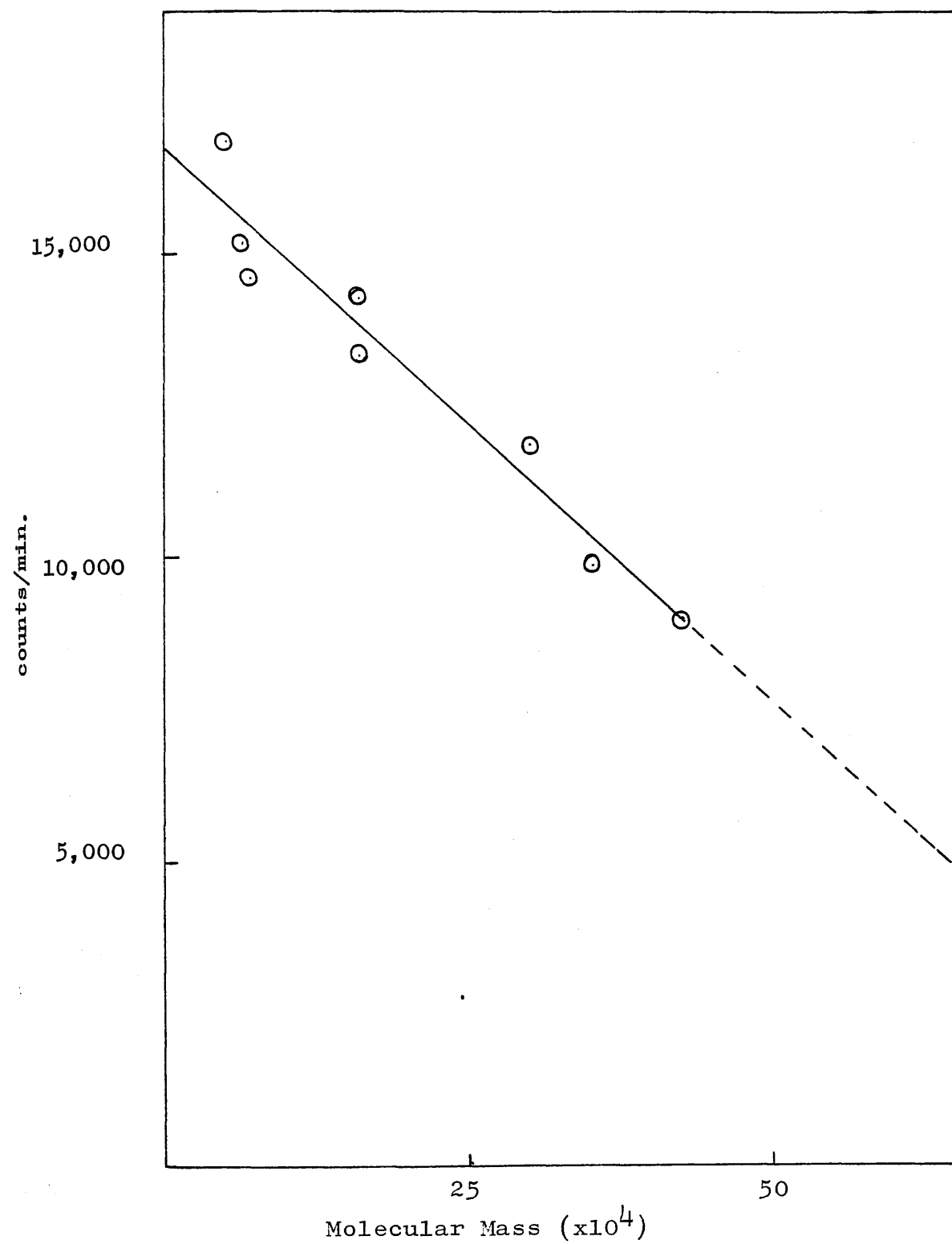


Fig.2.19: Relationship between molecular mass and counts/min for unirradiated PMA samples.

The variation in absorption of labelled solvent for samples of linear polymer with different molecular masses was also investigated. Count rates of films of equal weights of such polymers were measured after the standard sorption procedure as detailed above. It is obvious from the fig.2.19 that the absorption of the solvent decreases with the increase in molecular mass, approximately in direct proportions over the range studied. From this plot the molecular mass changes occurring during crosslinking of the polymer can be directly estimated over part of the measured count rate scale and can be measured approximately beyond the limit of the calibration graph, if a linear extrapolation is assumed. In practice, the relative behaviour of samples under various conditions is of more interest than the absolute values of the molecular masses.

CHAPTER THREE

PRELIMINARY INVESTIGATIONS

3.1 Introduction

Before a quantitative study of the photodegradation of the polyacrylates was taken, it was considered necessary to perform control experiments to characterise the irradiation apparatus. Thus the effects of lamp-to-sample distance, temperature, sample size and time of irradiation have been determined using PMA. The subambient TVA technique described in the preceding chapter was employed to obtain the preliminary information.

3.2 Preparation of the Polymer Film

A polymer solution in methylene chloride (redistilled) was prepared accurately to a concentration of 40 mg per ml (4%). 0.5 ml of the solution was transferred by means of a hypodermic syringe to a circular stainless steel support, having a flat recess of diameter 2.18 cm. The average film thickness was calculated from the weight of the polymer, the density and the area over which the sample was deposited. The solvent was allowed to evaporate slowly at room temperature over 24 hours. The film was then continuously pumped under vacuum at ambient temperature for another 24 hours and on the vacuum line for an additional two hours immediately before irradiation. After irradiation of the film, the

product analysis did not reveal the presence of any trace of methylene chloride. Hence the above drying procedure was adopted for the remainder of the studies.

3.3 Effect of Lamp-to-Sample Distance on Photodegradation Products

The medium pressure mercury lamp produces a large amount of heat during irradiation. A change in sample temperature was observed during variation of the lamp-to-sample distance. The effect of this variable on sample temperature and yield of volatile products was therefore examined. Films (20 mg) of PMA were irradiated for two hours at various distances viz., 5 cm, 10 cm, 15 cm, 16 cm and 20 cm from the radiation source. The products obtained were identified by employing the sub-ambient TVA technique described in the preceding chapter. The quantitative yield of each product was calculated from the corresponding peak area. Details of the product identification will be mentioned in the next chapter.

The results are shown in fig.3.1 and the data are summarised in table 3.1. At a lamp-to-sample distance of 5 cm, 11.84 mole per cent (based on number of moles of monomer units originally present in sample weight) of condensable liquid products were obtained while at 10 cm distance this reduces to 5.87 moles %. Further increase in the distance

TABLE 3.1

Lamp-to-Sample Distance	Total Yield of Products mole %	Temperature T°C
5 cm	11.84	59°C
6 cm	11.46	57°C
10 cm	5.87	37°C
15 cm	5.30	30°C
16 cm	5.20	30°C
20 cm	4.98	29°C

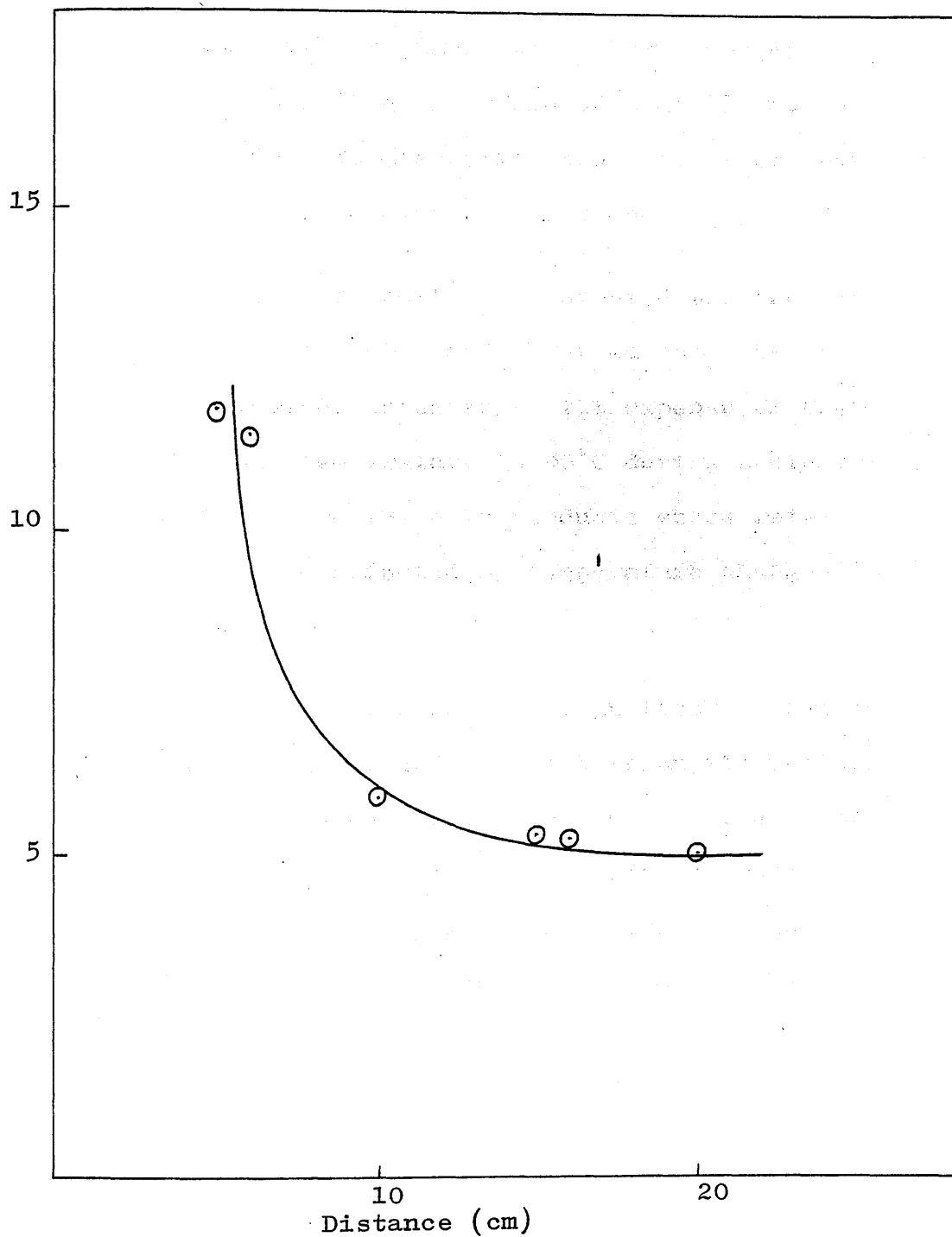


Fig. 3.1: Effect of lamp-to-sample distance on the mole % yield of the total condensable volatile products from PMA.

to 20 cm gave a decrease in yield to 4.98 mole %.

No linear relationship is observed. It is also shown in table 3.1 that the sample temperature decreases considerably with the increase in lamp-to-sample distance, from 59°C at 5 cm and 30°C at 15 cm. It was not possible to dissociate the effects of temperature rise and light intensity with distance.

Ackerman and McGill (20) studied the photolysis of PMA at 50°C and 80°C and observed that the rate of HCHO formation increases at the expense of CH₃OH on raising the temperature to 80°C during photolysis. HCHO and CH₃OH are the only products whose rates of formation are affected by temperature changes in this range.

One of the components of a photocuring system is a photosensitizer and its effects on the polyacrylate degradation was studied. The photosensitizers employed in these studies were found to be retained at 30°C under vacuum but at higher temperatures substantial amounts were observed to be sublimed under the normal conditions of photodegradation. Therefore a lamp-to-sample distance of 15 cm was used throughout these studies in order to keep the sample temperature at 30°C.

Film Thickness

Poly(methyl acrylate) films of different thickness were photodegraded for two hours and the mole % of the total and individual product is plotted against the film thickness as shown in figs. 3.2, 3.3, 3.4 and also tabulated in table 3.2.

The data shows that there is no appreciable influence of film thickness unless it is smaller than 20μ . Above this value there is a filtering effect of the upper layers of polymer in screening lower layers from irradiation.

The polymer film thickness employed throughout the rest of the studies was kept at approximately 22μ .

Effect of Time

In order to see the effect of time of irradiation on the formation of volatile products, 22μ films of the polymer were photodegraded for various time intervals as shows graphically in fig.3.5.

It is obvious from the graph that the total yield of the condensable volatiles is almost directly porportional to the time of irradiation for the first 30 minutes. After that the rate of product formation decreases. This effect is possibly due to the 'cage effect' due to crosslink formation which will reduce the diffusion of the products formed.

TABLE 3.2

Effect of film thickness on the mole % yield of condensable volatiles from PMA degradation

Film Thickness μ	CO ₂	HCHO	HCOOCH ₃	CH ₃ OH	Total Yield
7.34	0.65	0.6	0.96	1.01	3.22
15.12	1.01	0.94	1.39	1.22	4.55
18.3	1.00	1.01	1.46	1.22	4.69
20.49	1.08	1.01	1.65	1.2	4.94
21.92	1.11	1.15	1.75	1.29	5.30
26.85	1.16	1.16	1.74	1.24	5.30
32.88	1.24	1.29	1.82	1.28	5.63
43.84	1.19	1.28	1.87	1.33	5.67
52.83	1.24	1.25	1.91	1.32	5.72
63.58	1.24	1.34	1.91	1.40	5.89

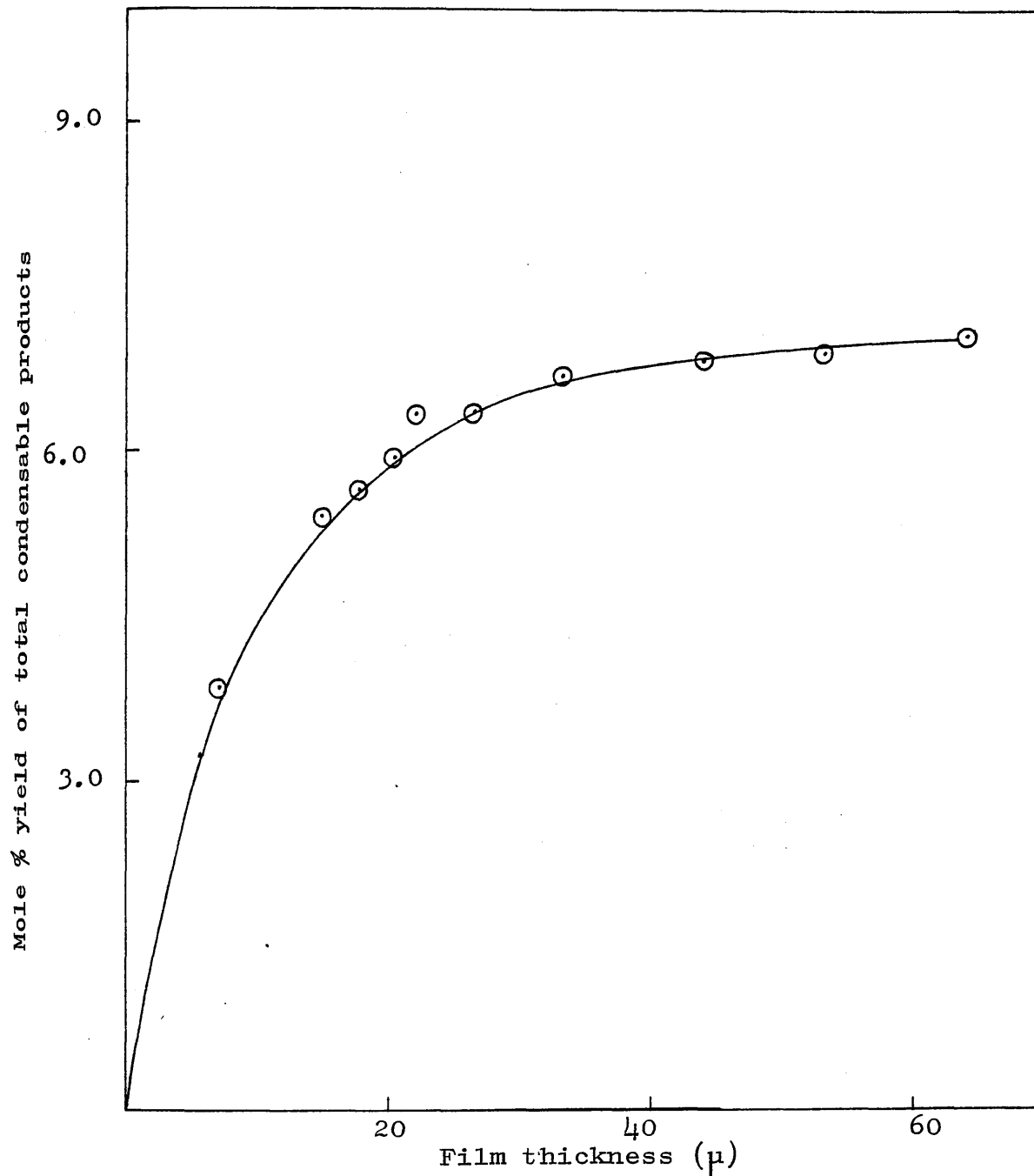


Fig. 3.2: Effect of film thickness on the mole % yield of the total condensable volatiles from PMA.

Mole % yield of condensable products

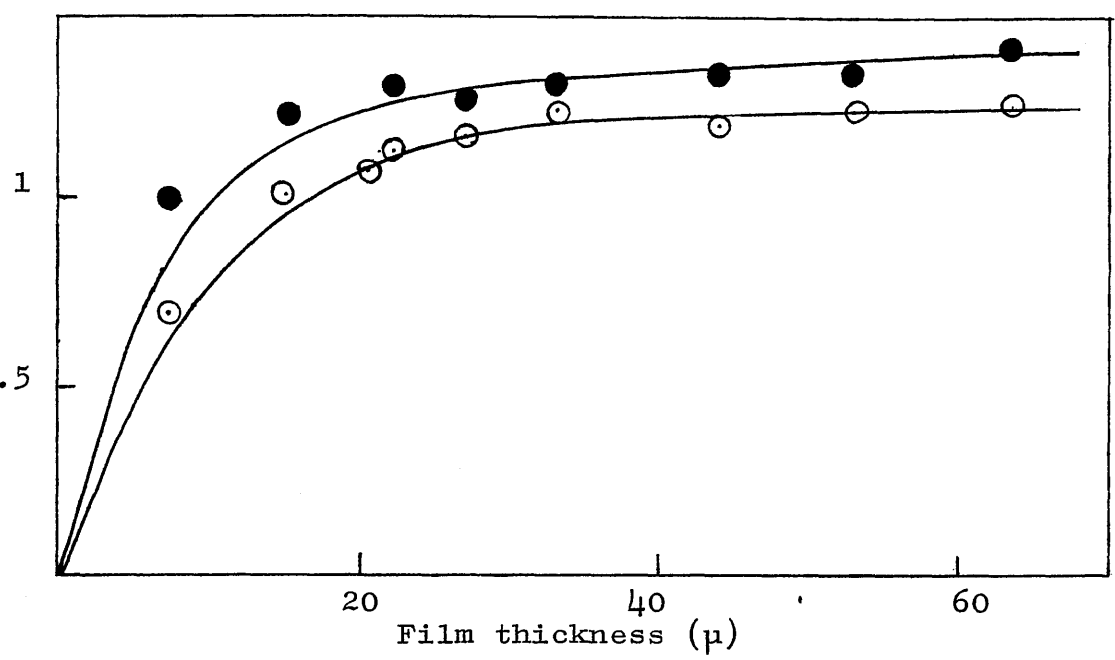


Fig. 3.3: Effect of film thickness on the mole % yield of condensable volatiles from PMA.
 ○ carbon dioxide ● methanol

Mole % yield of condensable products

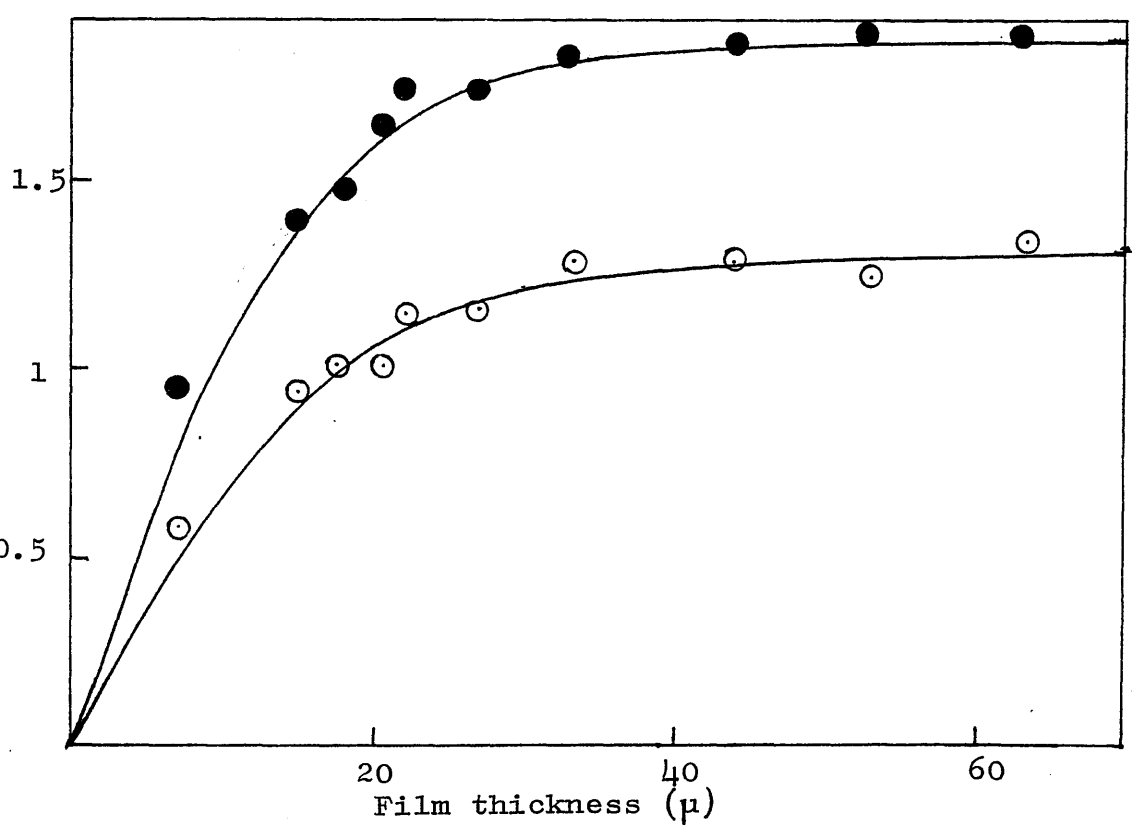


Fig. 3.4: Effect of film thickness on the mole % yield of condensable volatiles from PMA
 ○ formaldehyde, ● methyl formate

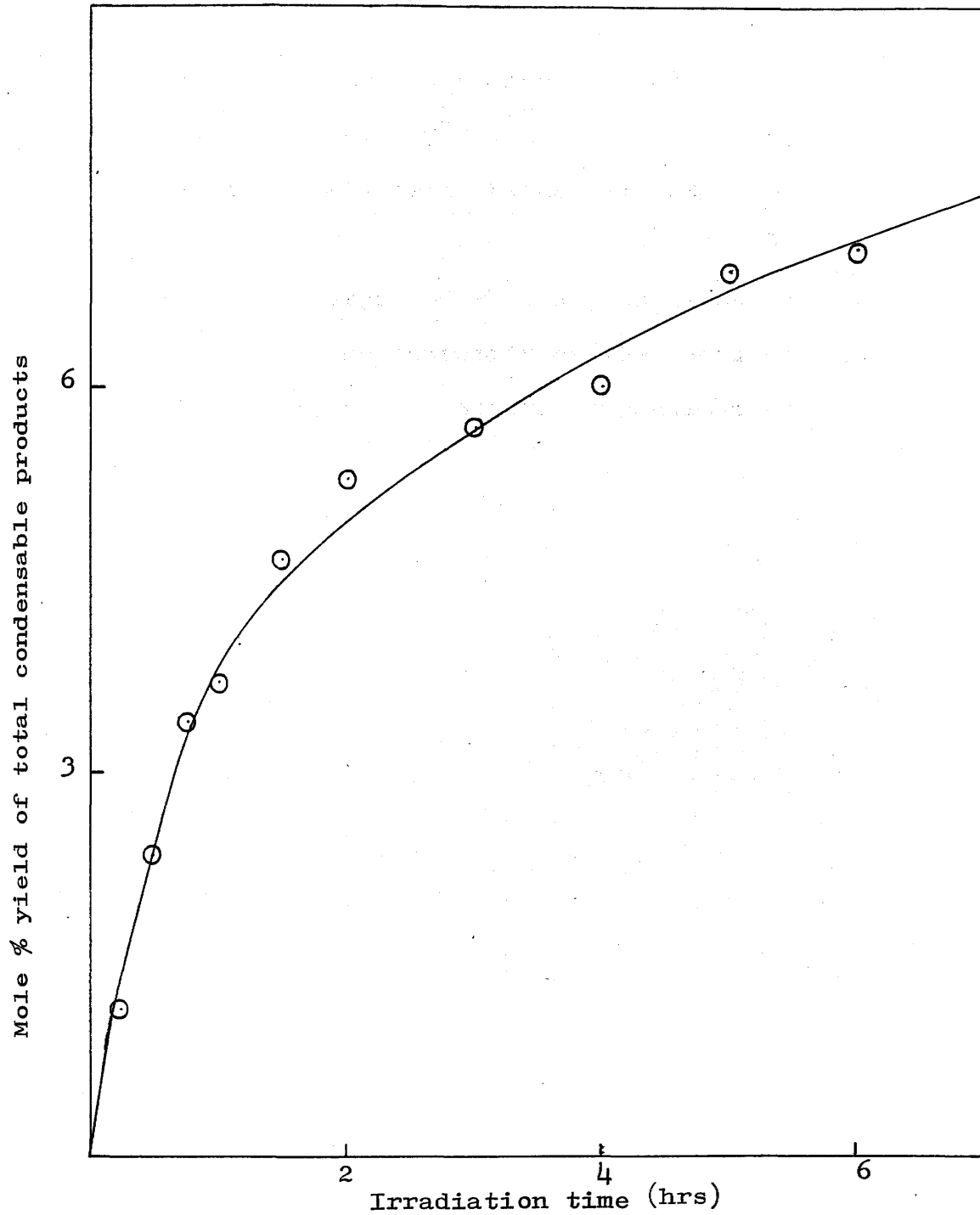


Fig. 3.5: Effect of irradiation time on the mole % yield of the total condensable products from PMA.

As a result of these preliminary experiments, the following conditions were selected as standard for quantitative studies subsequently described:

- lamp to sample distance: 15 cm
- temperature: 30°C ± 1
- sample (PMA) film thickness: 22μ

The spectral output of the lamp is given in table 2.2 (Chapter 2). The intensity of the incident light at this lamp-sample distance was approximately 10,080 μW/cm².

CHAPTER FOUR

PHOTODEGRADATION STUDIES ON POLY(METHYL ACRYLATE)

4.1 Introduction

Fox et al (19) reported the photolysis of thin films of PMA at room temperature, in air and in vacuum, by radiation from a low pressure mercury lamp source, and suggested a reaction mechanism for the degradation process. They found a number of gaseous and low boiling liquid products viz., carbon dioxide, formaldehyde, methanol and methyl formate. Ackerman and McGill (20) found methyl acetate along with the above mentioned products, when thin films of PMA were decomposed in vacuum at 50°C by irradiation with a high pressure mercury lamp.

In this investigation, the photodegradation of PMA films has been studied at $30^{\circ}\text{C} \pm 1^{\circ}\text{C}$ in vacuum by irradiation with a medium pressure mercury lamp, using the subambient TVA technique. The investigation has been approached from several angles in order that by combining the information obtained from each a more complete picture can be built up of the overall degradation reaction.

The main points of interest are:-

- (a) the evolution of volatile products during degradation,

- (b) spectroscopic changes in the film, and
- (c) the molecular mass changes in the film due to crosslinking.

A detailed description of the sample form, sample history and degradation apparatus, which consists of a photolysis cell, separation unit and analytical gas cell, has been given in the appropriate sections of the previous chapters, together with the techniques and procedure involved.

4.2 Product Analysis

Samples of approximately 22 μ thick and 7.46 cm² in area, cast from methylene chloride solution were degraded in the photolysis cell and the volatile products were trapped at liquid nitrogen temperature and subsequently examined by subambient TVA. Typical traces obtained from consecutive exposures of one hour and four hours respectively are illustrated in figs. 4.1 and 4.2.

In both cases six peaks can be distinguished corresponding to six condensed products. The first five peaks in the traces from PMA can each be assigned to a single product by consulting the data in table 4.1, where the distillation rate maxima of the reference compounds are given. Water which was responsible for the fifth peak (distillation rate maximum $-55^{\circ}\text{C} \pm 10^{\circ}\text{C}$), was not regarded as a genuine photolysis product,

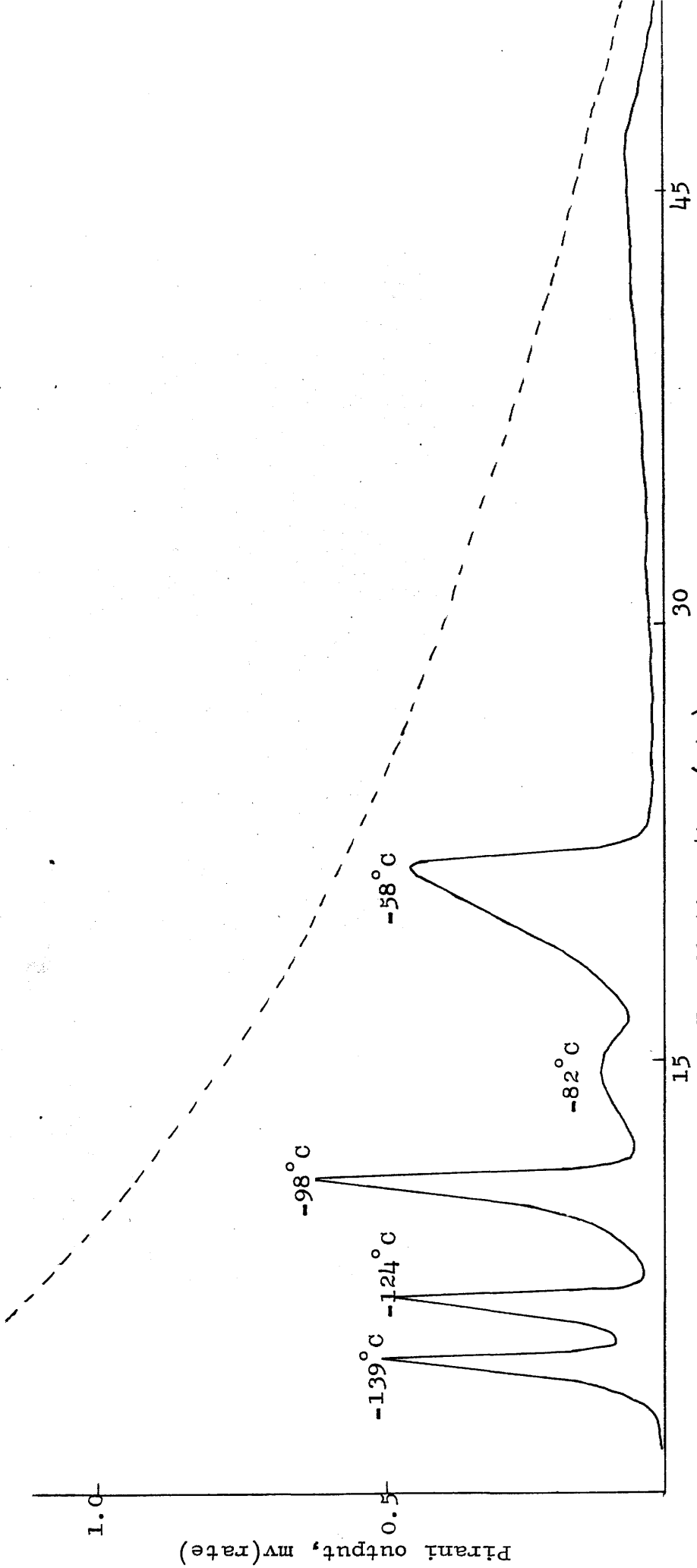


Fig. 4.1.1: Sub-ambient TVA curve for photodegradation products of PMA
 (One hour photodegradation of 22 μ film)

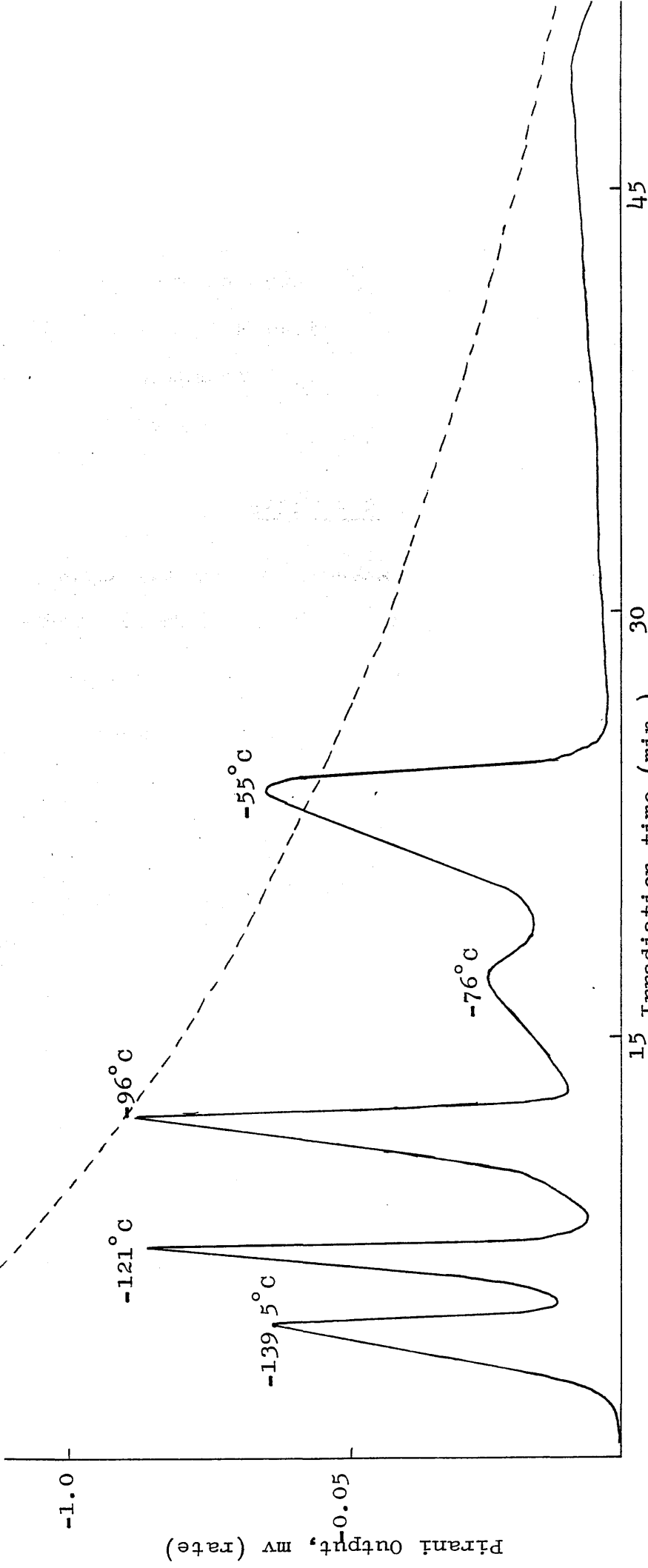


Fig. 4.2: Subambient TVA curve for photodegradation products of PMA (4 hours photodegradation of 22 μ film of PMA)

TABLE 4.1

<u>Product</u>	<u>Distillation Rate Maximum ($\pm 6^\circ\text{C}$)</u>
Carbon Dioxide	-140°C
Formaldehyde	-118°C
Methyl Formate	-90°C
Methanol	-76°C
Water	-55°C

TABLE 4.2

<u>Subambient TVA Rate Maximum</u>	<u>Infrared Absorptions</u>	<u>Mass Spectrometric Analysis (m/e)</u>	<u>Product</u>
-139°C	2300, 670 cm^{-1}	44/100, 16/9	Carbon Dioxide
-119°C	2900-2740, 1750 cm^{-1}	18/100, 29/85 30/51, 28/26	Formaldehyde
-92°C	3020-2880, 1740, 1220-1150 cm^{-1}	-	Methyl Formate
-76°C	3000-2840, 1030 cm^{-1}	31/100, 32/72, 29/70	Methanol

but considered as originating from glassware or from absorbed water on the acrylate film. In order to check this a blank run was performed using the same photolysis conditions with only the stainless steel sample support present. The trace obtained from the blank run showed a small quantity water, which could only have originated from the apparatus.

The peak assignments based on distillation rate maxima were confirmed by collection of the fractions responsible for each peak and analysis by infrared spectroscopy or mass spectrometry. Data are summarised in table 4.2.

The sixth peak was not identified as the amount of this high boiling liquid, probably short chain fragments, is too small. Similar products have been reported by other workers (19, 20) from their photolysis studies though the products were present in completely different ratios. See table 4.3.

According to Fox (3) the problem of finding a photolytically inert solvent is unlikely to be completely solved, hence residual solvent can affect the degradation behaviour. Ackerman and McGill (20) have reported the formation of methyl acetate, which has neither been reported previously nor observed in the present studies. They used acetone as film casting solvent which gives CH_3 and OCH_3 radical,

TABLE 4.3

<u>Study</u>	<u>Ackerman + McGill</u>	<u>Fox et al</u>	<u>Present Study</u>
Radiation Source	High pressure mercury lamp	Low pressure mercury lamp	Medium pressure mercury lamp
Temp.	50°C	Ambient Temp.	30°C ± 1
Film Thickness	44 u	30 - 50 μ	22 μ
Lamp-to-Sample Distance	10 cm	-	15 cm
Products	% (by vol)	Quantum Yield	Mole % (based on monomer unit)
CO ₂	11	Exponential Rate	22
HCOOCH ₃	30	0.008	37
CH ₃ COOCH ₃	13	Nil	Nil
CH ₃ OH	30	0.002	18
HCHO	16	0.02	23

on photolysis (56). The possibility of methyl acetate formation from these radicals could not be excluded.

4.2.1 Quantitative Analysis

The major volatile products formed during vacuum photolysis of PMA were identified as CO_2 , HCHO, HCOOCH_3 and CH_3OH . Permanent gases which do not condense at liquid nitrogen temperature in vacuum are generally accepted as carbon monoxide, methane and hydrogen. No attempt was made to detect and analyse these in this study.

The procedure for the stepwise quantitative analysis of condensable volatiles is described in Chapter Two. As the amount of products was small, the Pirani gauge response was linear (57) with rate of volatilization, hence the area under each peak gives a direct measure of the amount of the product.

Calibration graphs for each product were constructed as shown in Chapter Two figs. 2.8 - 2.11. The number of moles and hence the mole per cent (based on monomer unit present originally) of each product was determined quantitatively as follows.

22 μ thick films of PMA were degraded under identical conditions for various intervals of time, and from the peak area on the subambient TVA trace, the mole percentage of each product was calculated.

Results are given in table 4.4. Typical graphs obtained by expressing the mole percent yield as a function of irradiation time are displayed in fig 4.3. It is obvious from the plots that the rate of evolution of volatiles decreases with time, although for the first thirty minutes the rate is almost constant. The subsequent decrease is attributed to the internal filter effect of the upper layers of the polymer film and the 'cage effect' which will decrease the escape of products.

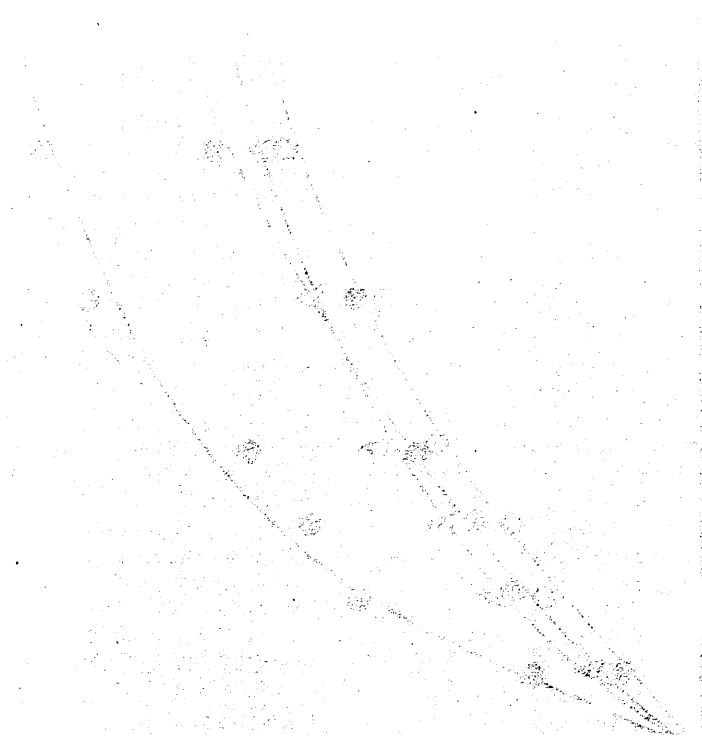
4.2.2 Methyl Formate Production

This is the major product of PMA photodegradation and constitutes 37-40% (based on number of moles) of the total condensable volatile products at least for the first 90 minutes of photolysis as shown in table 4.4.

It is suggested that after photolytic scission of PMA, the $\cdot\text{COOCH}_3$ radical formed abstracts a proton from the polymer. The radical left on the polymer may stabilize by forming a double bond in the polymer chain. After long exposures of the polymer samples slight yellowing is observed to develop, which is thought (57) to be due to formation of these double bonds in the polymer chain.

TABLE 4.4: Mole % yield of condensable volatiles
from the photodegradation of PMA

Irradiation <u>Time</u>	Mole % Yield of			
	<u>CO₂</u>	<u>HCHO</u>	<u>HCOOCH₃</u>	<u>CH₃ OH</u>
15 min	0.25	0.27	0.43	0.21
30 min	0.41	0.55	0.91	0.50
45 min	0.50	0.69	1.22	0.58
60 min	0.70	0.86	1.39	0.74
90 min	0.84	1.03	1.63	0.90
2 hrs	1.11	1.15	1.75	1.29
3 '	1.35	1.42	2.00	1.50
4 '	1.44	1.36	2.08	1.70
5 '	1.46	1.54	2.15	1.76
6 '	1.33	1.48	2.30	1.96



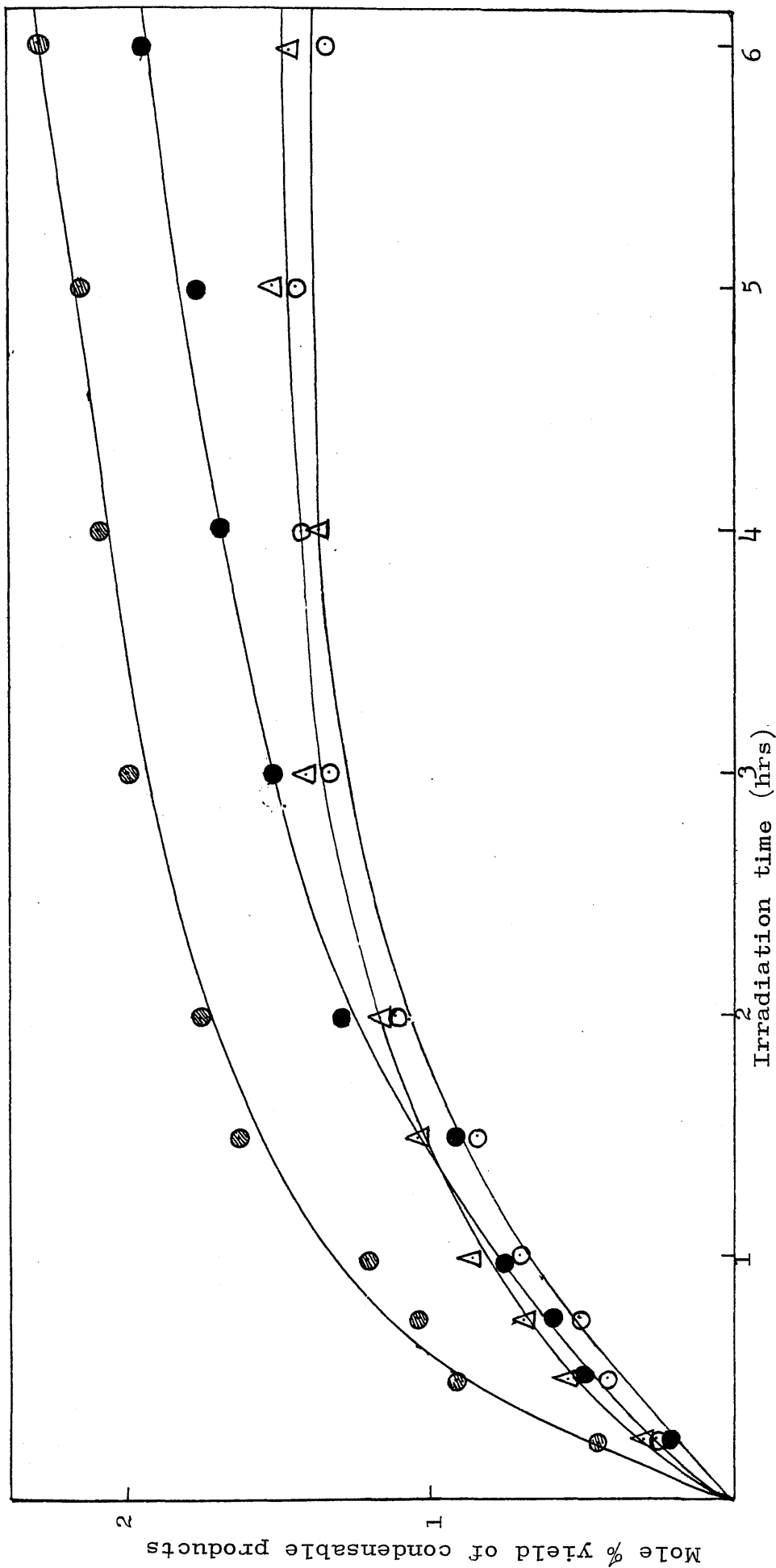
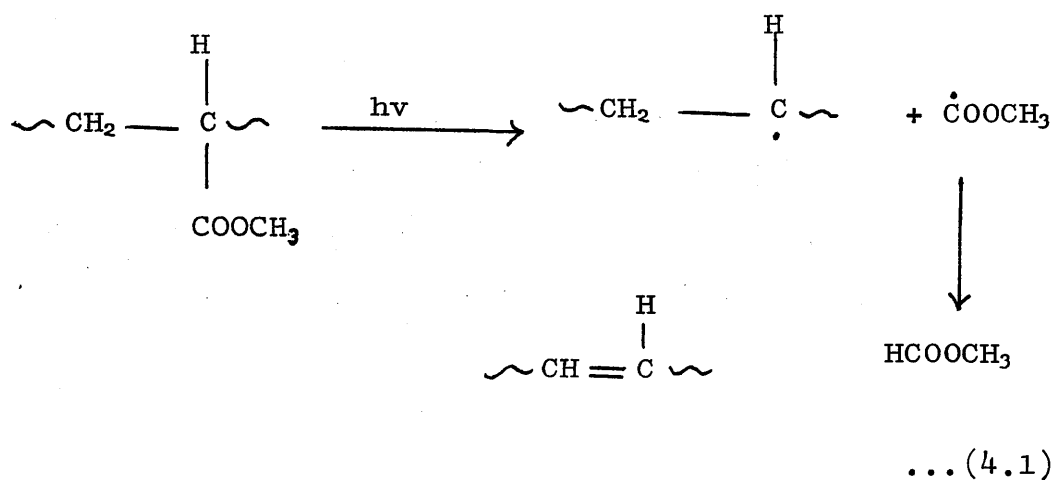


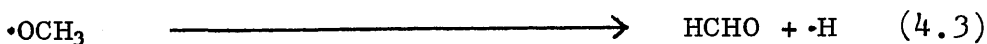
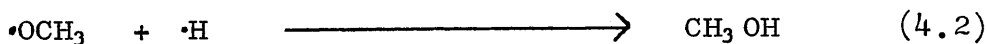
Fig.4.3: Effect of irradiation time on the condensable volatile products from PMA
 O carbon dioxide, ● formaldehyde, ⊗ methyl formate.



Ackerman and McGill (20) found that $\text{CH}_3/\text{HCOOCH}_3$ accounted for about 40% by volume of total volatiles formed on photolysis in vacuum, as shown in table 4.3. It was suggested that $\text{CH}_3/\text{HCOOCH}_3$ may result from abstraction by the $\cdot\text{COOCH}_3$ radical of a methyl group or a proton, respectively from the polymer.

4.2.3 Production of Formaldehyde and Methanol

Both products are thought to originate from the methoxy radical formed during the photo-decomposition of the ester group of PMA, hence their formation is discussed together. The methoxy radical $\cdot\text{OCH}_3$ may either abstract a hydrogen from the polymer to form methanol or convert to give formaldehyde and a proton.



In fig. 4.3 the rates of production of methanol and formaldehyde are seen to increase linearly with time, but after 60 minutes to decrease slowly.

By comparing the total yield of HCHO + CH₃OH, 42% (based on the number of moles of total volatile products) found in this study with those reported by other workers as shown in table 4.3, it is evident that our results are in better agreement with Ackerman and McGill's value of 46% by volume of total volatiles.

Fox et al obtained excessively large volumes of HCHO relative to all other products, when compared to our results. They suggested the possibility of a significant fraction of the formaldehyde resulting from biradical reactions of the type:



This possibility is discounted on the evidence obtained from our experiments. The production of both HCHO and CH₃OH depends upon the intensity of radiation and also upon temperature, suggesting the methoxy radical as a common precursor to the production of both compounds (see fig. 4.4). The results are summarized in table 4.5. The production of HCHO increases at the expense of CH₃OH production on increasing the photolysis temperature and intensity of radiation by decreasing the lamp to sample distance,

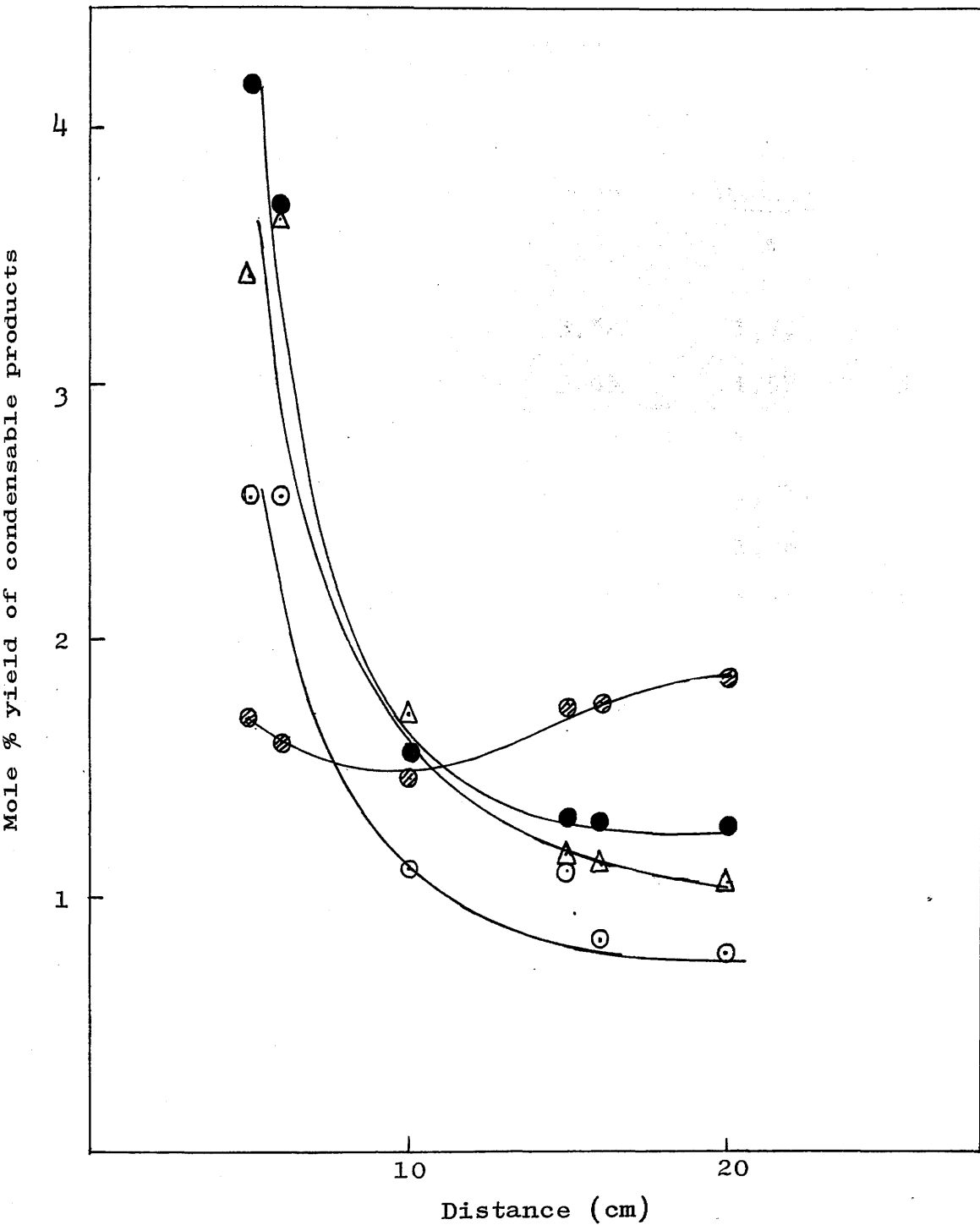


Fig. 4.4: Effect of lamp-to-sample distance on the mole % yield of condensable volatile products from PMA, ○ carbon dioxide, △ formaldehyde, ● methanol, ⊗ methyl formate.

TABLE 4.5: Effect of lamp-to-sample distance on the mole % yield (per monomer unit) of condensable volatiles from PMA Photodegradation

<u>Lamp-to-Sample Distance</u> (cm)	<u>CO₂</u>	<u>HCHO</u>	<u>HCOOCH₃</u>	<u>CH₃ OH</u>
5	2.55	3.52	1.70	4.17
6	2.55	3.65	1.59	3.67
10	1.13	1.72	1.48	1.54
15	1.11	1.15	1.75	1.29
16	0.83	1.12	1.76	1.29
20	0.79	1.05	1.86	1.26

while methyl formate production is more or less unaffected by both of these factors. Ackerman and McGill also argued the dependence of the rate of formation of these two compounds upon the reaction temperature.

For irradiations up to a total exposure time of 90 minutes, the ratio $\text{HCHO}/\text{CH}_3\text{OH}$ remains constant, but with increasing exposures the ratio decreases slowly see table 4.6. The ratio $(\text{HCHO} + \text{CH}_3\text{OH})/\text{HCOOCH}_3$, corresponding to the ratio of the rates of two photolysis reactions, remains constant, for film thicknesses above 20μ .

Ackerman and McGill (20) argued that the $\cdot\text{OCH}_3$ radical would undergo fragmentation if it possessed the necessary energy and this energy could be supplied thermally or by the absorption of radiation in the shorter wavelength region of the broad 275 nm absorption band. This helps to explain the observations of Fox et al (19) who used a low pressure mercury lamp emitting 88% of its energy at 254 nm and obtained much larger volumes of HCHO relative to all other products, than in this work and that of Ackerman and McGill. Motimoto and Suzuki (51) have shown that the 254 nm line is the most effective in decomposing polyacrylates.

TABLE 4.6

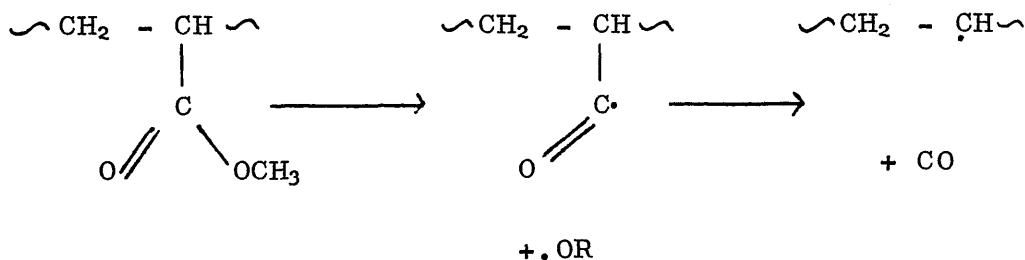
<u>Irradiation Time</u>	<u>HCHO/CH₃ OH</u>	<u>(HCHO + CH₃ OH)/HCOOCH₃</u>
15 min	1.28	1.11
30 '	1.10	1.15
45 '	1.18	1.04
60 '	1.17	1.14
90 '	1.19	1.15
2 hrs	0.89	1.39
3 '	0.94	1.46
4 '	0.79	1.47
5 '	0.87	1.53
6 '	0.75	1.49

... (H) have suggested the following

... the abstraction of OH OH in the thermal

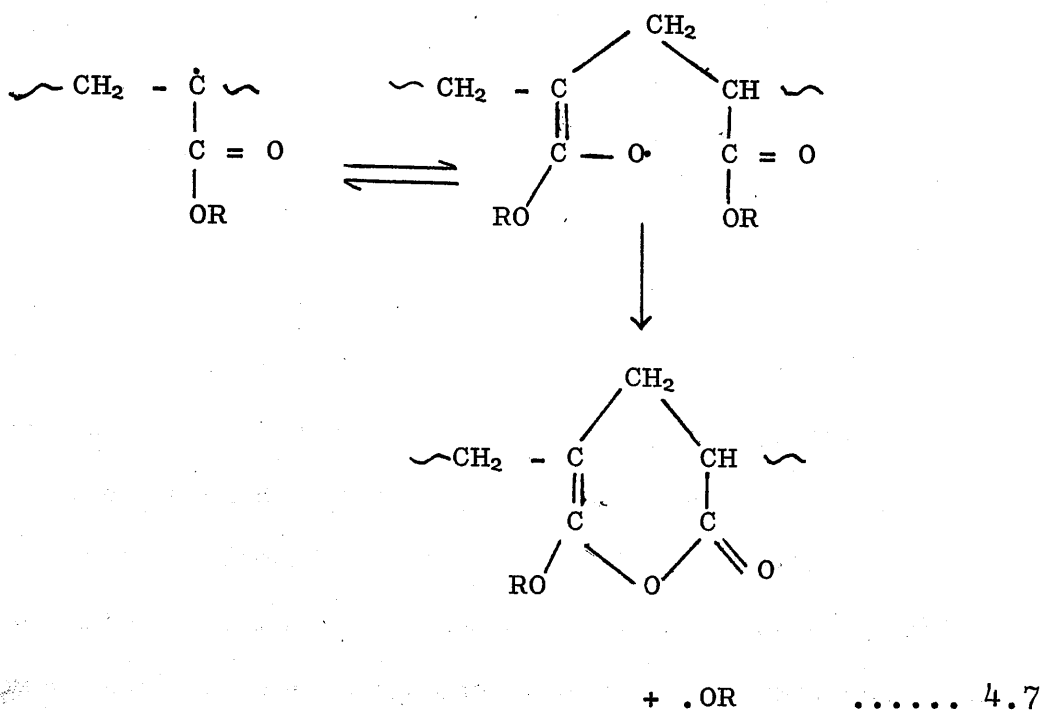
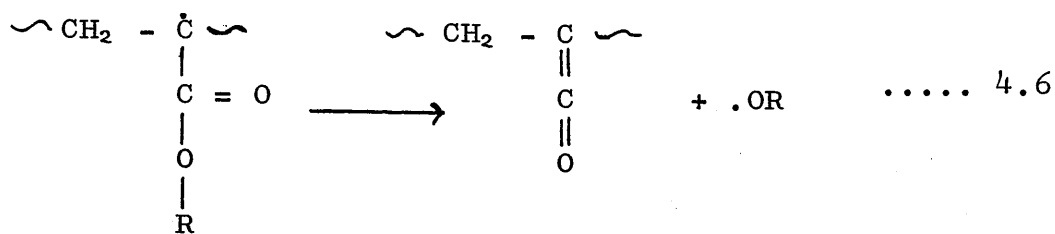
Table 4.4 and fig. 4.3 show that initially the yield of methanol is less than that of formaldehyde but after 90 minutes it exceeds the latter. It appears that there are two reaction mechanisms operative in the formation of the methoxy radical, the activating radiation for one process being more readily filtered out by the polymer.

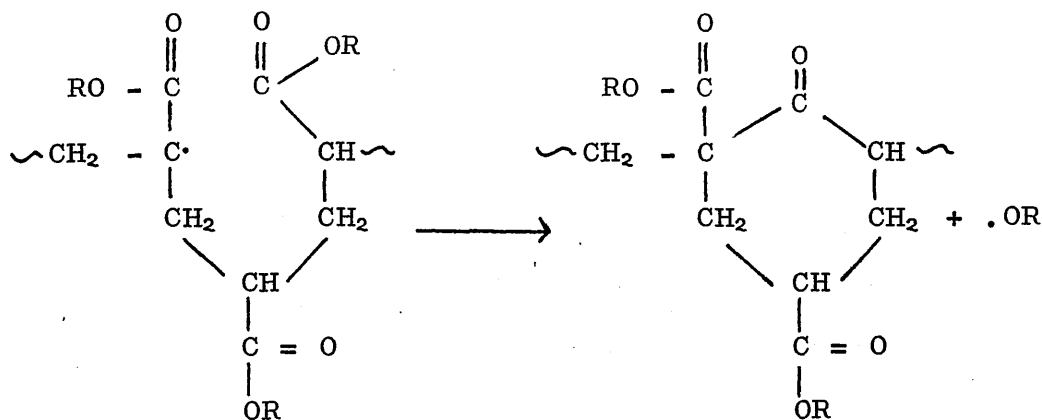
Various mechanisms have been proposed (20,24,58,59) to account for the formation of CH₃OH without the concurrent evolution of CO, which is a product of PMA photolysis(19,20) and which would be expected if CH₃OH formation involved the straightforward decomposition of the ester side group, since ^{the} RCO· macroradical is unstable (Reaction 4.5).



..... 4.5

Cameron and Kane (24) have suggested the following mechanism for the formation of CH₃OH in the thermolysis of PMA, viz.





Reactions 4.7 and 4.8 can also proceed via intermolecular reaction routes. Both these reactions involve either the formation of a ring (intramolecular) or a crosslink (intermolecular). Loss of the tertiary H-atom is proposed as the initiating step. Reaction 4.6 involves the formation of ketene, which reaction was considered unlikely by Cameron and Kane (24) as the infrared spectra in their studies had shown no characteristic ketene absorption around 2160 cm^{-1} . They also discounted it as copolymer studied (60) had suggested that neighbouring rather than isolated ester groups were involved in alcohol formation. Reaction 4.7 would create a structure which would contribute to a broadening of the carbonyl absorption in the infrared spectra. The unsaturated ether structure would also increase absorption around

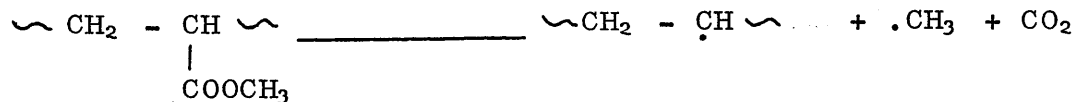
1600 cm^{-1} (61). Cameron and Kane (24) also suggested from the study of molecular models that reaction 4.8 involving radical attack on the carbonyl group and displacement of a methoxy radical in the process, was sterically favoured. The resulting cyclic ketone would contribute to the infrared and ultra-violet spectra of the polymer residue only by broadening the regions of carbonyl absorption. The mechanisms proposed by Cameron and Kane were supported by Grassie et al. (40) from results found in the thermolysis of poly (n-butyl acrylate).

In this study we are unable to detect any broadening of the carbonyl peak, possibly due to the small amount of methanol produced by this mechanism.

4.2.4 Carbon Dioxide Production

The results of figure 4.3 have shown that CO_2 is evolved at a constant rate initially, up to approximately 30 minutes and the rate then decreases. This decrease in the rate of CO_2 formation with time is similar to the decrease found for all other products evolved.

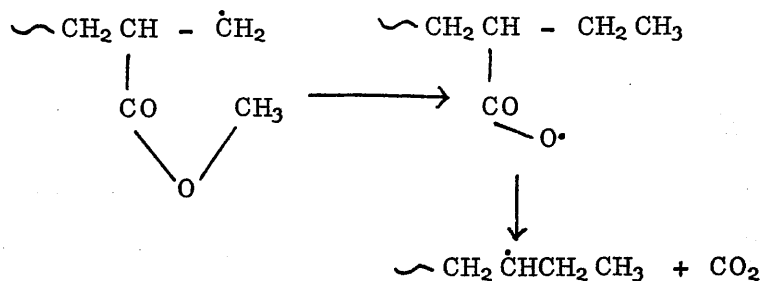
The absence of both methane and CO_2 as products in experiments using glass filtered radiation led Ackerman and McGill (20) to suggest that their formation may be linked, and that they may result from the reaction



However, considerably more CO₂ than CH₄ was evolved, which indicated that an alternative or perhaps a second mechanism must be operative in producing CO₂.

Both CO₂ and CO have been observed in the photolysis of methyl formate (62) and CO₂ was a major product in the methyl radical sensitized decomposition of this ester (63). Our experiments do not prove this route for CO₂ formation.

It is evident from fig. 4.4 that CO₂ production is also temperature and intensity dependent, since it decreases with the increases in the lamp-to-sample distance, while HCOOCH₃ production is unaffected. If CO₂ is a product of photolytic scission of HCOOCH₃, then the production of the latter must be affected. The possibility of CO₂ formation involving the 'back-biting' mechanism suggested by Fox et al (19), cannot be ruled out.



4.3 Molecular Mass Changes

The evaluation of molecular mass changes occurring during the photolysis of polyacrylates is complicated by the simultaneous occurrence of crosslinking and chain scission (19,21,25,51). Jacob and Steele, (25) have shown that theories applied to calculate the degree of crosslinking in the case of poly(ethyl acrylate) were in satisfactory agreement only when used to calculate the crosslinked contents of less than 10^{-5} moles of crosslinked unit per cm^3 .

In the case of systems with high crosslink density it is very difficult to see any molecular mass changes by means of existing methods.

An attempt has been made in this investigation to develop a new sorption technique for following molecular mass changes in such systems. The sorption technique is described in detail in Chapter Two. It was considered important to test the applicability of the technique in the case of poly(methyl acrylate).

Films of PMA 22 μ thick cast on stainless steel supports of area 7.46 cm^2 were irradiated under identical conditions for different time intervals. After exposure, the films were pumped in vacuum for 15 minutes to ensure removal of all volatile products, before the films were soaked in 5% labelled styrene dichloride solution in pet. ether as non-solvent

(b.p. 40°C - 60°C) for two hours.

The formation of crosslinked polymer was followed from the uptake of labelled styrene dichloride, measured by the counting technique described in Chapter Two. The measured count rates are plotted as a function of irradiation time as shown in fig. 2.18 (Chapter Two) and tabulated in table 4.7. The decrease in the count rate with extended irradiation time may be related to the increase in the extent of crosslinking as follows:-

A calibration graph was constructed to show the effect of molecular mass of unirradiated polymer on the count rate as shown in fig. 2.19 (Chapter Two) with data summarised in table 4.8. It is clear from the graph that the count rate decreases considerably with increase in molecular mass for linear polymer molecules. This is due to the smaller tendency of the higher molecular mass polymers to absorb the radioactive solvent.

Molecular mass increases during crosslinking, while it decreases during chain scission. By making the assumption that a similar relationship between count rate and average molecular mass is applicable to the irradiation situation, it is possible to obtain an approximate quantitative measure of extent of crosslinking.

TABLE 4.7: Effect of Irradiation time on count rate of PMA and extent of crosslinking % (based on the assumption that decrease in count rate is proportional to the extent of crosslinking).

Time (min)	Counts/min	Extent of crosslinking %
0	9868	0
15	7900	19.68
30	5625	42.43
45	1750	81.18
60	600	92.68
90	400	94.68
120	200	96.68
150	300	95.68
180	250	96.18

TABLE 4.8: Effect of molecular mass on the count rate

<u>Molecular Mass</u> (10^4)	<u>Counts/min</u>
42.5	9,001
35.2	9,867
29.7	11,823, 13,649
16.0	13,301, 14,249
7.1	14,622
6.51	15,171
5.11	16,858

The data of fig. 2.18 may on this basis be presented in a form which shows the increase in crosslinking with irradiation time as shown in fig 4.5, results are summarised in table 4.7. The percentage crosslinked material is calculated as:-

$$\% \text{ crosslinked} = \frac{\text{decrease in count rate of irradiated sample due to crosslinking}}{\text{count rate of the unirradiated sample}}$$

Ackerman and McGill (21) calculated the amount of crosslinked polymer formed upon irradiation from the weight of the insoluble material for polyacrylates (PMA, PEA, PBA) and found an increase in the amount of % crosslinked material as a function of irradiation time. Jacob and Steele (25) have shown that the vacuum photolysis of PEA leads to a decrease in the swelling ratio of the polymer as well as to a decrease in viscosity of the soluble fraction. Fox et al (19) have noted a similar effect for PMA.

Subambient TVA studies showed a high boiling liquid peak (sixth peak) most probably due to short chain fragments. The formation of chain fragments can be attributed to random scission of polymer molecules by a free radical chain reaction. Cameron and Kane (24) explained the maximum in the rate of thermal decomposition of PMA in terms of such a mechanism leading to the accumulation of chain fragments.

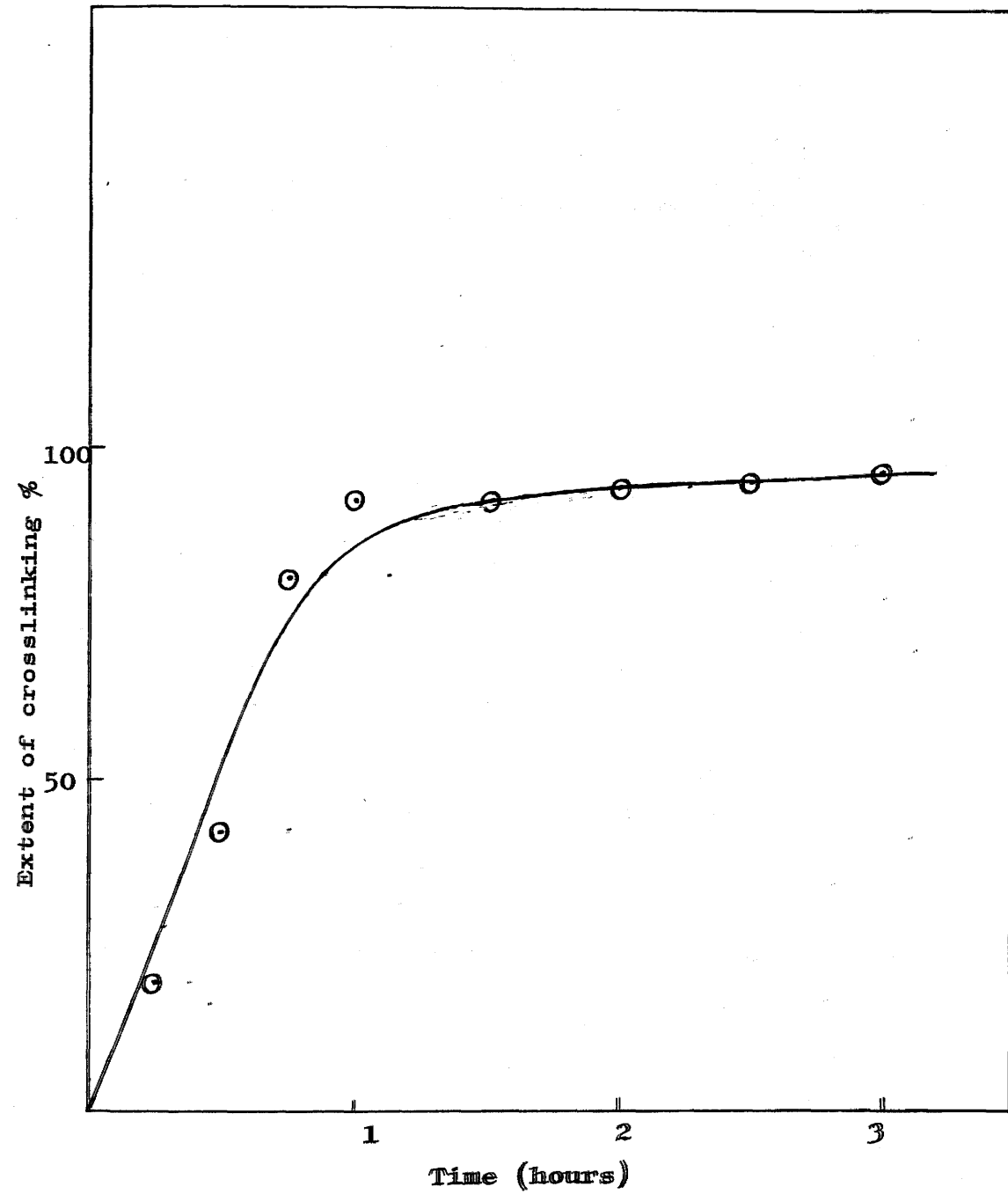
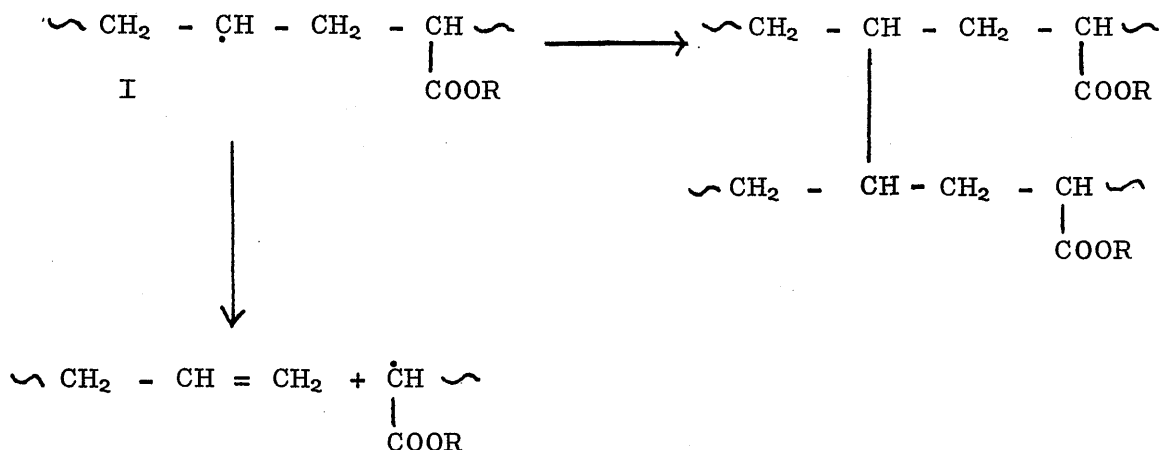


Fig.4.5: Relationship between irradiation time and extent of crosslinking %

Taking all the above observations into consideration, the following reaction sequences are proposed as the most probable mechanism involved in scission and crosslinking.

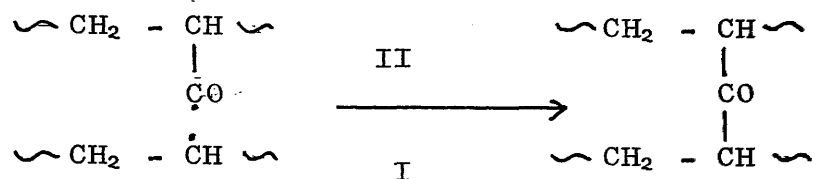


It is also possible that the original polymer molecule abstracts a tertiary hydrogen from another polymer molecule and transfers the radical site from one molecule to another.

Electron spin resonance (ESR) investigations (30) to identify the radicals formed on radiolysis of polyacrylates have shown the presence of the following radicals.



Ackerman and McGill argued that the radical I is a common precursor for scission and crosslinking and suggested the formation of crosslinks by the combination of I with the radical II as follows.



This seems unlikely because the carbonyl radical is very unstable (64) and will decompose immediately to give carbon monoxide.

4.4 Spectral Changes Occurring During Degradation

4.4.1 Ultra-Violet Region

The absorbance of poly(methyl acrylate) film in the ultra-violet region was measured before and after irradiation. Significant changes were observed in the polymer. The spectra in fig.4.6 of PMA film after three successive exposure periods show that a progressive increase in absorption occurs. No distinct peaks were observed, but it can be reasonably assumed that new chromophores are being formed during degradation.

After exposure for long periods of irradiation, the polymer film acquires a yellow tint. This colouration is due to an increase in absorption in the blue-violet

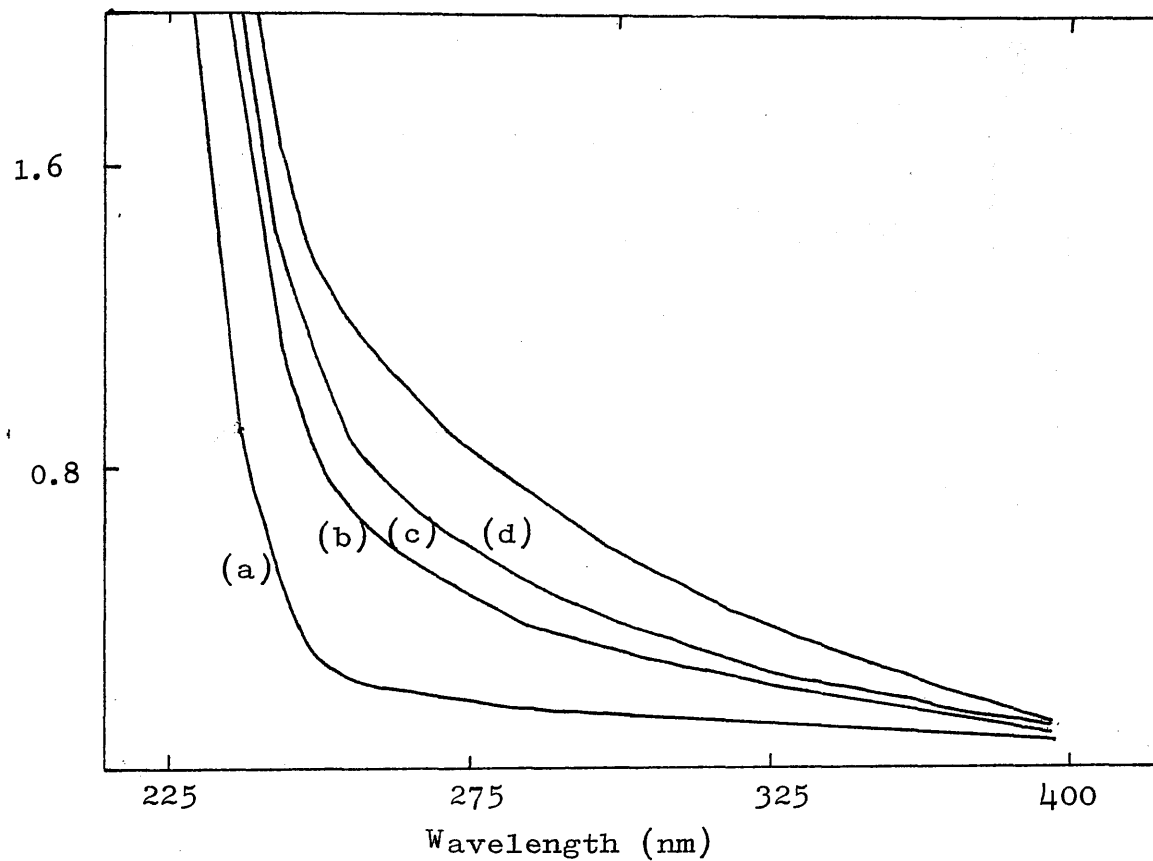


Fig.4.6: Ultra-violet absorption spectrum of PMA film cast from methylene chloride solution and irradiated under the conditions described in Chapter Two.

- (a) Prior to degradation
- (b) Exposed for 3 hours.
- (c) Exposed for 6 hours.
- (d) Exposed for 12 hours.

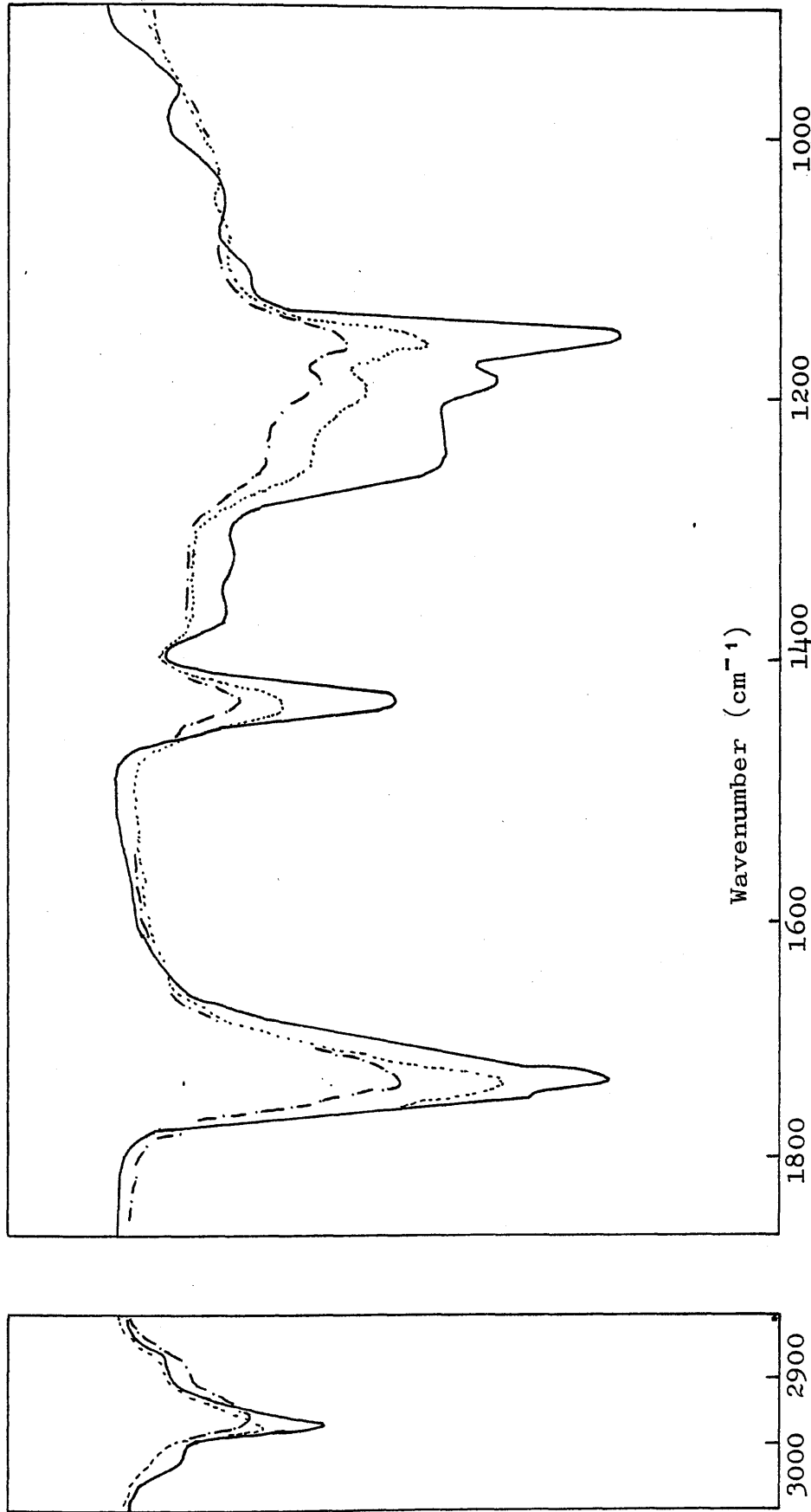


Fig.4.7: IR absorption spectra of; -PMA, PMA photodegraded for 6 hours and ---- PMA photodegraded for 12 hours.

region of the spectrum which is a 'tail' of the absorption in the ultra-violet.

Colour in organic compounds is usually associated with unsaturated groups such as $-C = C-$, $-C = O$, $-C = N$ etc., Approximately six groupings in conjugation are sufficient for colouration in aliphatic systems.

4.4.2 Infrared Region

Spectra obtained from irradiated PMA films, cast from methylene chloride solution as described in chapter two, are shown in fig. 4.7, together with the spectrum of the original polymer. After irradiation for six hours and twelve hours, the C-H bond stretching at 2980 cm^{-1} and carbonyl bond stretching at 1755 cm^{-1} decrease markedly. Similarly the intensities of the other bonds at 1465 cm^{-1} , 1190 cm^{-1} , 1160 cm^{-1} and 820 cm^{-1} decrease gradually. Thus photodegradation does not yield new bands.

CHAPTER FIVE

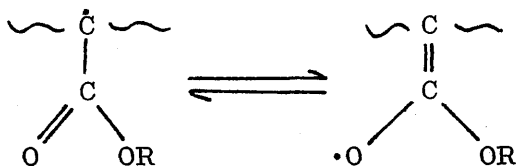
PHOTODEGRADATION OF POLY(2-ETHYLHEXYL ACRYLATE)

5.1 Introduction

2-Ethylhexyl acrylate is used as a viscosity reducer in some photocuring systems, hence it is of interest to study the effect of ultra-violet radiations on films of the homopolymer.

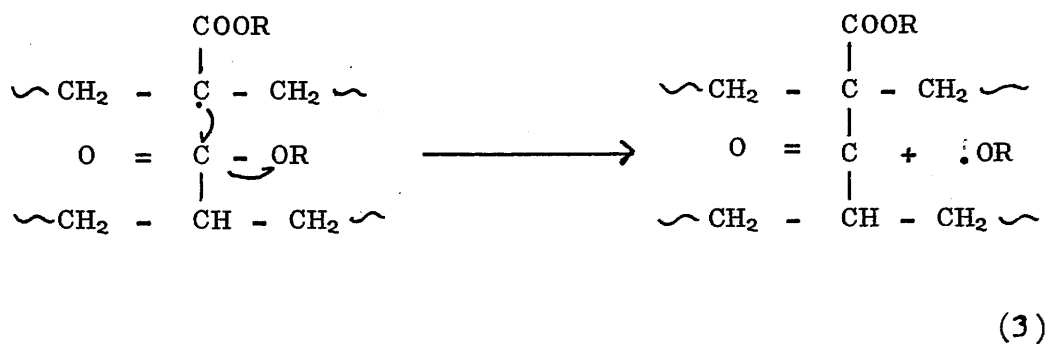
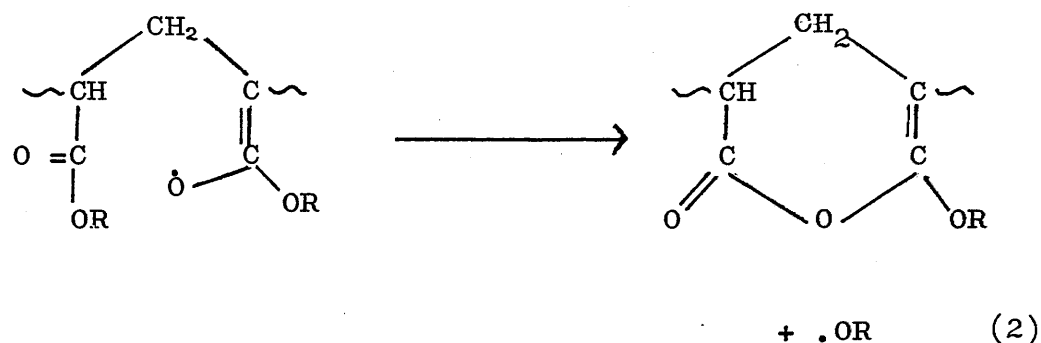
Morimoto and Suzuki (51) investigated the molecular mass changes of the irradiated polymer by means of gel permeation chromatography (GPC), while Grassie et al(58) reported on the thermal degradation of P(2EHA). Carbon dioxide, 2-ethyl-1-hexene and 2-ethyl-1-hexanol were the major volatile products. Monomer, 2-ethylhexyl methacrylate and short chain fragments were also found as a result of thermal degradation.

A free radical mechanism has been suggested to explain the product formation, and all the major decomposition reactions are thought to be initiated by the radical I



I

Formation of alcohol is thought to be through similar reaction mechanisms as proposed by Cameron and Kane (24) for the production of methoxy radical in PMA. Two of these are represented in reactions (2) and (3)



The suggested mechanisms (24) are supported by Grassie et al. (58) who used infrared spectral changes in the polymer to monitor its thermal degradation behaviour.

A study of the mechanism of photodegradation P(2-EHA) requires a knowledge of the products of reaction and molecular mass changes. Accordingly, polymer in film form was degraded by ultra-violet

radiation and products were characterised by spectroscopic techniques following separation by the procedure described in Chapter Two. The degraded films were examined by infrared and ultra-violet spectroscopy in order to determine structural changes.

5.2 Product Analysis

The photolysis apparatus and conditions and the techniques of product collection, separation and identification have been described in detail in previous chapters. As before, films were prepared from solutions using methylene chloride as film casting solvent, residual solvent being removed by treatment in a vacuum oven. The products were separated according to their volatility at liquid nitrogen temperature under low pressure conditions as described in Chapter Four. Typical traces obtained from exposure of one hour and two hours respectively are illustrated in figs. 5.1 and 5.2.

In both cases six peaks can be distinguished corresponding to the condensed products. Each peak in the trace can be assigned to a product by consulting the data in table 5.1. As the difference between the distillation maxima of 2-ethyl-1-hexene and 3 methylheptane is small, these two products could not be separated, and distil simultaneously at peak (2).

TABLE 5.1: Distillation rate maxima of condensable volatiles from P(2-EHA)

<u>Product</u>	<u>Distillation Rate Maximum</u> (<u>± 10° C</u>)
Carbon Dioxide	-140°C
3-Methylheptane	-66°C
2-Ethyl-1-Hexene	-63°C
2-Ethyl-1-Hexanal	-47°C
2-Ethylhexyl Formate	-31°C
2-Ethyl-1-Hexanol	-18°C

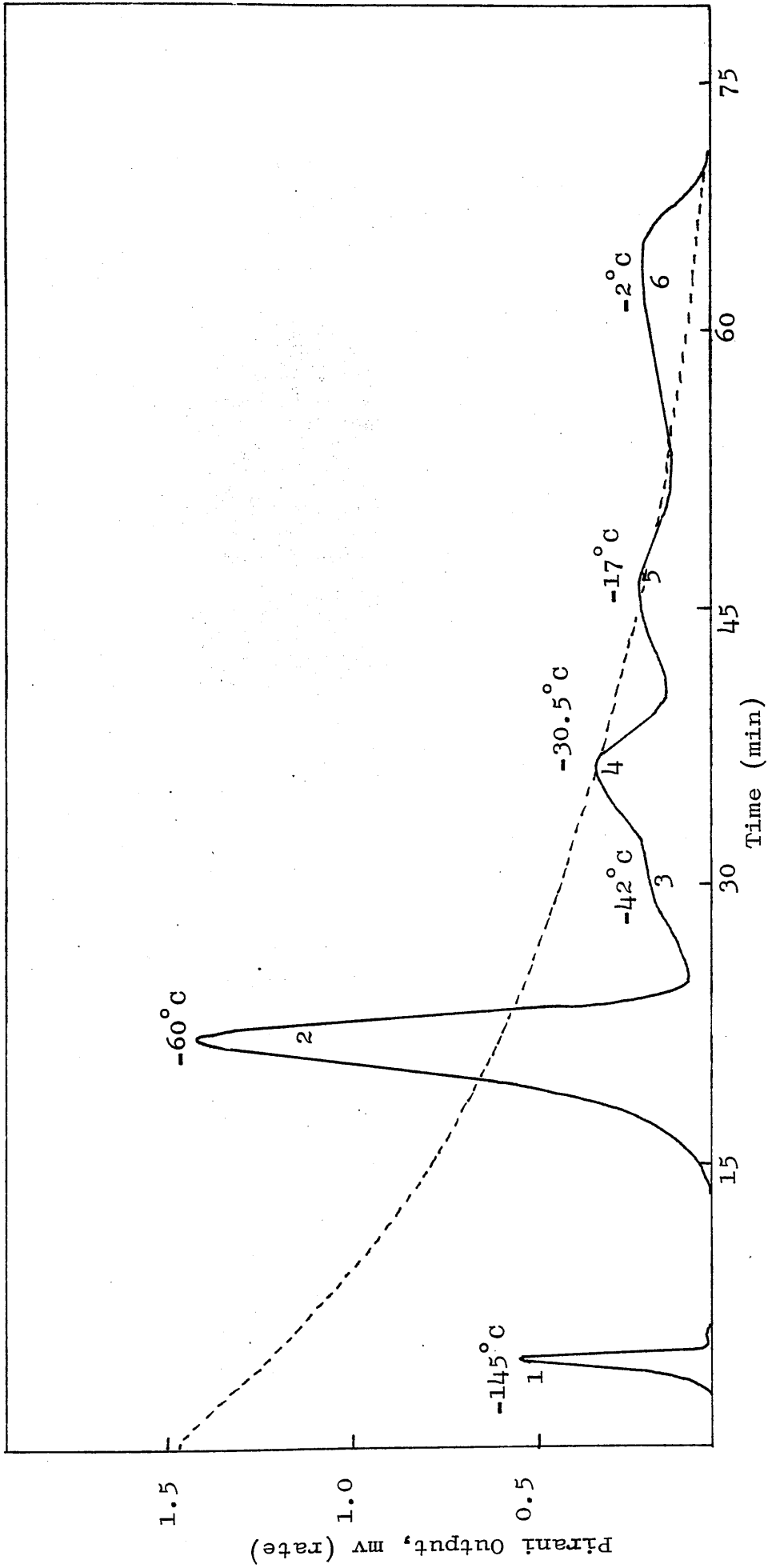


Fig. 5.1: Subambient TVA curve for photodegradation products of P(2-EHA) (one hour photodegradation of 23.5 μ film)

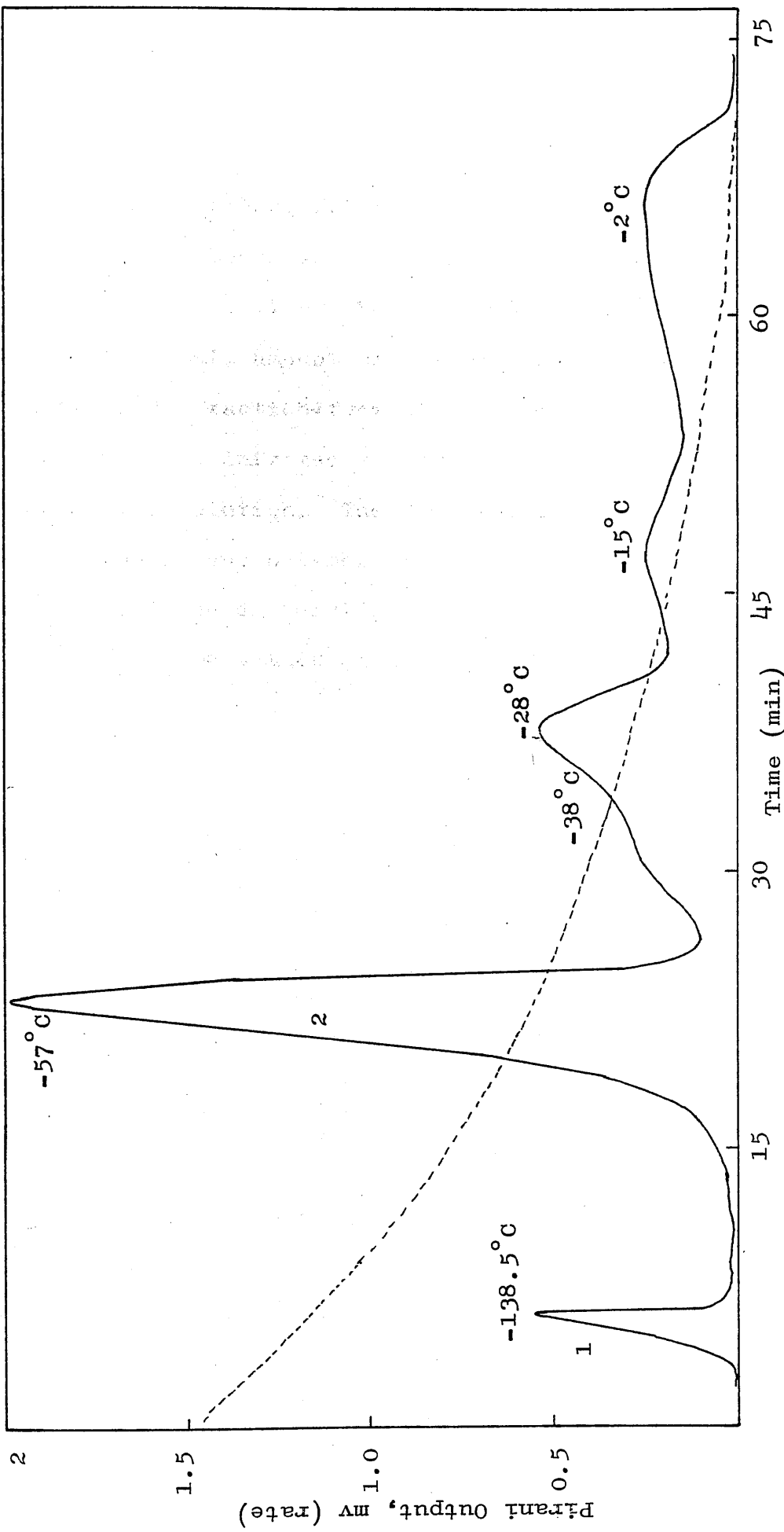


Fig. 5.2.2: Subambient TVA curve for photodegradation products of P(2-EHA) (two hours photodegradation of $23.5\ \mu$ film)

Products were also identified by the conventional methods, IR spectroscopy and GLC, as shown in table 5.2.

As the sixth subambient TVA peak is due to a very high boiling fraction, most probably some short chain fragments such as dimer or trimer, it was difficult to collect the sample for IR spectroscopy. Owing to the small amount of material available, the chain fragment fractions from all the degradations were combined and the infrared spectrum was run in carbon tetrachloride solution. The spectrum was similar to those of the parent polymer with the following minor differences. The carbonyl peak at 1730 cm^{-1} and the peaks in the $1500 - 1000\text{ cm}^{-1}$ region show a general broadening. Two shoulders at about 1755 cm^{-1} and 1715 cm^{-1} appear on the carbonyl peak.

5.2.1 Liquid Products Analysis by Gas Liquid Chromatography (GLC)

GLC was performed on liquid volatiles from photodegradation of P(2-EHA) sample in the form of a film, the products being collected and analyzed as described in Chapter Two, using methyl acetate as a solvent.

A typical GLC trace is shown in fig. 5.3. Altogether there are five peaks: peak A is due to solvent methyl acetate and peak B to ethyl acetate present as impurity in the solvent, and therefore these materials are not

TABLE 5.2

<u>Subambient TVA Rate Maximum</u>	<u>Infrared Absorptions</u>	<u>GLC Analysis Retention Time</u>	<u>Product</u>
-138.5°C	2300, 670cm ⁻¹	-	Carbon Dioxide
-57°C	2960 - 2860, 1460, 1380 cm ⁻¹	2 min 12 sec	3-Methylheptane
-57°C	3080, 2970-2860, 1642, 1455, 1372, 890 cm ⁻¹	2 min 12 sec	2-Methyl-1-1-Hexene
-38°C	3020, 2980-2860, 2720, 1740, 1460, 1380 cm ⁻¹	6 min 42 sec	2-Ethyl-1-1-Hexanal
-28°C	2960-2860, 1730, 1465, 1380, 1175 cm ⁻¹	11 min. 18 sec	2-Ethylhexyl Formate
-15°C	3642, 2960-2860, 1465, 1380, 1035 cm ⁻¹	15 min	2-Ethyl-1-1-Hexanol
-2°C	2960-2860, 1730	-	Short chain fragments

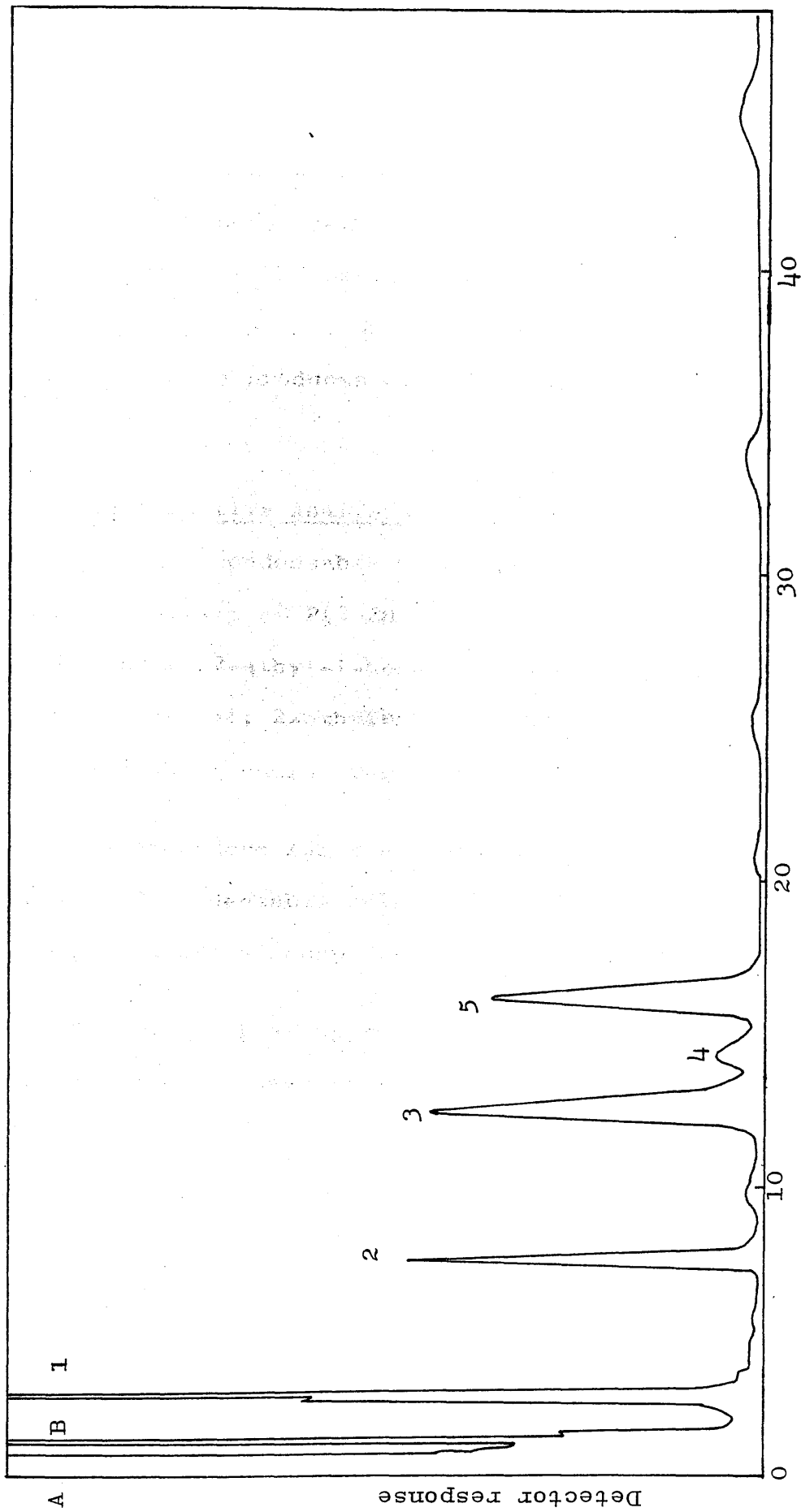


Fig. 5.3: GLC analysis of liquid degradation products of P(2-EHA), column temperature 80°C, Nitrogen Carrier gas, 0.33m³/sec.

110.

accounted as degradation products. The rest of the peaks were assigned by injecting reference compounds and then comparing their retention times with those of the unknown degradation products. Only a minor peak is unassigned. 2-Ethyl-1-hexene and 3-methylheptane could not be completely separated even by GLC, the latter appears as a shoulder in peak no.1. Apparently these products are present in approximately 1:2 ratio.

5.2.1 Quantitative Analysis

The main condensable volatile products of vacuum photolysis of P(2-EHA) were identified as carbon dioxide, 2-ethyl-1-hexene, 3-methylheptane, 2-ethyl-1-hexanal, 2-ethylhexyl formate, 2-ethyl-1-hexanol along with short chain fragments.

The procedure for the stepwise quantitative analysis of condensable volatiles is described in preceding chapters (Chapters Two and Four).

Polymer samples approximately 23.5 μ thick and 7.46 cm² in area, cast from methylene chloride solution, were degraded under identical conditions for various intervals of time and from the peak area on the subambient TVA trace, the mole per cent (based on no. of moles of monomer originally present) of each product was calculated from the corresponding calibration graphs (fig. 2.12 - 2.15).

Results are given in table 5.3. Mole per cent yield of each product is plotted against the irradiation time ⁱⁿ figs. 5.4 (a) and (b). It is seen from the plot that the rate of evolution of volatiles remains constant for the early stages of reaction (first 30 minutes) but decreases with further increase in irradiation time. It is not possible to calculate the mole % yield in the case of short chain fragments, hence peak area (arbitrary units) is plotted against the irradiation time as seen in fig. 5.5. The rate of formation of short chain fragments with irradiation time shows a similar trend as for the other degradation products.

5.3 Dependence of Product Evolution on Film Thickness

Samples of P(2-EHA) as films cast from methylene dichloride solution were degraded under identical conditions and product evolution was measured in the normal manner. Samples with different film thickness but the same area were examined. In fig. 5.6, the mole percent yield is plotted as a function of film thickness and the data are summarised in table 5.4.

It is apparent that after an initial dependence of rate of product formation on sample thickness (up to 23.5μ for 20 mg sample size), the film thickness plays little part in determining the quantity of product formation in a given time.

A similar effect was observed in the case of

TABLE 5.3: Effect of irradiation time on the mole % yield per monomer unit of P(2-EHA)

Time (mins)	Carbon Dioxide	2-Ethyl-1-1-Hexene	3-Methyl heptane	2-Ethyl-1-1-Hexanal	2-Ethyl-1-1-Hexanol	2-Ethyl hexyl Formate
15	0.39	0.44	0.22	0.129	0.212	0.407
30	0.71	0.49	0.24	0.28	0.325	0.46
45	1.15	0.89	0.445	0.379	0.46	0.71
60	1.50	1.148	0.574	0.43	0.61	0.805
120	2.31	1.80	0.9	0.805	0.95	1.48
180	2.77	2.05	1.03	0.916	1.32	1.71
240	3.1	2.27	1.13	1.01	1.37	1.93
300	3.47	2.45	1.22	0.99	1.50	1.98
360	3.70	2.61	1.30	1.10	1.57	2.01

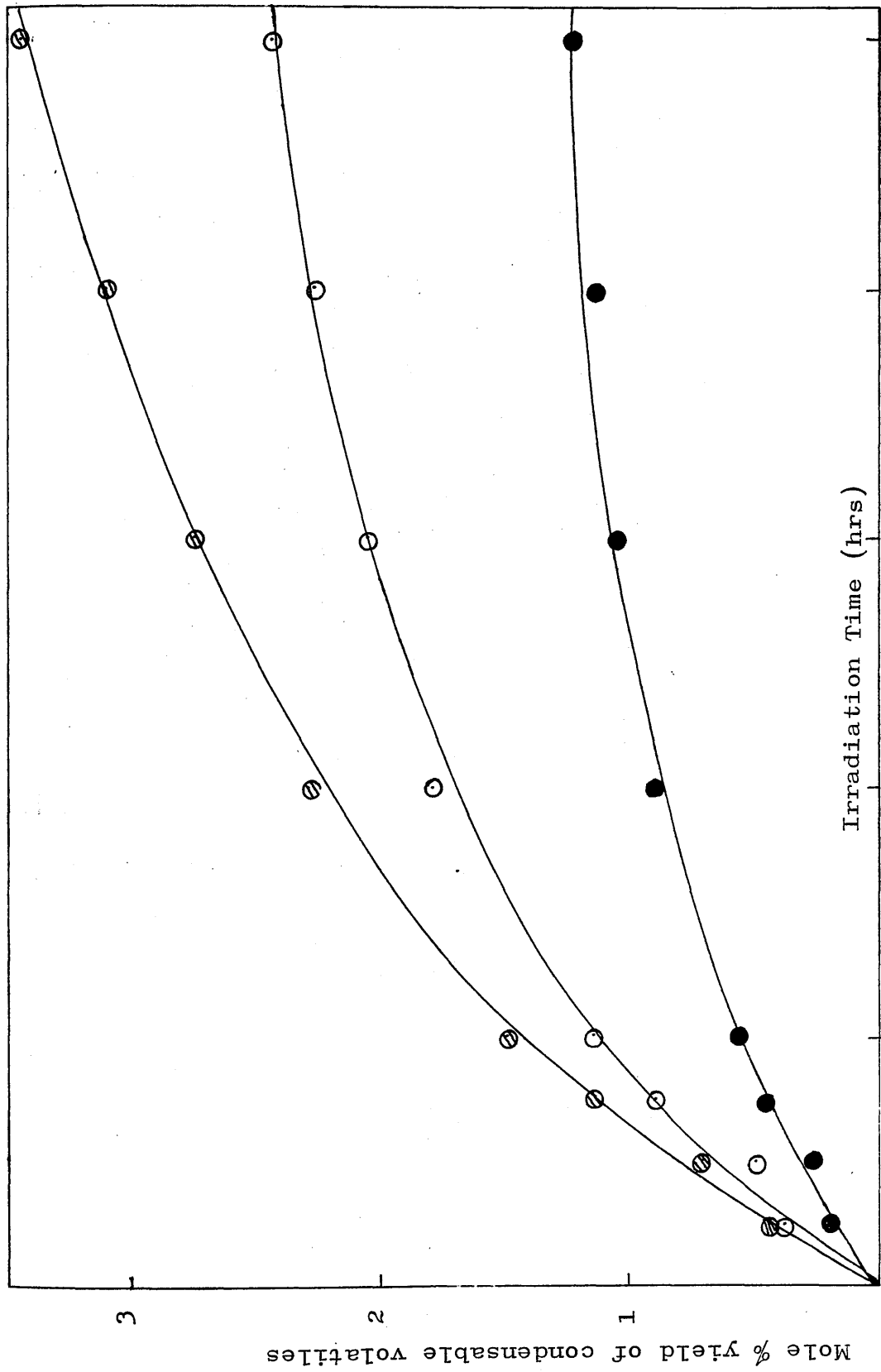


Fig. 5.4(a): Effect of irradiation time on the condensable volatile products from P(2-EHA)

○ 2-ethyl-1-1-hexene, ● 3-methylheptane, ⊘ carbon dioxide

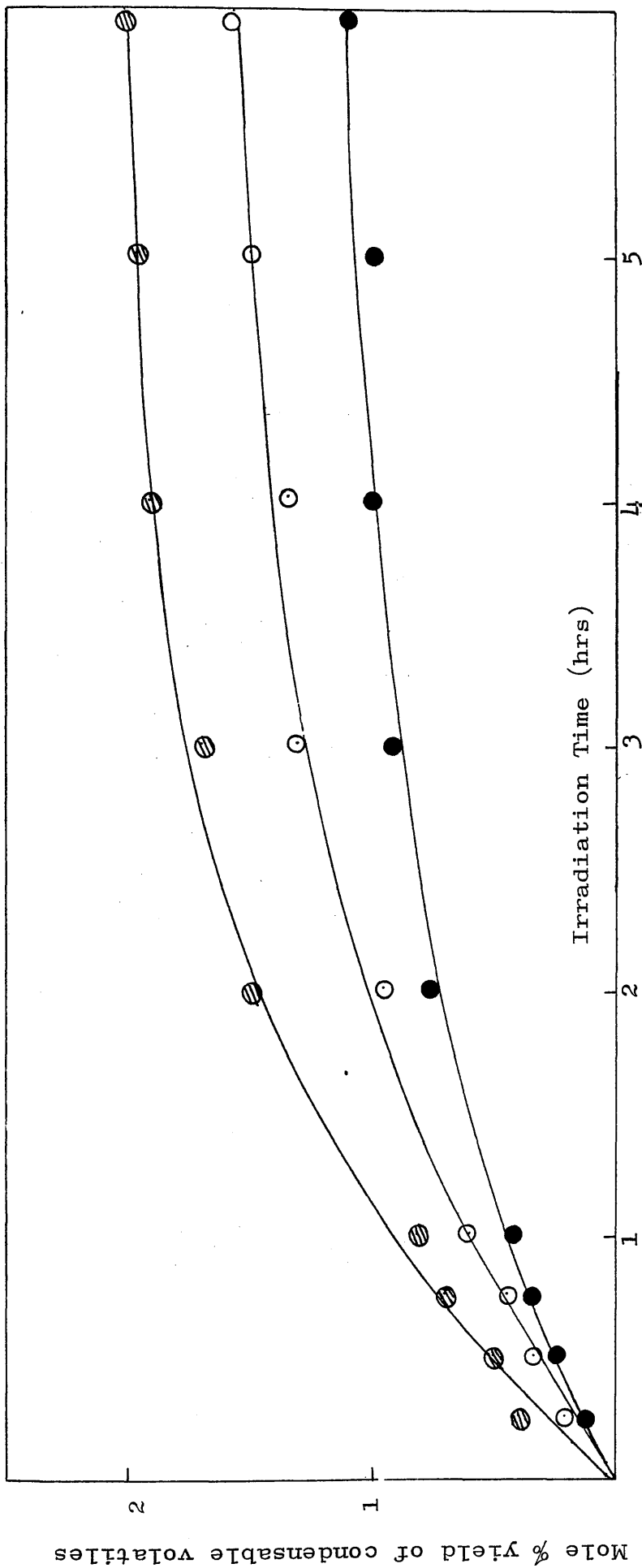


Fig. 5.4(b): Effect of irradiation time on the condensable volatile products from P(2-EHA)

● 2-ethyl-1-hexanol, ○ 2-ethyl-1-hexanal, ⊗ 2-ethylhexyl formate

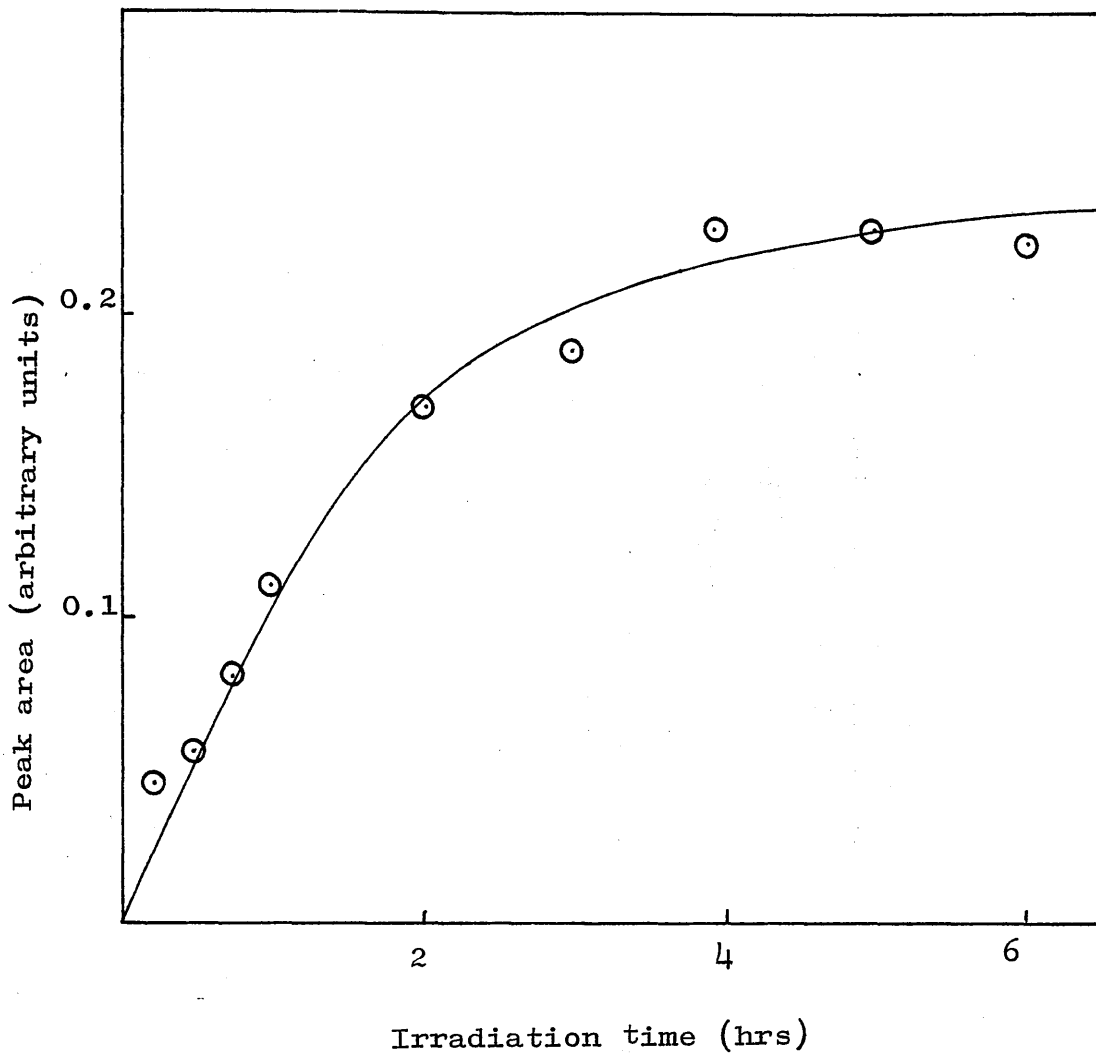


Fig. 5.5: Effect of irradiation time on the production of short chain fragments from P(2-EHA).

TABLE 5.4: Effect of film thickness on the mole % yield per monomer unit of P(2-EHA).

Film Thickness [μ]	Carbon Dioxide	2-Ethyl-1-1- Hexene	3-Methyl- heptane	3-Ethyl-1-1- Hexanal	2-Ethyl-1-1- Hexanol	2-Ethylhexyl formate
8.69	1.29	1.19	0.59	0.46	0.42	0.89
11.75	1.87	1.28	0.64	0.59	0.70	1.09
17.62	2.19	1.54	0.77	0.67	0.76	1.17
23.50	2.31	1.80	0.90	0.805	0.95	1.48
38.77	3.1	1.87	0.935	0.91	1.21	1.65
47.0	2.99	1.99	0.99	0.85	1.54	1.92
60.5	3.30	2.1	1.05	0.98	1.48	1.86
87.0	3.25	2.3	1.15	1.12	1.62	1.98

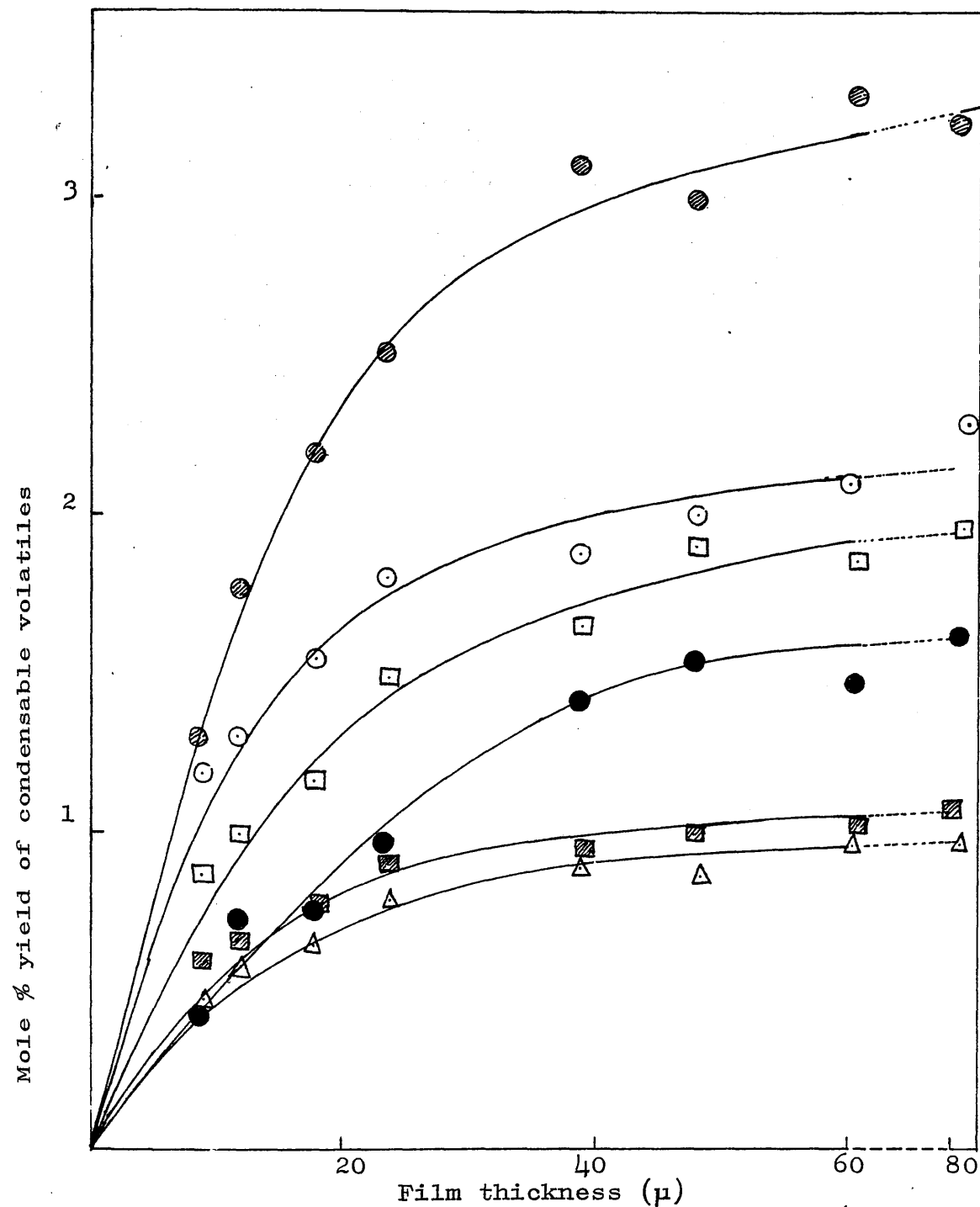


Fig.5.6: Effect of film thickness on the mole % yield of condensable volatiles from poly(2-ethylhexyl acrylate). ● carbon dioxide, ○ 2-ethyl-1-hexene, □ 2-ethylhexyl formate, ● 2-ethyl-1-hexanol, ▨ 3-methylheptane, △ 2-ethyl-1-hexanal

short chain fragments, where it is difficult to determine the mole % yield. In this case peak area (arbitrary units) is plotted against film thickness (fig. 5.7).

5.4 Molecular Mass Changes

Polyacrylates undergo extensive crosslinking as well as chain scission during thermal and photo-degradation.

Grassie et al(58) observed that during thermal degradation of polyacrylates, crosslinking occurs in the case of the ethyl, propyl and butyl esters, which become insoluble, and may occur to some extent in the 2-ethylhexyl ester, although scission predominates since the polymer remains soluble. Insolubility develops faster in the lower homologs, which was explained as probably due to a steric effect, since the bulky ester groups should be expected to inhibit intermolecular reactions.

Morimoto and Suzuki (51) irradiated polyacrylates using a low pressure mercury lamp in presence of air and followed molecular mass changes of the irradiated polymers by gel permeation chromatography (GPC). It was found that both crosslinking and chain scission take place in P(2-EHA).

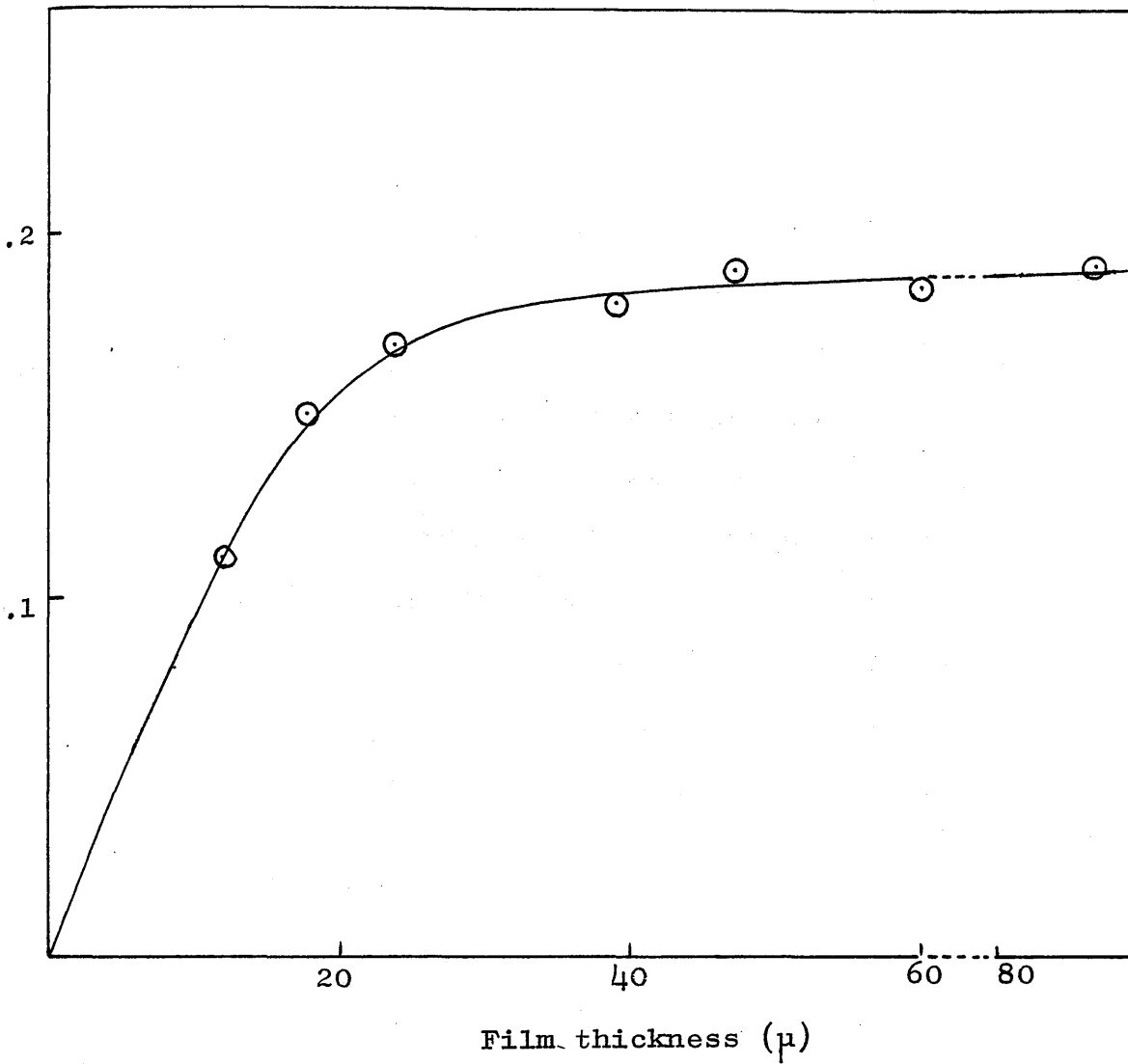


Fig. 5.7: Effect of film thickness on the production of short chain fragments from P(2-EHA).

It is important to examine the effect of ultra-violet radiation on the rate of crosslinking of P(2-EHA) by the new sorption technique described in Chapter Two.

Samples of P(2EHA) film 23.5μ thick were irradiated for different intervals of time under identical conditions. These polymer films were cast on special stainless steel supports of area 7.46 cm^2 as described previously (Chapter Three). After each exposure the uptake of the labelled styrene dichloride was determined by sorption and counting techniques described in Chapter Two. The decrease in the uptake of styrene dichloride indicated by a decrease in count rate, is a measure of the formation of crosslinked polymer. The measured count rates are plotted as a function of irradiation time in fig. 5.8 and data are summarised in table 5.5.

It was shown in case of PMA, in Chapter Four, that in this sorption procedure, the count rate is inversely proportional to the molecular mass of linear polymer and a similar relationship was assumed to be applicable to the irradiation conditions, so that count rate could be related to extent of crosslinking.

On a similar basis, the data derived from graph 5.8 for P(2-EHA) may be presented in a form which shows the increase in crosslinking with irradiation time, as shown in fig. 5.9, table 5.5. By comparing

TABLE 5.5: Effect of irradiation time on count rate of P(2-EHA) and extent of crosslinking % (based on the assumption that decrease in count rate is proportional to the extent of crosslinking).

<u>Time (hrs)</u>	<u>counts/min</u>	<u>Extent of Crosslinking %</u>
0	8453	0
0.5	7450	11.86
1	7361	12.91
2	6379	25.54
3	6285	25.65
4	4639	45.13
5	4621	45.34
7	4248	49.75
8	3198	62.17
10	1771	79.05
12	1265	85.04
15	939	88.9
20	666	92.13
24	513	93.94

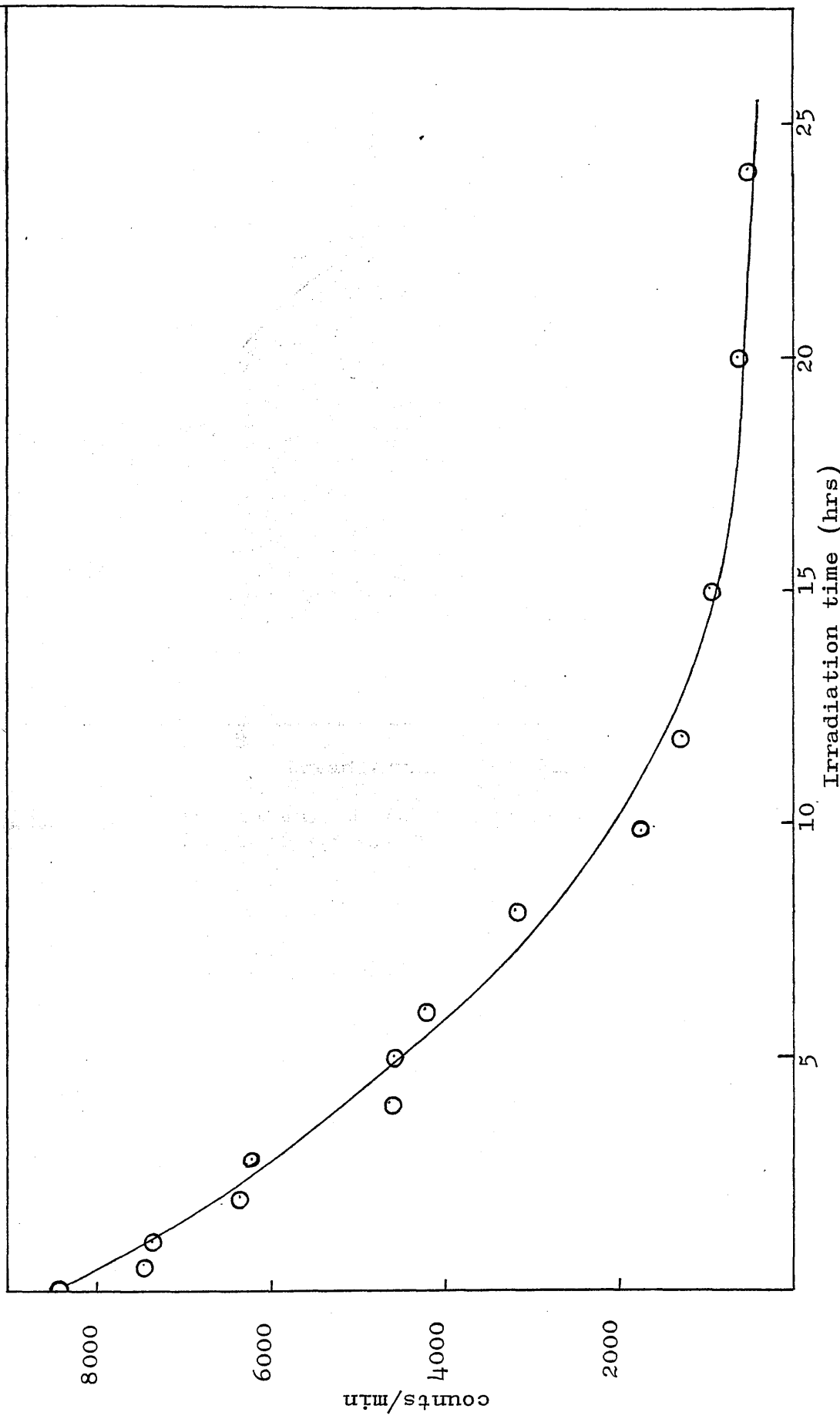


Fig. 5.8: Relationship between irradiation time and count rate for P(2-EHA)

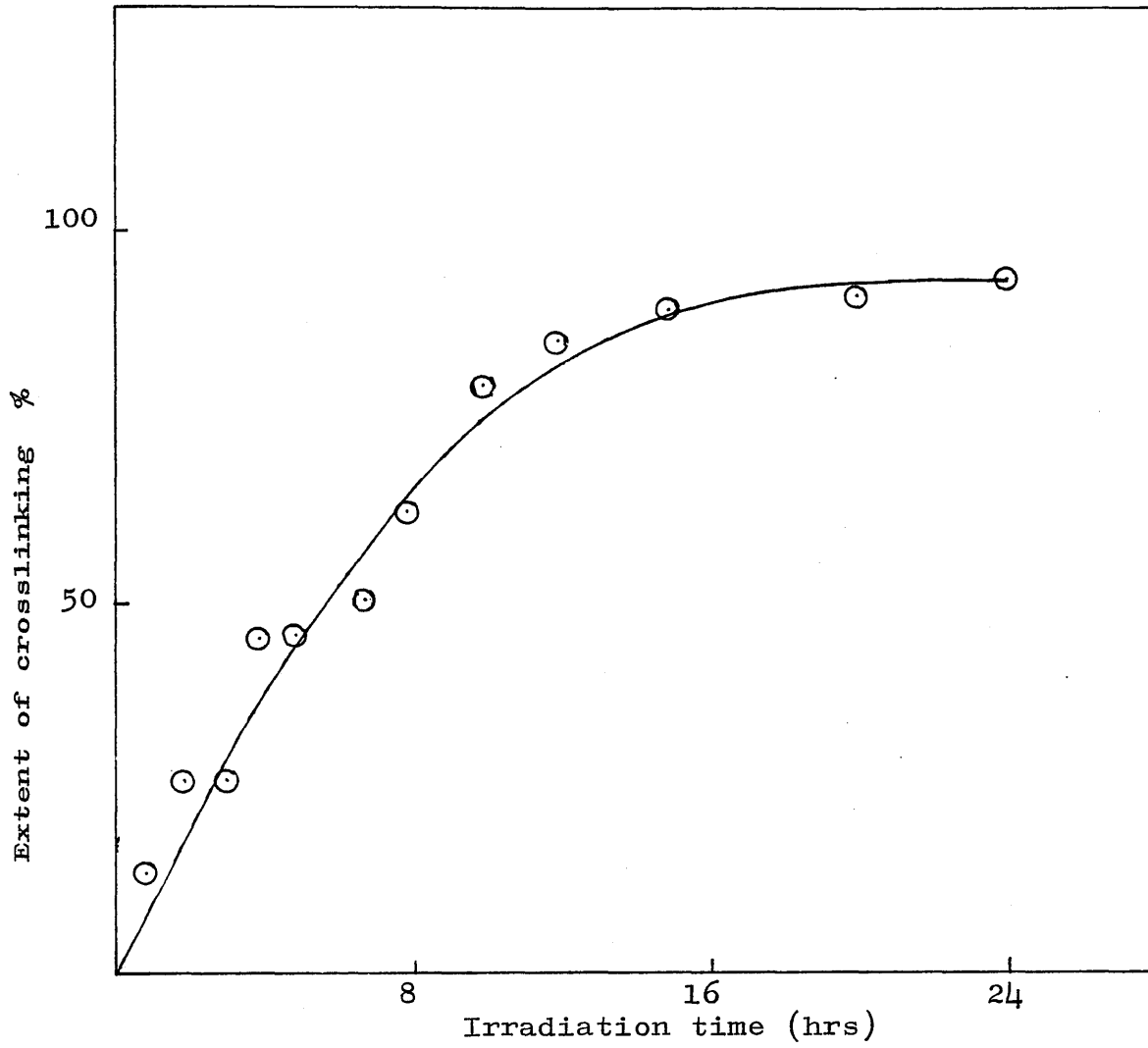


Fig.5.9: Relationship between irradiation time and extent of crosslinking %

127.

these results with those for PMA (Chapter 4), crosslinking in P(2-EHA) seems to occur to a lesser extent than in the former. This is probably a steric effect since bulky ester groups should be expected to inhibit intermolecular reactions.

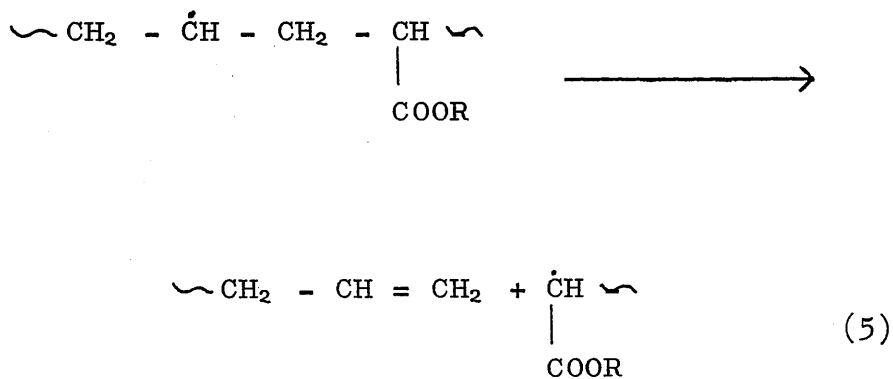
Subambient TVA studies show a considerable amount of short chain fraction present in the degradation products, indicating a considerable degree of chain transfer. Cameron and Kane(24,65) suggested that intramolecular transfer predominates in the thermal degradation of PMA since this favours the production of small chain fragments. They described as 'unbuttoning' the process whereby a radical moves along the polymer chain eliminating small polymer molecules in contrast to 'unzipping' in which monomer units are progressively eliminated as in the degradation of PMMA. The main feature of interest in the 'unbuttoning' reaction as it occurs in the present work is that it increases as the size of the alkyl group increases. This is probably because as the length of the alkyl group increases, the polymer becomes less polar, so that attractive forces between neighbouring molecules, or segments of the same molecule, become smaller.

The combination and disproportionation reactions leading to crosslinking and scission have been proposed for the mechanism of thermal and photodegradations of polyacrylates.

The irradiation results primarily in a scission of the ester side chains from the polymer backbone. Crosslinking results from the combination of two polymer radicals formed in this process as follows:



The polymer radicals can also decompose according to equation (5), which results in main chain scission.



The polyacrylates have a tertiary hydrogen atom on every alternate carbon atom along the chain. This provides a reactive site for hydrogen abstraction processes, hence transfer of radical site from one molecule to another could occur.

5.5 Spectral Changes During Photodegradation

5.5.1 Infrared Region

Fig. 5.10 (a) illustrates the infrared region of primary interest in a P(2-EHA) film cast from methylene chloride as stated in the experimental section. After four hours of irradiation, the infrared spectrum shows an overall decrease in the intensity of the bands, fig. 5.10 (b). No new bands appear.

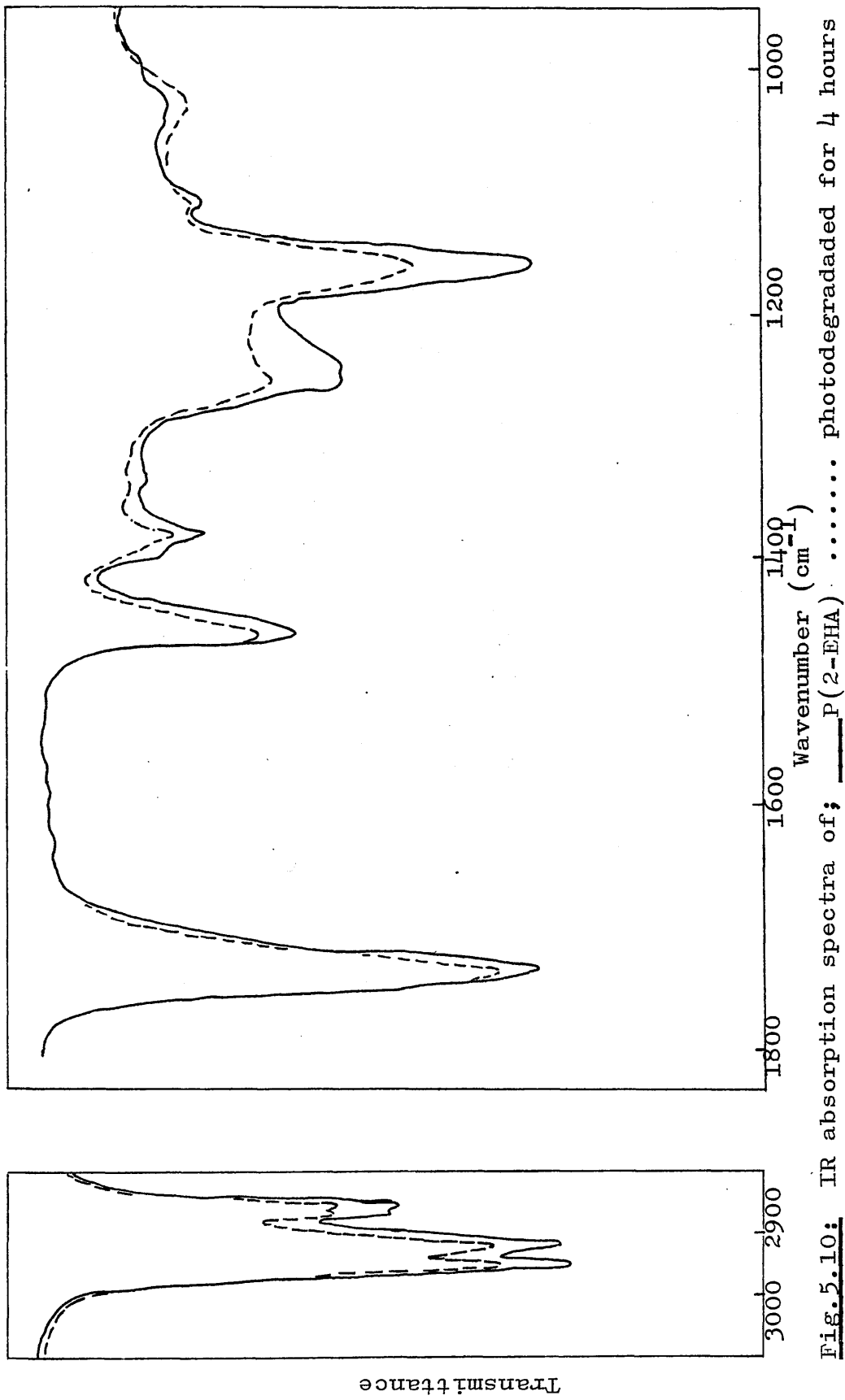
5.5.2 Ultra-Violet Region

The ultra-violet spectra of P(2-EHA) films were measured before and after irradiation as shown in fig. 5.11. The spectra after successive exposures show a gradual increase in absorption during degradation, which occurs in the region usually associated with conjugated double bonds.

Yellowing of the films may be due to conjugated double bond formation.

5.6 Mechanism of Degradation

In thick films of polyacrylates a very weak absorption band, generally associated with the $n \rightarrow \pi^*$ transition in the carbonyl, can be seen around 275 nm, and it is commonly accepted that the decomposition of methacrylates and acrylates is due to energy absorbed in this broad band.



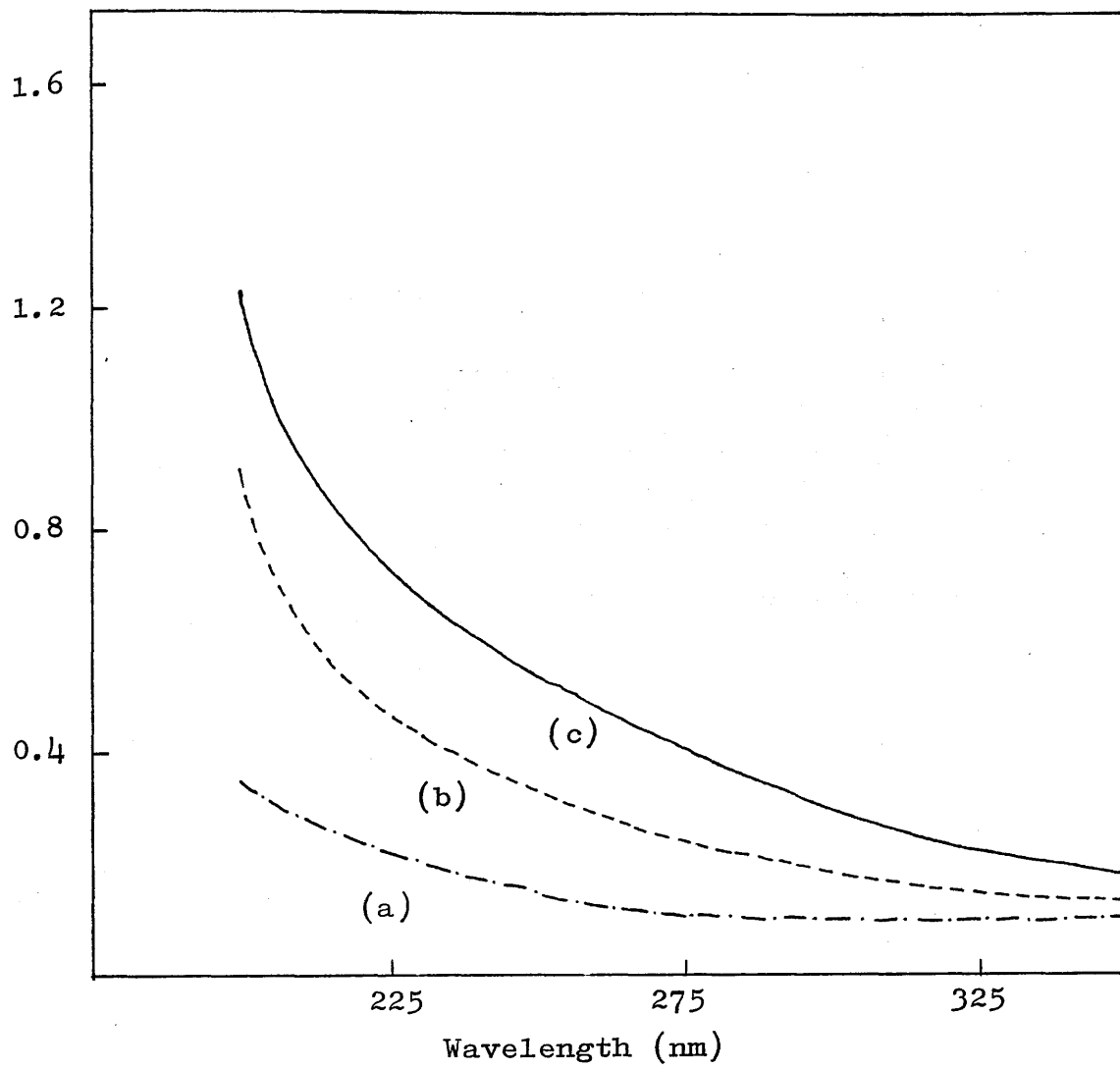
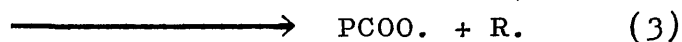
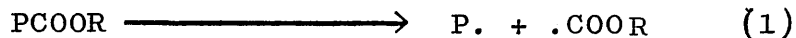


Fig.5.11: Ultra-violet absorption spectrum of P(2-EHA) film.

- (a) Prior to degradation
- (b) Exposed for 2 hours
- (c) Exposed for 6 hours

The formation of most of the products evolved in the photolysis of P(2-EHA) can be visualised as originating from the ester group as a result of three homolytic reactions as proposed by Fox et al (19) for PMA:



The bond strengths(25) involved here decrease in the order $\text{C=O} > \text{C-H} > \text{C-O} > \text{C-C}$. Similar decomposition reactions have been suggested for PMMA (31) and for other acrylates (19,25) but little quantitative information has been available for the acrylates.

5.6.1 Formation of 2-Ethylhexyl Formate

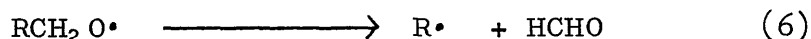
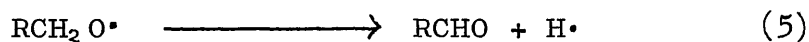
2-Ethylhexyl formate may result from the .COOR radical abstracting an H atom in reactions similar to those proposed for PMA and other acrylates (25).

The radical left on the polymer may be stabilized by forming a double bond in the polymer chain. Slight yellowing observed to develop after long exposures of the polymer films is thought to be due to double bond formation. Formation of double bonds can also be seen in the ultra-violet spectrum of irradiated polymer films.

5.6.2 Alkoxy Radical Reactions

Alkoxy radicals may result from reaction (2), and the unstable PCO. radical will decompose to give CO (64).

On hydrogen abstraction from the polymer, the alkoxy radical will produce an alcohol, while on fragmentation it will yield an aldehyde. Two reactions are possible [eqs. (5) and (6)] (66).

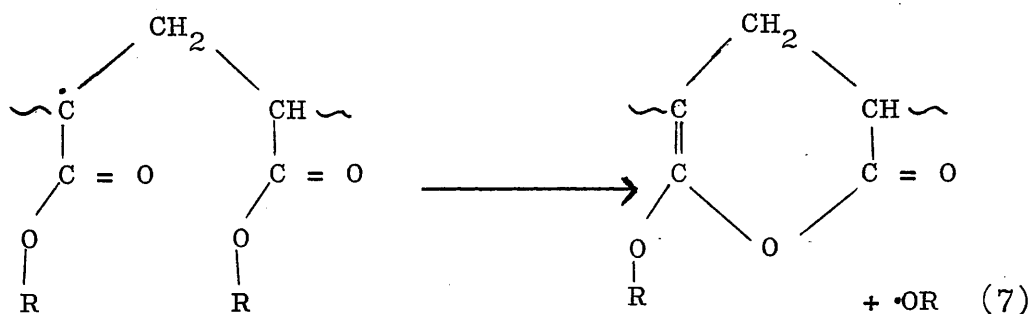


In the gas phase reaction(6) is the preferred fragmentation process. No formaldehyde was detected in P(2EHA) degradation.

McBay and Tucker (67) have shown that in solution, in the temperature range 110 - 155°C, the alkoxy radicals can react either by hydrogen abstraction from a solvent molecule to give alcohol or by disproportionation with another alkoxy radical to give equal yields of alcohol and aldehyde. Rust, Suebold, and Vaughan (68) studying the reaction of alkoxy radicals with cyclohexane in the gas phase at 195°C, showed that both hydrogen abstraction and disproportionation occur. By consulting table 5.3 it can be seen that the ratio of ROH/RCHO is more than unity and remains almost constant irrespective of irradiation time.

The ratio of $[(ROH + RCHO)/HCOOR]$ corresponding to the ratio of the rates of two photolytic reactions, increases with the increase in film thickness as calculated from table 5.4. It appears there are two reaction mechanisms operative in the formation of the alkoxy radical, the activating radiation for one process being more readily filtered out by the polymer.

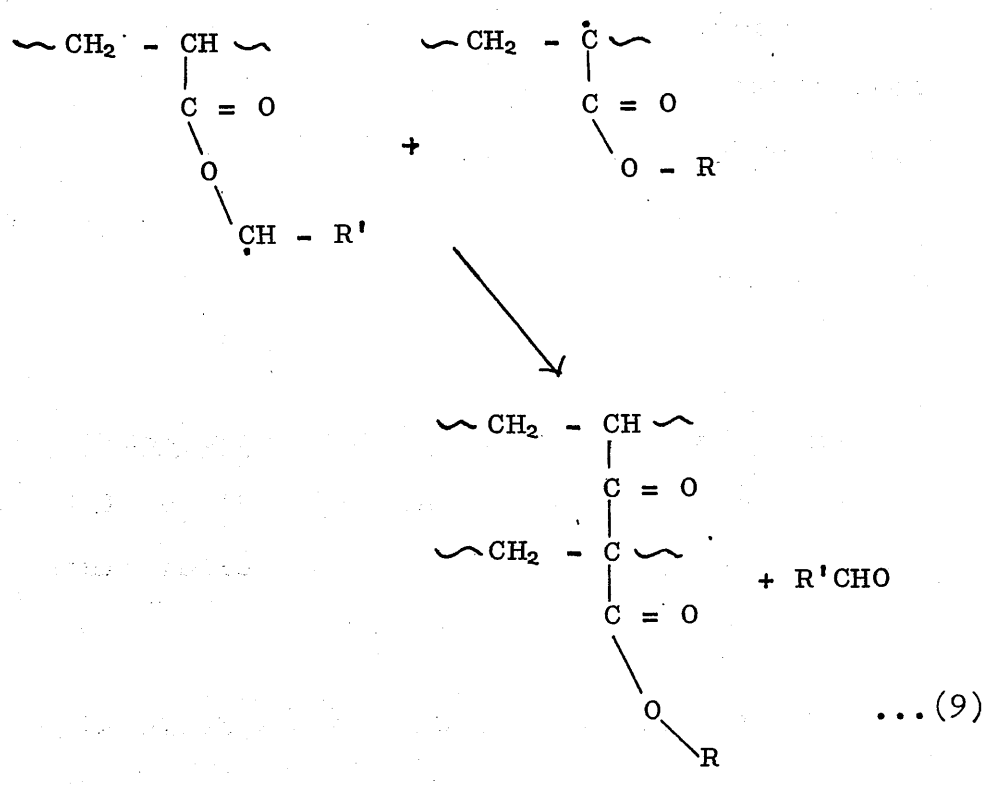
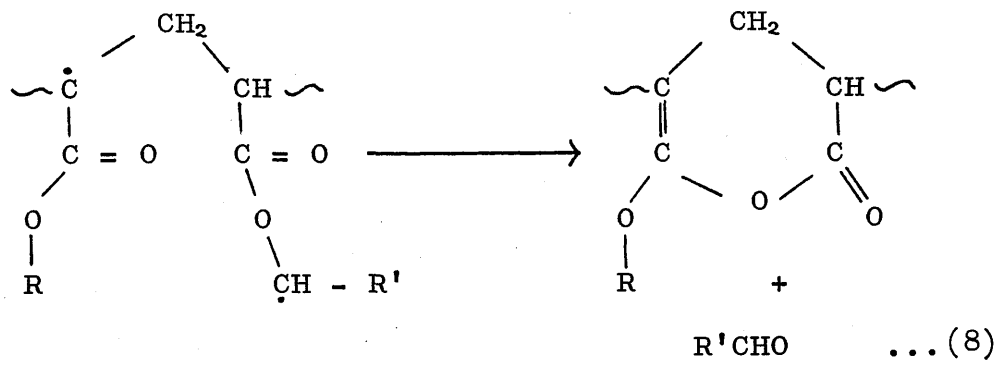
The other reaction for alkoxy radical formation may be through the lactone formation reactions proposed by Cameron and Kane (24) for PMA [eq.(7)].



also suggested for methanol formation in the photolysis of PMA in Chapter 4.

It has been shown (29) by deuteration experiments that in the radiolysis of PEA, abstraction of the α -hydrogen atom on the ester played an important role in the subsequent degradation of the ester group into CO and aldehyde. Two further aldehyde-forming reactions involving abstraction of the α -hydrogen,

suggested by Ackerman and McGill (23), may be visualized [eqs. (8) (9)].



The latter reactions are similar to those proposed by Cameron and Kane (24) for the formation of alkoxy radicals [reaction (5)] but involve two radical positions.

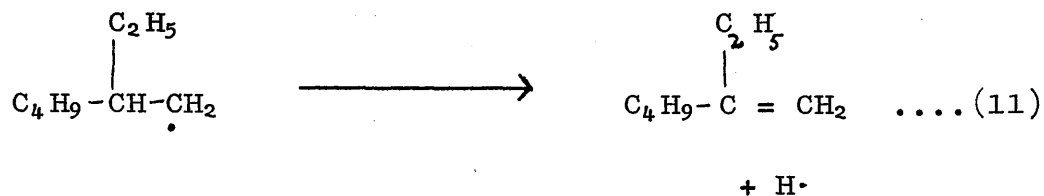
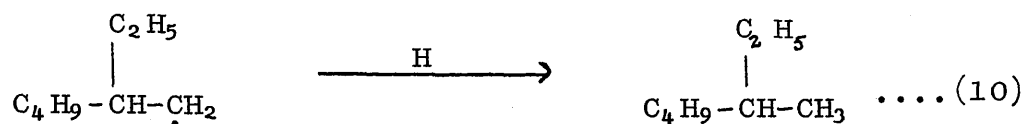
Table 5.3 shows that the total yield of ROH + RCHO production for P(2-EHA) degradation is considerably less than that for PMA under similar conditions (Chapter Four), the values being 21 and 46%, respectively.

Rust, Suebold and Vaughan (68) have shown that in the gas phase, the alkoxy radicals have stabilities in the order $CH_3O \cdot > CH_3CH_2O \cdot > CH_3CH_2CH_2CH_2O \cdot > (CH_3)_2CHCH_2O \cdot$. Thus it may be expected that alkoxy radical elimination reactions will be less likely to occur in polymers with fewer β -hydrogen atoms in the ester group, and this will account for the decreasing yield of RO. in P(2-EHA).

5.6.3 Production of Carbon Dioxide, Olefin and Alkane

All the three products, an alkane, olefin and CO₂, may result following degradation according to reaction (3).

The alkyl radical $(C_4H_9\overset{C_2H_5}{\underset{\cdot}{C}}HCH_2)$ formed in reaction(3) can either abstract a H atom to form an alkane or disproportionate to give olefin as follows [eqs.(10) and (11)]:



to form 3-methylheptane and 2-ethyl-1-hexene respectively. The amount of olefin formation is approximately double the amount of alkane production, as seen by GLC analysis. This might be due to the fact that the tertiary hydrogen next to the free radical is very reactive and hence the disproportionation reaction is preferred to hydrogen abstraction.

Carbon dioxide is the major photolysis product of P(2EHA) and constitutes about 28 - 30% of the total yield of condensable volatile products.

The ratio R./CO₂ (where R. equals alkane + olefin) is slightly higher than unity in the early stages of reaction, but approaches unity in the later stages. There may be a possibility of acid group formation due to incomplete decarboxylation, when CO₂ is not liberated in the early stages of reaction. The infrared spectra did not show any changes in absorption

due to acid group formation along the polymer chain.
 This might, however, be due to the very small amount
 present, which would be difficult to detect in the
 presence of a great excess of ester structures.

CHAPTER SIX

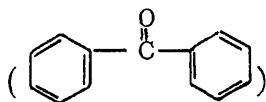
EFFECT OF PHOTSENSITIZERS ON THE PHOTODEGRADATION OF POLYACRYLATES

6.1 Introduction

One of the important components of a photocuring system is a photosensitizer. Therefore it is of practical importance to examine the effect of photosensitizers on the degradation behaviour of polymers.

The photoinitiation of polymerization and crosslinking of polymers by a free radical mechanism are well known (69). Photopolymerization might be defined as the process whereby light is used to induce an increase in molecular weight. Photopolymerization involves the addition chain polymerization of vinyl monomer while photocrosslinking is also a type of photopolymerization concerned with the crosslinking of pre-existing low polymer. The distinction between these two processes is not always clear cut.

Aromatic carbonyl compounds have been widely investigated as sensitizers in photoreactions of polymers. Benzophenone



and its

derivatives cause extensive crosslinking of polyethylene (70, 71) and can also be used as sensitizers for photo-chemical grafting of monomers onto polymers (72).

Benzoin O=C(c1ccccc1)C(O)c2ccccc2 and benzoin alkyl
ethers O=C(c1ccccc1)C(OR)c2ccccc2 have been most widely used
as sensitizers for vinyl polymerization.

In the first detailed study of the benzoin -
photoinitiated polymerization of vinyl monomers
(styrene, butyl acrylate, methyl acrylate and methyl
methacrylate), Melville (73) obtained kinetic evidence
for photochemical production of radicals from benzoin.

Benzoin has been investigated as a photosensitizer
for accelerating the formation of free radicals under ultra-
violet light in the case of poly(vinyl pyrrolidone),
poly(vinyl butyral) and poly(oxyethylene) (46). It
has been shown that sensitizer added to the polymers
functions as source of radicals under irradiation and
these excited radicals transfer energy to the polymer
molecules, so accelerating formation of radicals of the
matrix.

Fluorenone O=C1c2ccccc2c3ccccc13 and 2-chlorothioxanthone
O=C1c2ccccc2Sc3cc(Cl)ccc13 are both used as photoinitiators for
vinyl polymerization in industry (42, 74, 75).

In this, the final chapter, the normal degradation behaviour of the polymer is compared to that of a polymer sample containing photosensitizer in order to determine the effect of photosensitizers on the photo-degradation process.

6.2 Experimental Results

6.2.1 Apparatus and Conditions

The following photosensitizers were used in the study.

- a) benzoin (Hopkin and Williams Ltd.)
- b) fluorenone
- c) 2-chlorothioxanthone

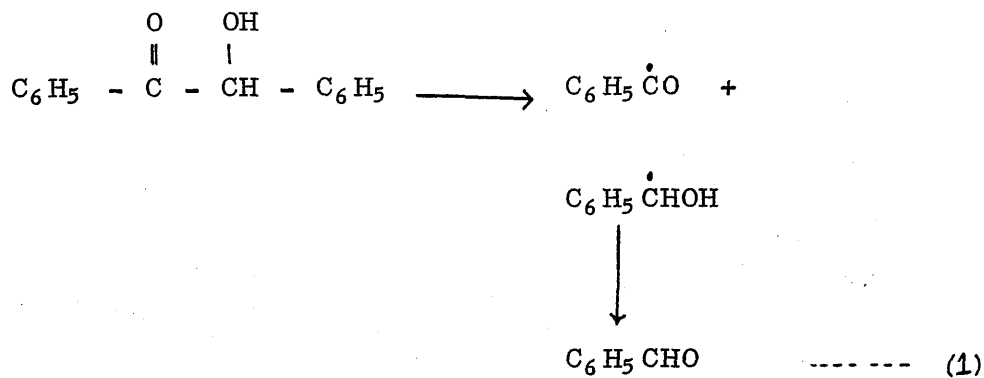
Samples (b) and (c) were kindly supplied by ICI Ltd.

Benzophenone was found to sublime under the experimental conditions used, hence its effect as a sensitizer was not examined in this study.

Polymer films (22 μ thickness in case of PMA and 23.5 μ in the case of P(2-EHA), containing different concentrations of photosensitizers, were prepared from methylene chloride as casting solvent, as described in Chapter Two. Photolysis apparatus and techniques were described in the preceding Chapters. The polymer films were irradiated for various time intervals under identical experimental conditions and the photolysis products were studied.

6.2.2 Product Analysis

Products were analyzed and identified using the subambient TVA technique, as described before, together with infrared spectroscopy and gas liquid chromatography (GLC). The product trace obtained from the degradation of a PMA film containing 4% benzoin, fig. 6.1, consists of peaks corresponding to CO₂, HCHO, HCOOCH₃, CH₃OH, H₂O, short chain fragments (all photodegradation products of the polymer) and a seventh species (peak no. 6) giving rise to the infrared spectrum in fig. 6.2, which is characteristic of benzaldehyde. The benzaldehyde peak in the subambient TVA trace is not obvious till the benzoin concentration is more than 2%. Benzaldehyde is a photodegradation product of benzoin. Photochemical cleavage of benzoin gives rise to benzoyl (C₆H₅·C=O) and hydroxybenzyl radical (C₆H₅·CHOH) (73,76). Benzaldehyde is formed by hydrogen transfer of the hydroxyl proton of the hydroxybenzyl radical to the benzoyl radical (77) as follows:



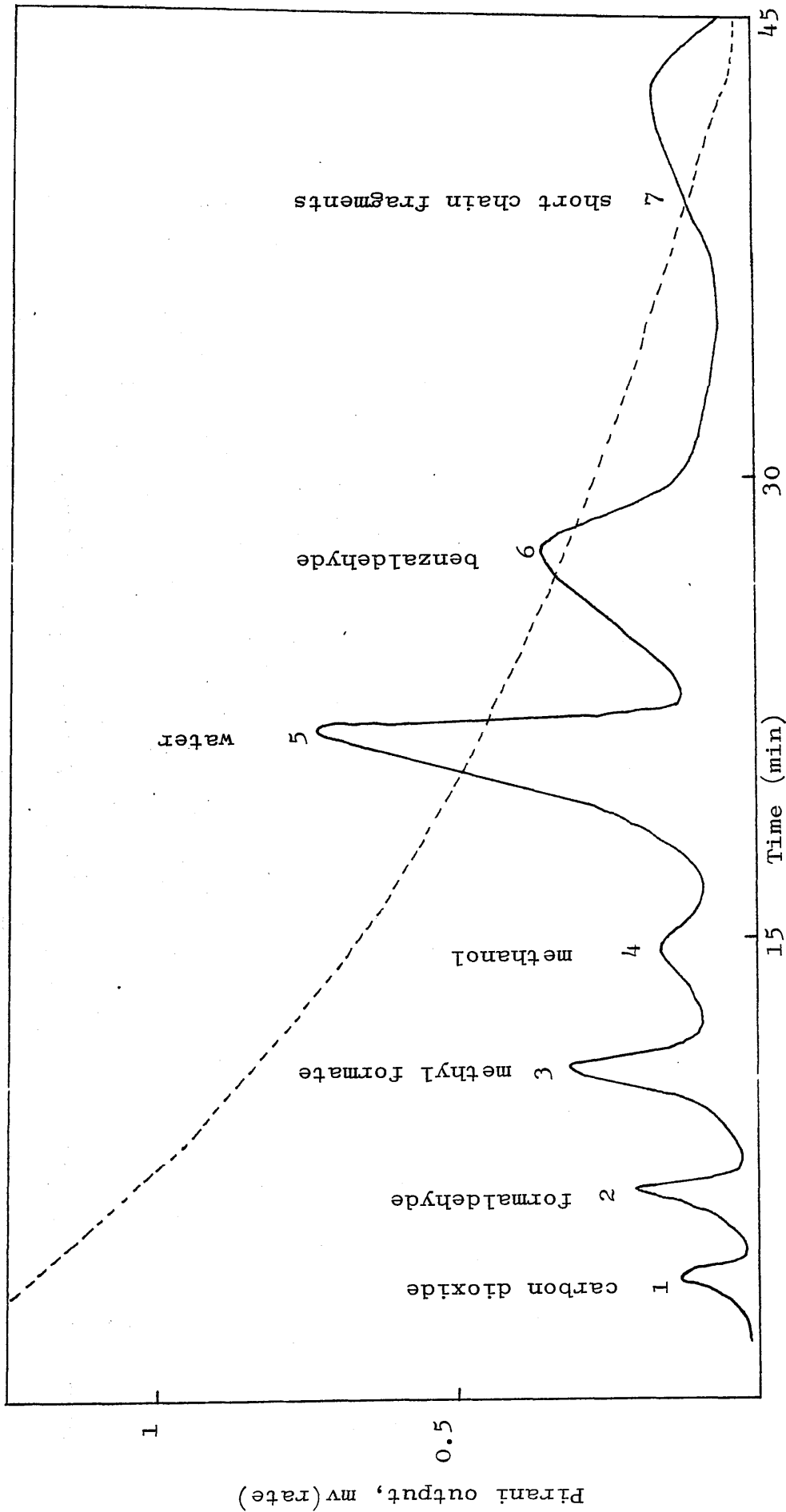


Fig. 6.1: Subambient TVA trace for photodegradation products of P(2-EHA) containing 4% benzoin, (60 minutes irradiation time under vacuum)

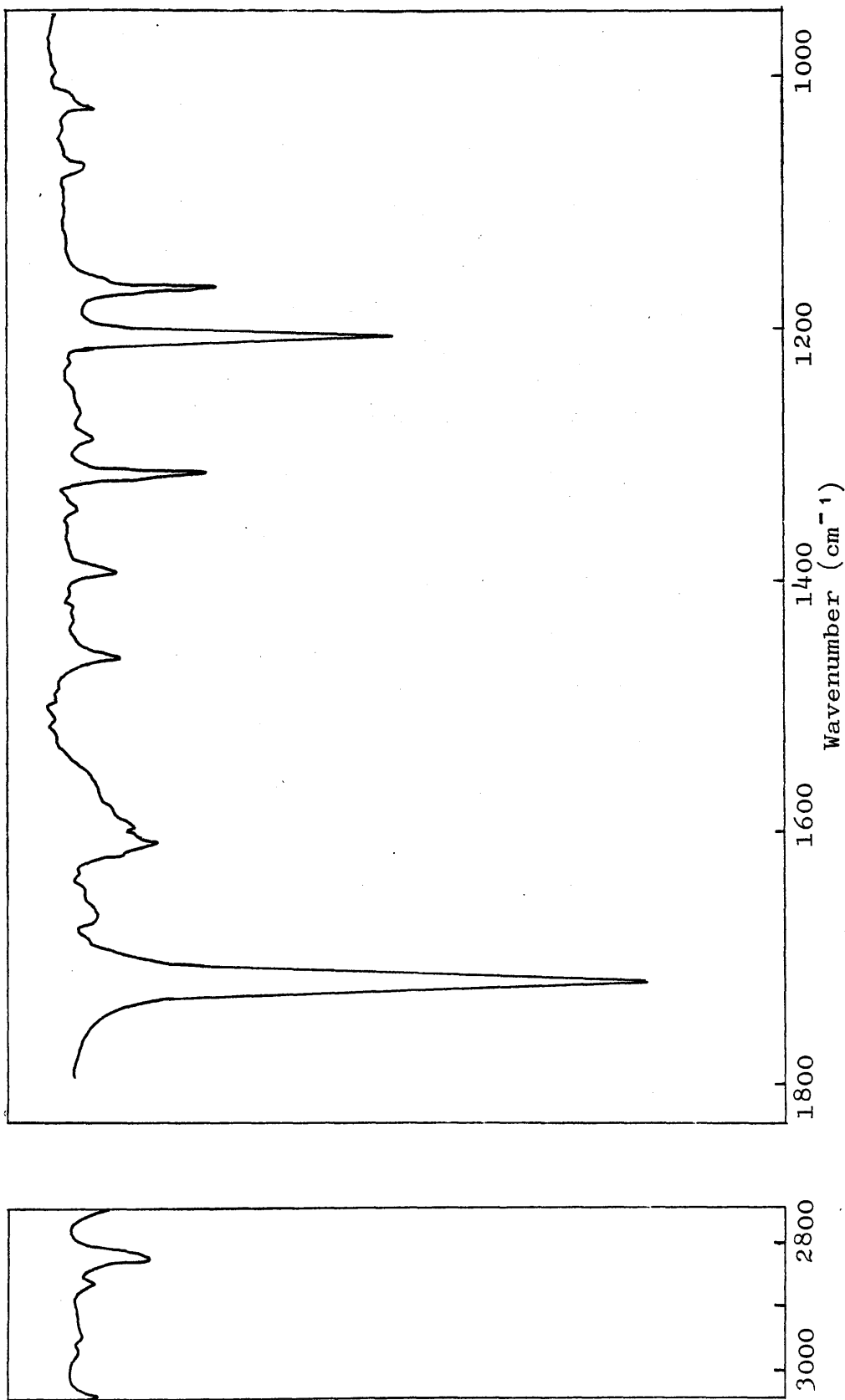


Fig. 6.2: Infrared spectrum (in CCl_4) obtained from products corresponding to peak 6 in the product trace from photodegradation of PMA containing benzoin. The product was identified as benzaldehyde.

As all the photolysis products of P(2-EHA) are high boiling liquids, and no benzaldehyde peak can be detected in the subambient TVA trace for the sample at this benzoin concentration (fig.6.3), it was decided to analyse the products by GLC.

Gas liquid chromatography of liquid photolysis products from P(2-EHA) and 4% benzoin system was performed as described in Chapter Five, and benzaldehyde was identified by the retention time as shown in fig. 6.4, along with the condensable volatile products of P(2-EHA), which are carbon dioxide, 2-ethyl-1-hexene, 3-methylheptane, 2-ethyl-1-hexanal, 2-ethylhexyl formate, 2-ethyl-1-hexanol and short chain fragments, as analyzed and identified in Chapter Five. Comparison of subambient TVA traces fig. 6.3 and fig.5.1 (Chapter Five) suggests that there is an apparent decrease in short chain fragments formation in presence of photosensitizer.

Fluorenone and 2-chlorothioxanthone were also investigated as photosensitizers for PMA photolysis. No new peaks were observed and only the photolysis products of PMA were found.

An increase is observed in the amount of short chain fragments in the case of PMA and photosensitizer systems. By comparing the subambient traces fig.6.1 and fig.4.1(Chapter Four), this increase in short chain fragments (last peak of the trace) can be seen for PMA containing benzoin. Due to the small amount of material

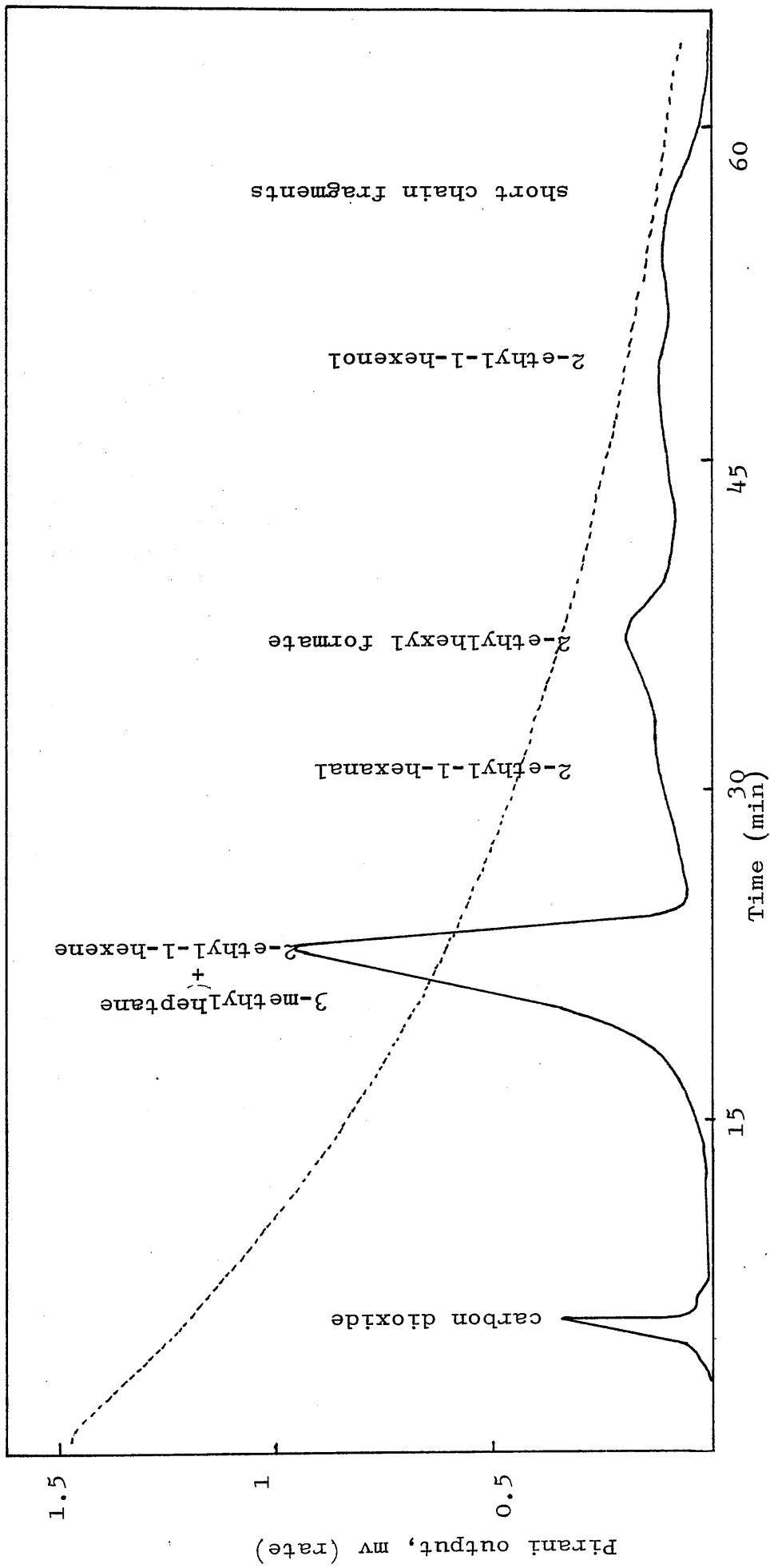


Fig. 6.3: Subambient TVA trace for photodegradation products of P(2-EHA) containing 1% benzoin (60 min irradiation time under vacuum).

the chain fragment fractions from all the degradations were combined and the infrared spectrum was run in carbon tetrachloride as shown in fig. 6.5. The spectrum was similar to those of the parent polymer with the following minor differences: the carbonyl peak and the peaks in the $1500 - 1000 \text{ cm}^{-1}$ region show a general broadening.

6.2.3 Quantitative Analysis

The effect of different concentrations of benzoin on the mole % yield of condensable volatile products from PMA was studied as a function of irradiation time. The procedure for the stepwise quantitative analysis of condensable volatiles is described in previous chapters. The yields of volatile products from 0.25%, 1% and 4% benzoin + PMA are summarised in tables 6.1, 6.2 and 6.3 respectively and shown graphically in fig. 6.6 - 6.9, with corresponding data for PMA alone included. It is clear from the graphs that there is a general decrease (compared to PMA alone) in the yield of volatiles (except short chain fragments) in presence of increasing amounts of benzoin. This might be due to the fact that benzoin absorbs strongly in the ultra-violet region of spectrum and an increase in its concentration means more absorption, leaving less energy for the decomposition of the ester group of the PMA.

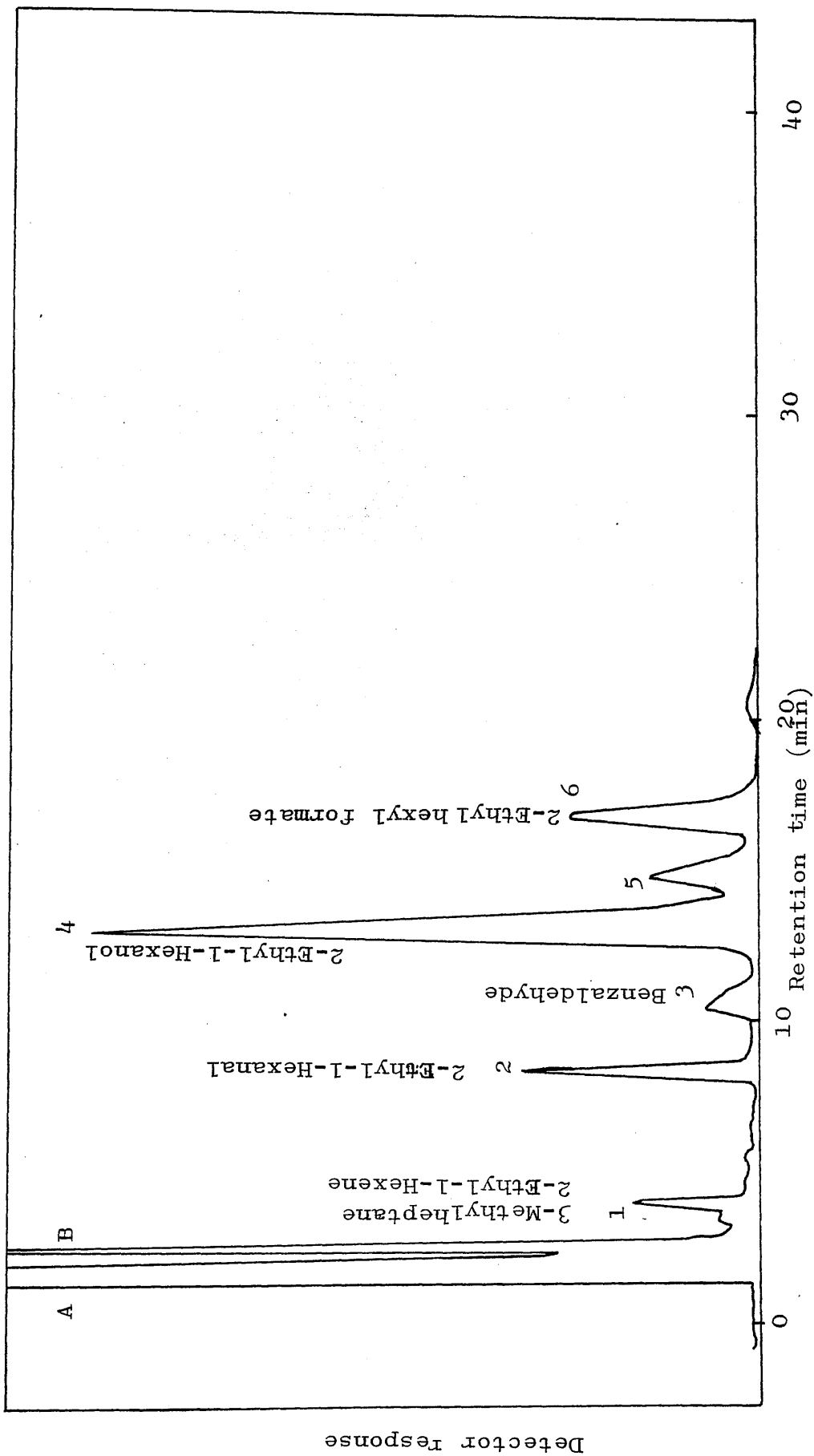


Fig. 6.4: GLC analysis of liquid degradation products of P(2-EHA) containing 4% benzoin, column temperature 80°C, Nitrogen carrier gas, 0.33m³/sec.

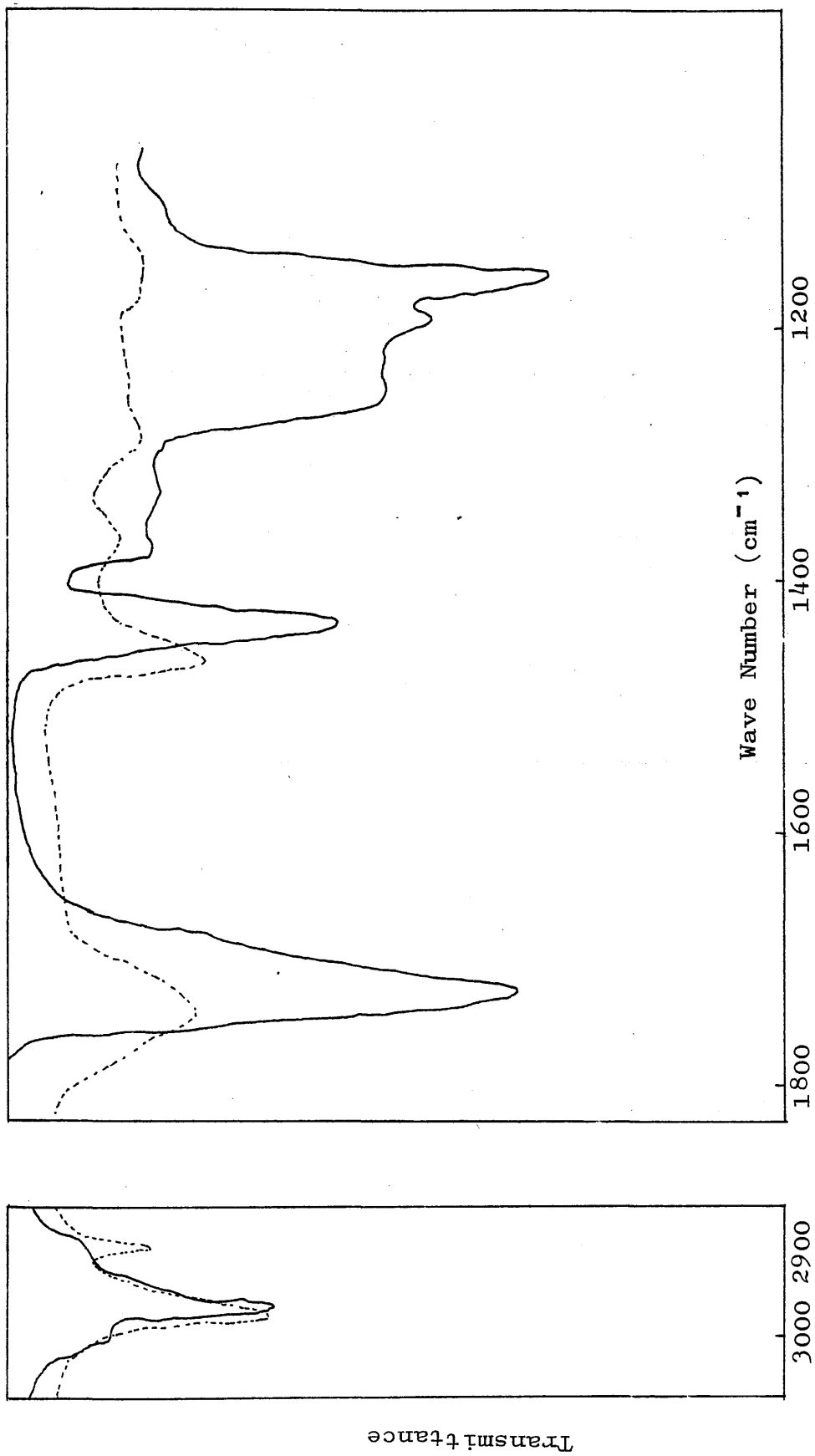


Fig. 6.5: Infrared spectra of: — PMA, short chain fragments from PMA containing benzoin.

TABLE 6.1: Mole % yield of volatiles per monomer unit from PMA containing 0.25% benzoin (w/w)

Time (min)	CO ₂	HCHO	HCOOCH ₃	CH ₃ OH
15	0.17	0.21	0.40	0.20
30	0.38	0.38	0.86	0.49
45	0.44	0.55	0.99	0.56
60	0.56	0.64	1.16	0.69
90	0.72	0.77	1.4	0.87
120	0.85	0.92	1.54	1.05

TABLE 6.2: Mole % yield per monomer unit
of volatiles from PMA containing
1% benzoin (w/w)

Time (min)	CO ₂	HCHO	HCOOCH ₃	CH ₃ OH
15	0.16	0.15	0.34	0.19
30	0.32	0.26	0.64	0.46
45	0.38	0.46	0.86	0.53
60	0.47	0.55	0.99	0.66
90	0.60	0.62	1.24	0.75
120	0.69	0.77	1.33	0.88

TABLE 6.3: Mole % yield per monomer unit of
volatiles from PMA containing
4% benzoin (w/w)

Time (min)	CO ₂	HCHO	HCOOCH ₃	CH ₃ OH
15	0.11	0.12	0.25	0.20
30	0.25	0.23	0.53	0.47
45	0.28	0.30	0.52	0.53
60	0.32	0.32	0.64	0.61
90	0.31	0.32	0.74	0.72
120	0.36	0.4	0.81	0.75

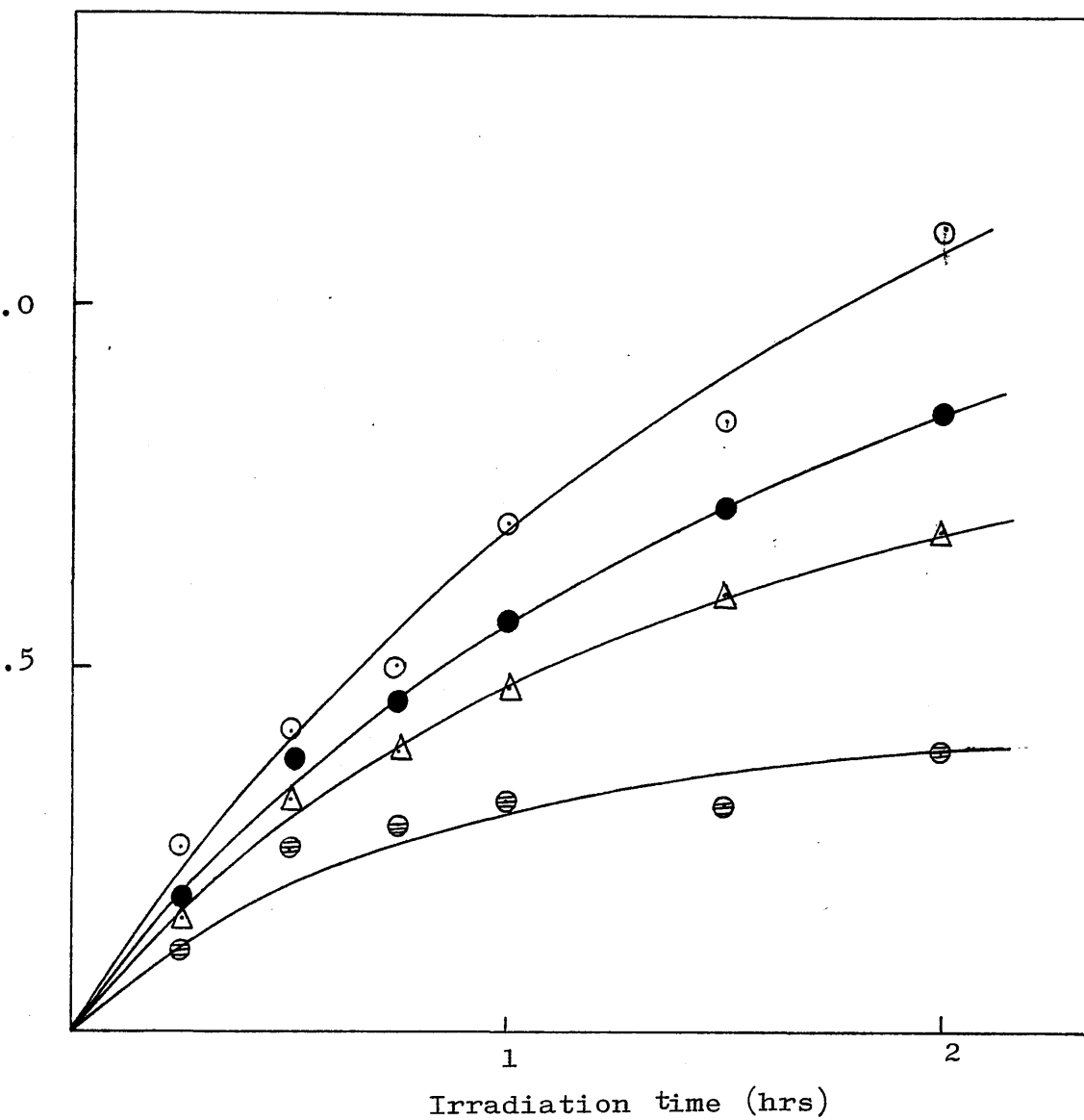


Fig. 6.6: Effect of benzoin on the production of carbon dioxide from PMA as a function of irradiation time, ○ without benzoin, ● 0.25% benzoin, △ 1% benzoin, ⊖ 4% benzoin.

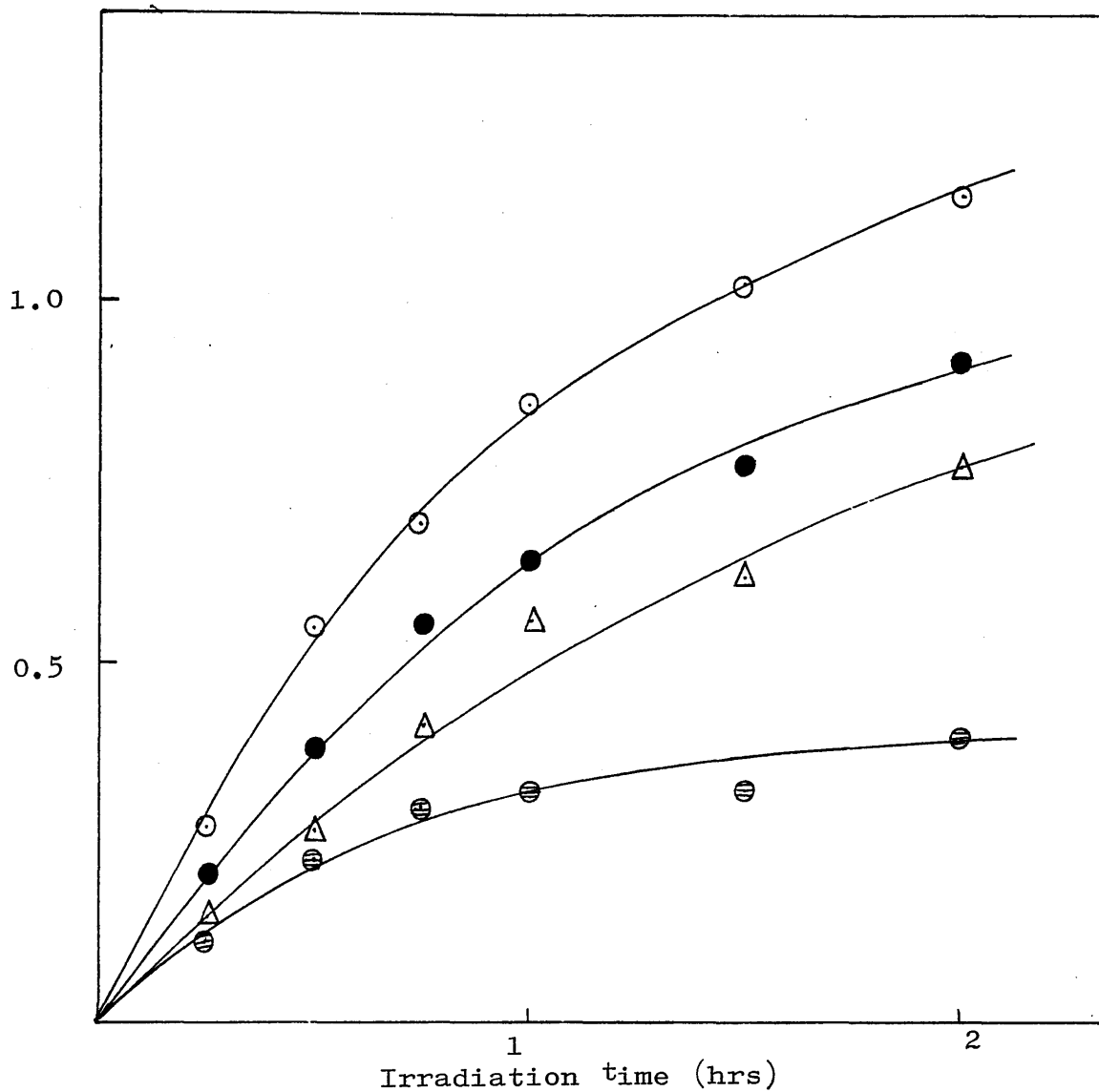


Fig.6.7: Effect of benzoin on the production of formaldehyde from PMA as a function of irradiation time, ○ without benzoin, ● 0.25% benzoin, △ 1% benzoin, ⊖ 4% benzoin.

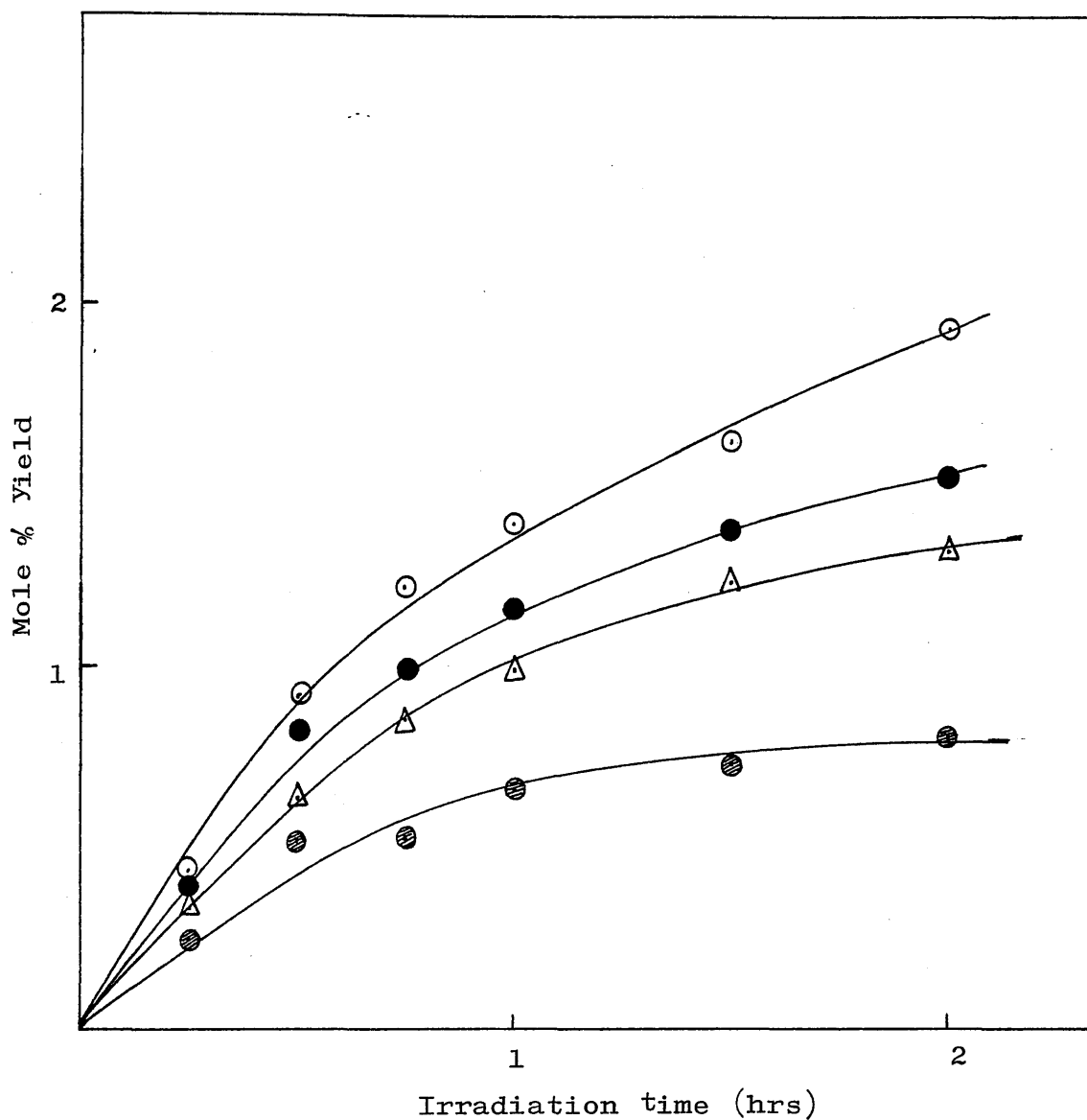


Fig. 6.8: Effect of benzoin on the production of methyl formate from PMA as a function of irradiation time, ○ without benzoin, ● 0.25% benzoin, △ 1% benzoin, ⊖ 4% benzoin.

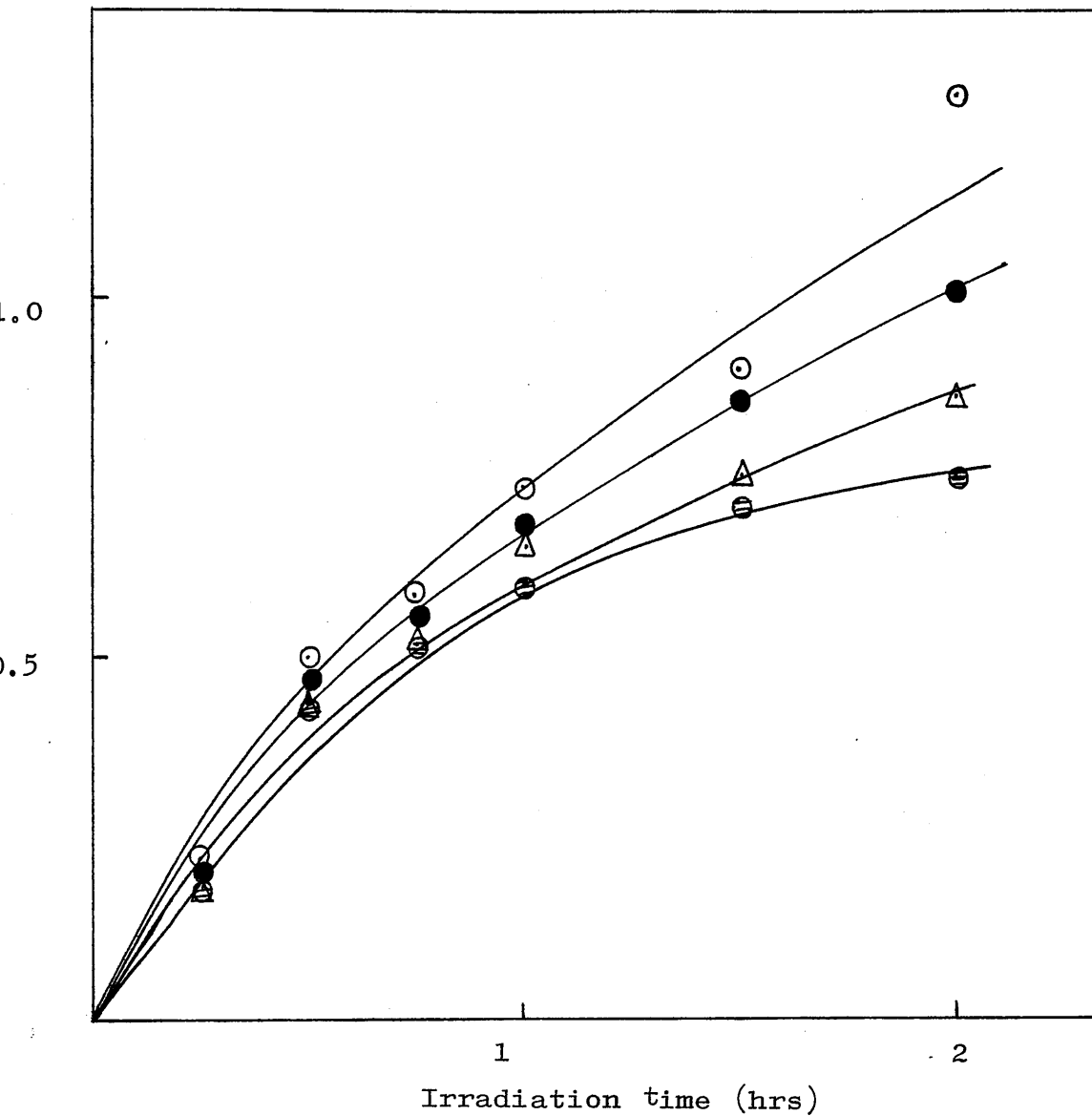


Fig.6.9: Effect of benzoin on the production of methanol from PMA as a function of irradiation time, ○ without benzoin, ● 0.25% benzoin, △ 1% benzoin, ⊖ 4% benzoin.

The other two photosensitizers, fluorenone and 2-chlorothioxanthone, have similar effects on the yields of the volatile products from PMA degradation. Results are given in tables 6.4 and 6.5 for fluorenone and 2-chlorothioxanthone respectively, while comparison plots are shown in figs. 6.10 - 6.13 for the former and figs. 6.14 - 6.17 for the latter. The effect of benzoin on the amount of condensable volatile products from P(2-EHA) was also studied quantitatively as a function of irradiation time, and data are presented in table 6.6. The mole % yields of the products from P(2-EHA) are shown in figs. 6.18 - 6.23. It is not possible to determine the mole % yield in the case of short chain fragments, hence comparison has been made between peak areas (arbitrary units) of the subambient TVA traces as shown in fig. 6.24. It is clear from the plots that the presence of benzoin decreases the volatile product formation from P(2-EHA).

6.3 Molecular Mass Changes

Polyacrylates undergo chain scission and cross-linking during photolysis as stated in the preceding chapters.

It is important to examine the effect of photosensitizers (which form radicals under appropriate circumstances under ultra-violet light) on the extent of crosslinking and chain scission of polyacrylates.

TABLE 6.4: Mole % yield per monomer unit of volatiles from PMA containing 1% fluorenone (w/w)

Time (min)	CO ₂	HCHO	HCOOCH ₃	CH ₃ OH
15	0.61	.21	.36	.16
30	.25	.32	.50	.36
45	.31	.46	.83	.40
60	.43	.52	1.16	.49
90	.47	.76	1.27	.67
120	.51	.90	1.4	.71

TABLE 6.5: Mole % yield per monomer unit of volatiles from PMA containing 2-chlororthioxanthone

Time (min)	CO ₂	HCHO	HCOOCH ₃	CH ₃ OH
15	0.11	0.17	0.38	0.10
30	0.16	0.27	0.62	0.33
45	0.19	0.45	0.78	0.35
60	0.25	0.53	0.81	0.46
90	0.37	0.73	1.01	0.61
120	0.40	0.84	1.17	0.66

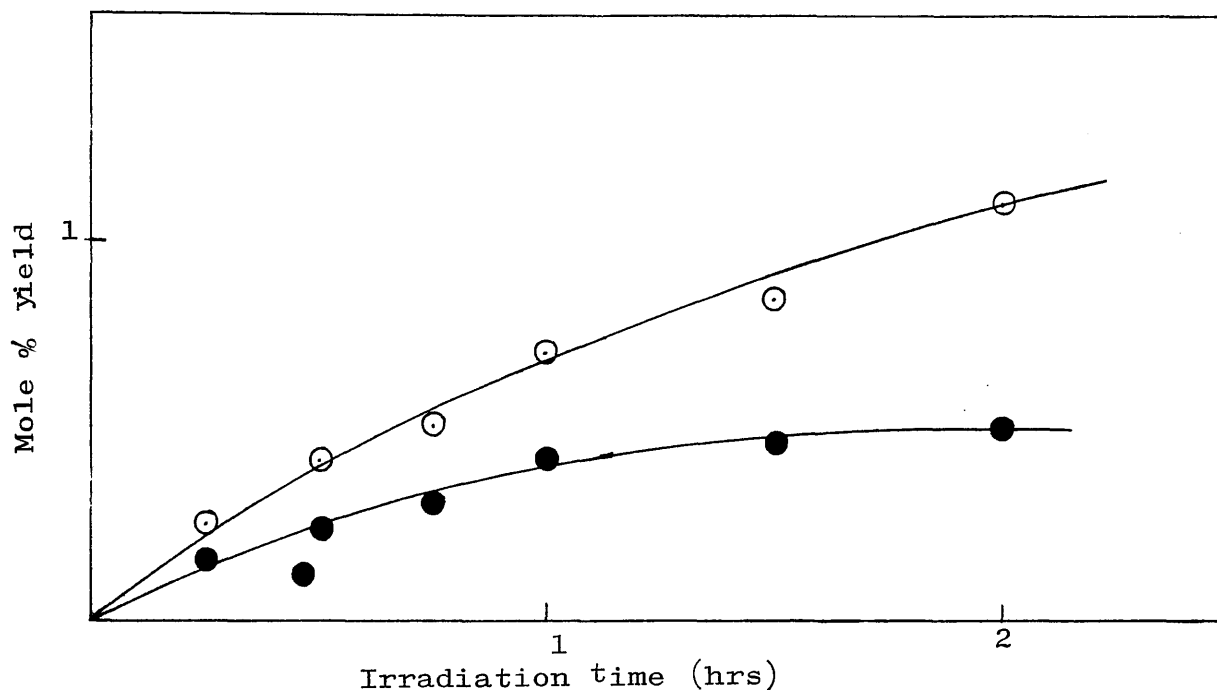


Fig.6.10: Effect of fluorenone on the production of carbon dioxide from PMA as a function of irradiation time; ○ without fluorenone, ● 1% fluorenone.

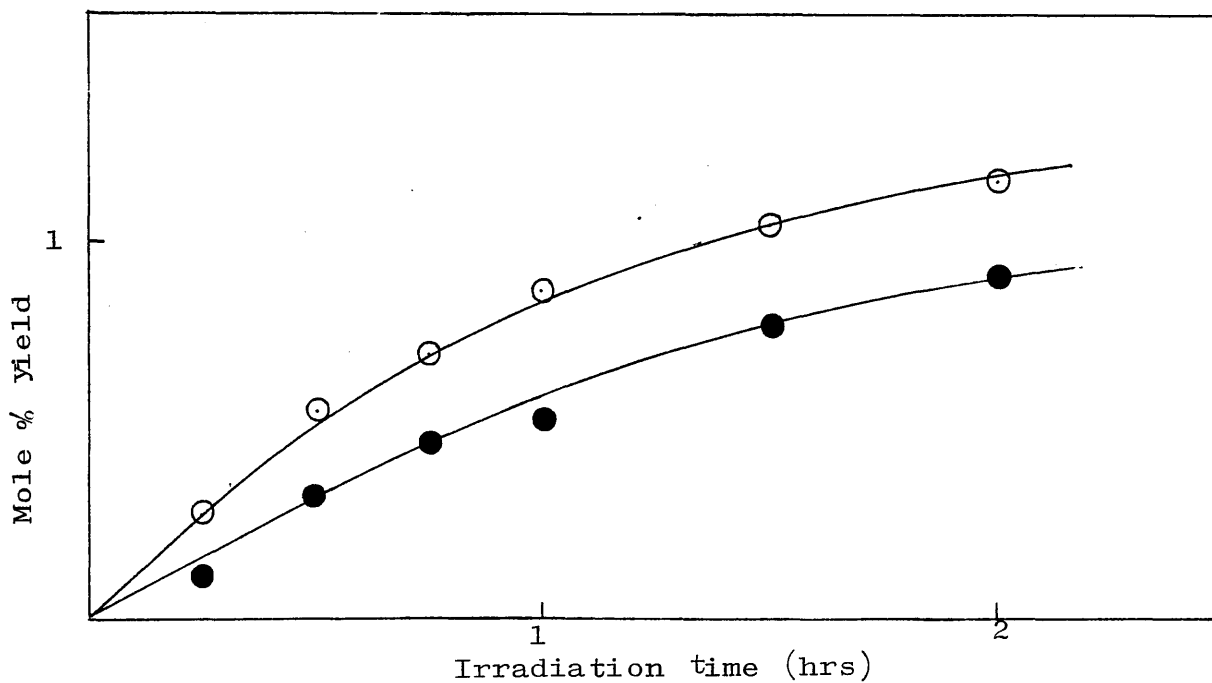


Fig.6.11: Effect of fluorenone in the production of formaldehyde from PMA as a function of irradiation time; ○ without fluorenone, ● 1% fluorenone.

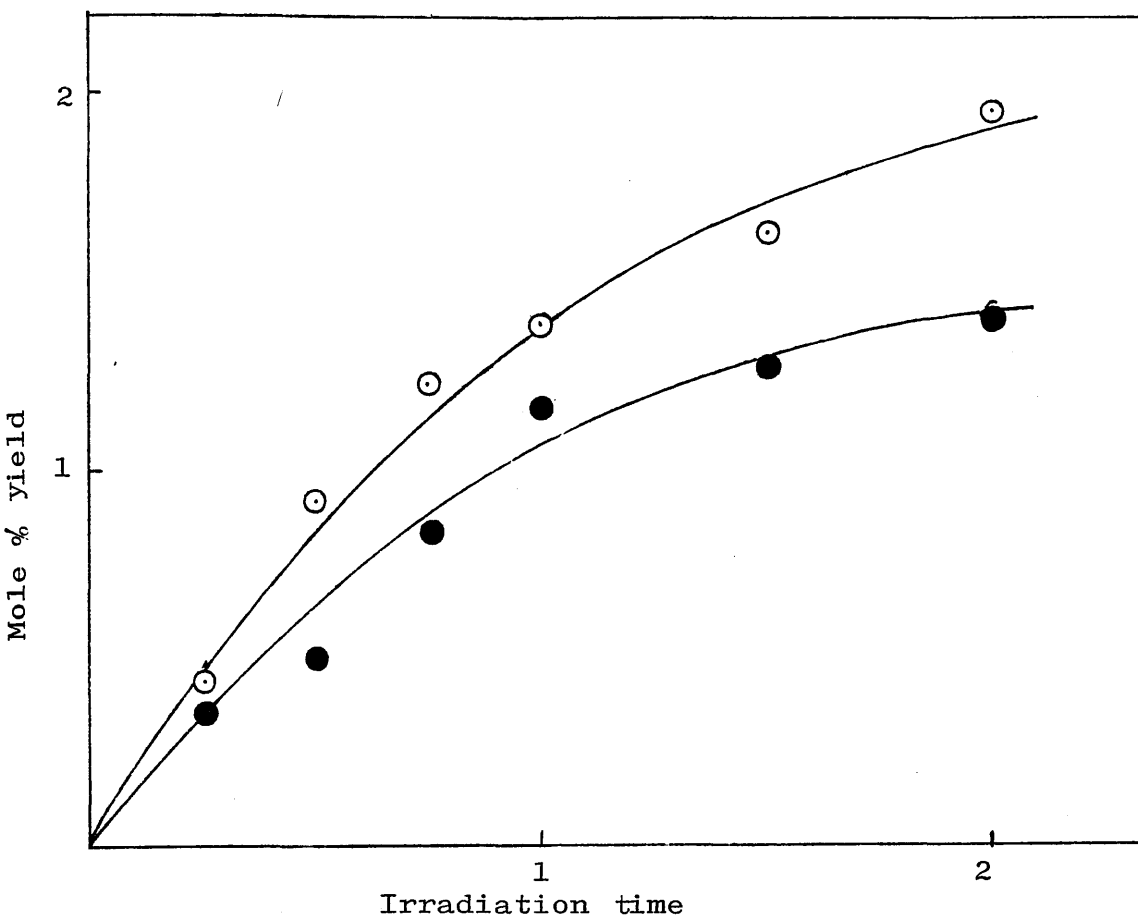


Fig. 6.12: Effect of fluorenone on the production of methyl formate from PMA as a function of irradiation time, \odot without fluorenone, \bullet 1% fluorenone.

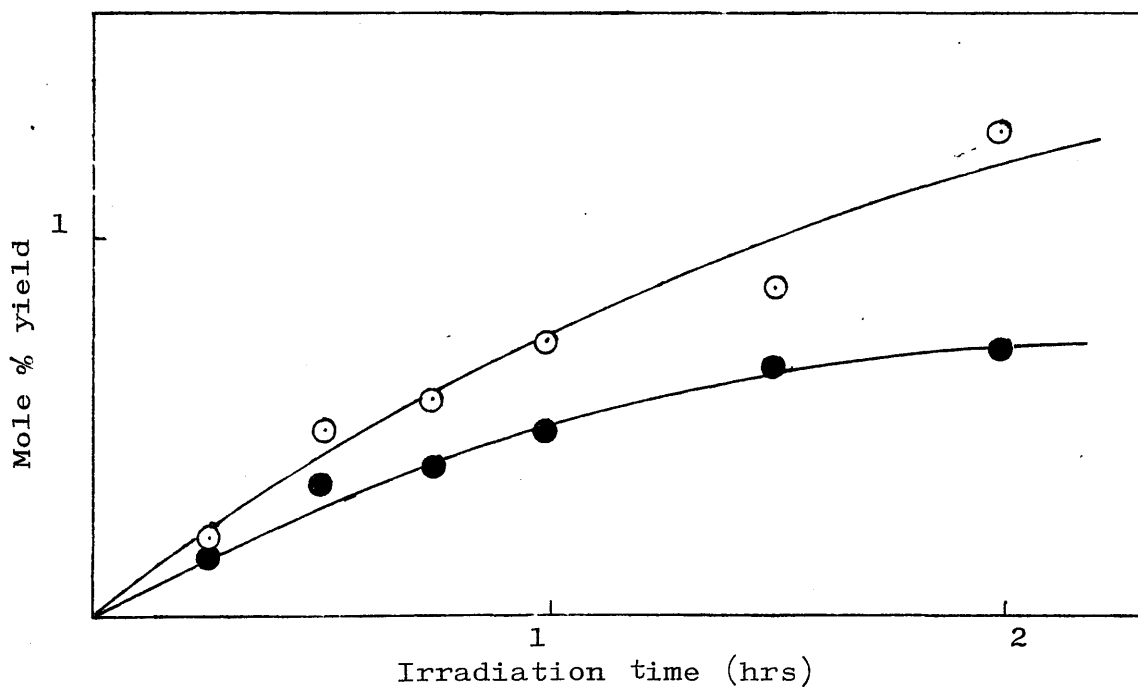


Fig. 6.13: Effect of fluorenone on the production of methanol from PMA as a function of irradiation time, \odot without fluorenone, \bullet 1% fluorenone.

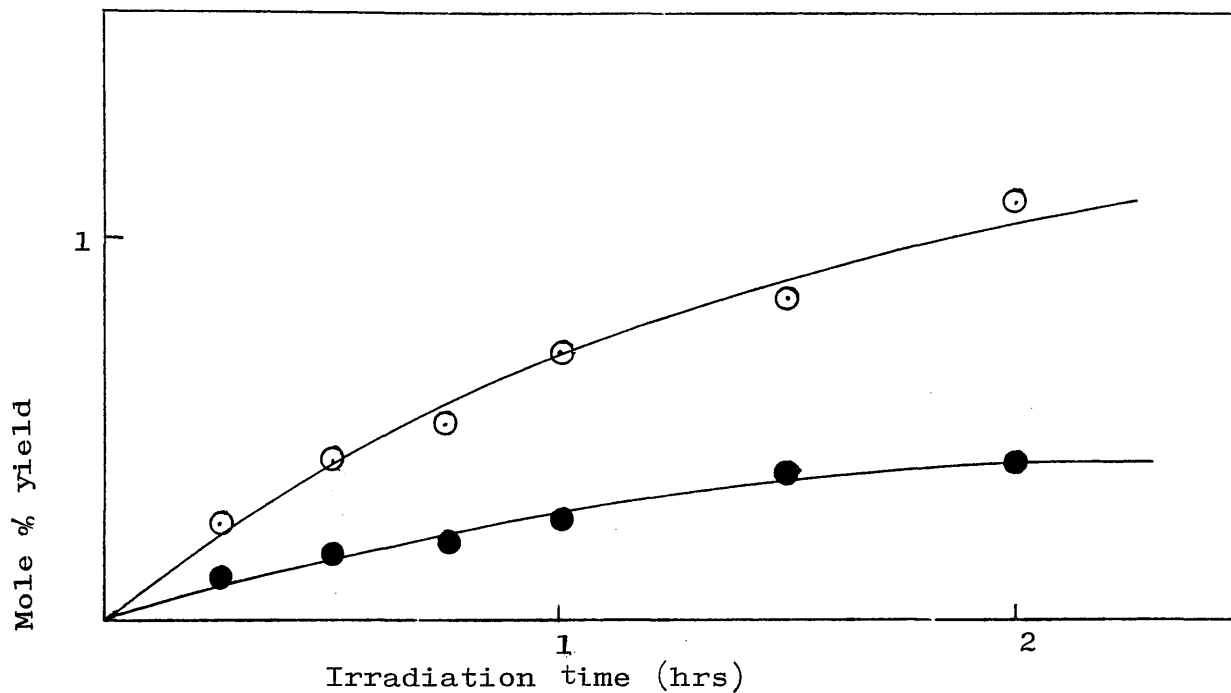


Fig.6.14: Effect of 2-chlorothioxanthone on the production of carbon dioxide from PMA as a function of irradiation time, ○ without 2-chlorothioxanthone, ● 1% 2-chlorothioxanthone

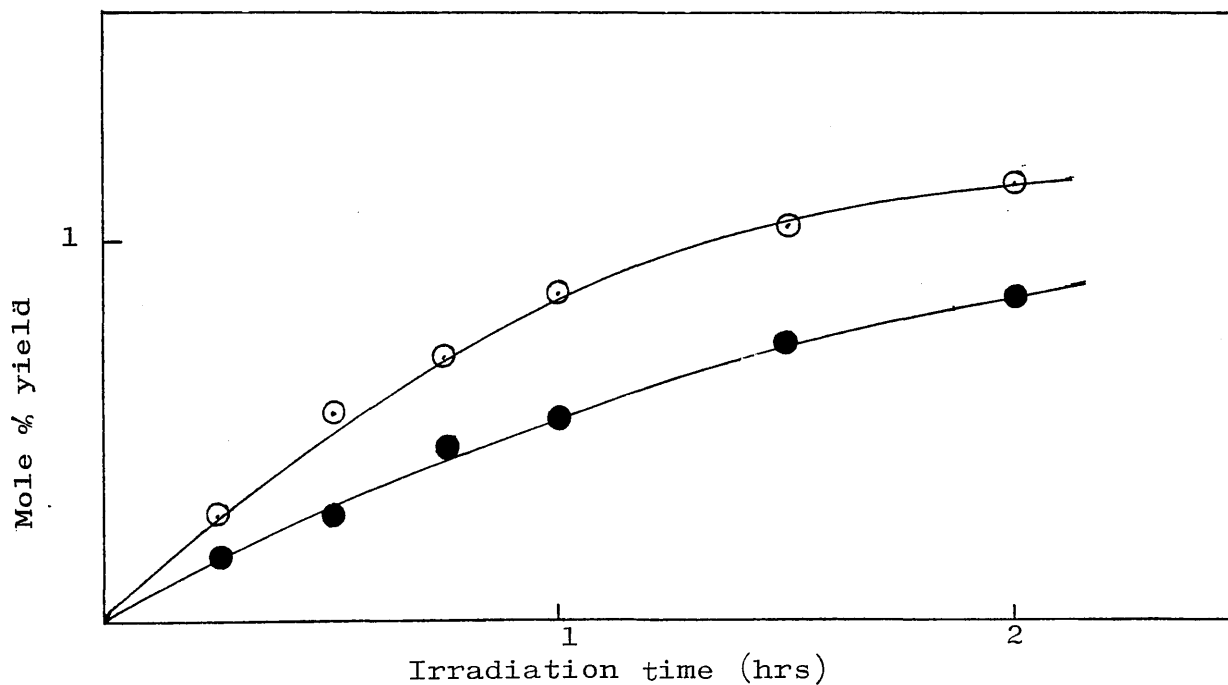


Fig.6.15: Effect of 2-chlorothioxanthone on the production of formaldehyde from PMA as a function of irradiation time, ○ without 2-chlorothioxanthone, ● 1% 2-chlorothioxanthone.

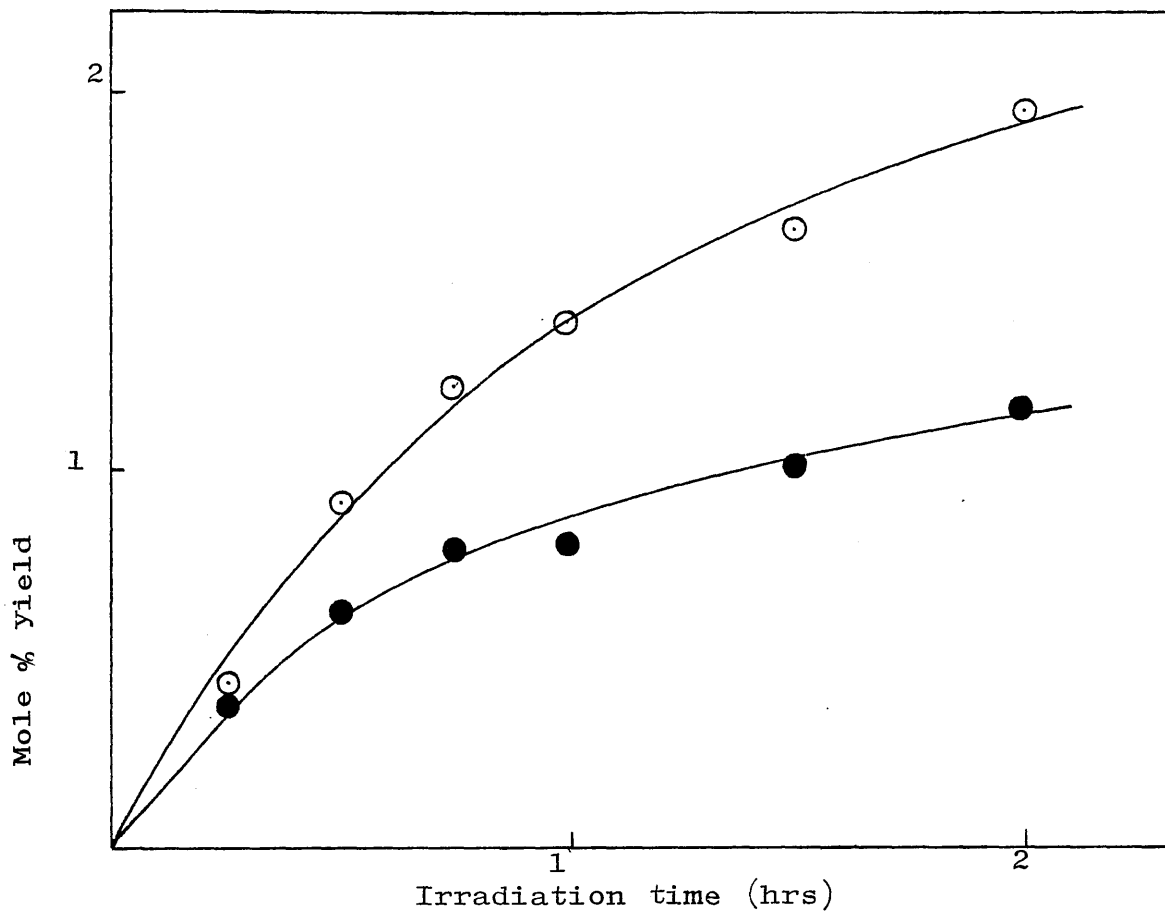


Fig. 6.16: Effect of 2-chlorothioxanthone on the production of methyl formate from PMA as a function of irradiation time, \odot without 2-chlorothioxanthone, \bullet 1% 2-chlorothioxanthone.

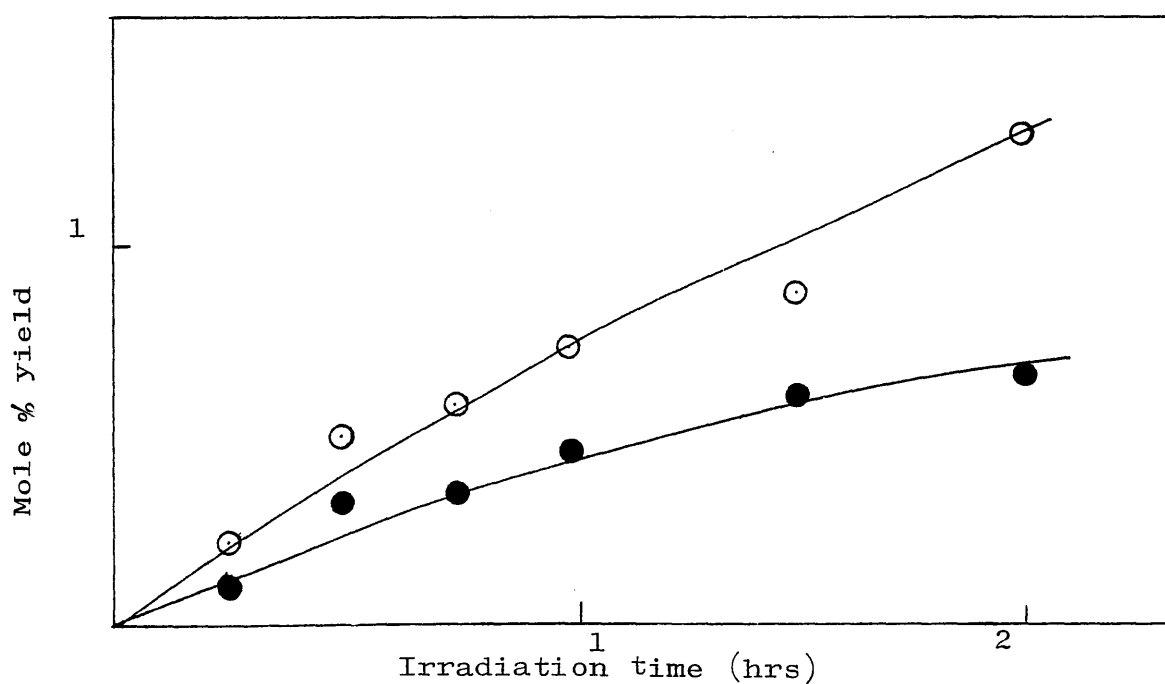


Fig. 6.17: Effect of 2-chlorothioxanthone on the production of methanol from PMA as a function of irradiation time, \odot without 2-chlorothioxanthone, \bullet 1% 2-chlorothioxanthone.

Time min	CO ₂	2-Ethyl-1- Hexene	3-Methyl heptane	2-Ethyl-1- Hexanal	2-Ethylhexyl Formate	2-Ethyl-1- Hexanol	Short Chain fragments (Peak area)
15	0.23	0.17	0.085	0.103	0.175	0.13	0.014
30	0.35	0.22	0.113	0.22	0.29	0.20	0.03
45	0.60	0.424	0.212	0.255	0.35	0.25	0.026
60	0.88	0.51	0.259	0.35	0.60	0.42	0.04
120	1.71	0.95	0.475	0.67	0.92	0.76	0.08
180	2.4	1.22	0.66	0.86	1.19	1.12	0.12
240	2.82	1.75	0.87	0.905	1.57	1.25	0.15
360	3.21	1.87	0.93	0.91	1.60	1.48	0.19

Table 6.6: Mole % yield per monomer unit of volatiles from P(2-EHA) containing 1% benzoin (w/w). Short chain fragments are given as peak areas of the subambient TVA peaks (arbitrary units).

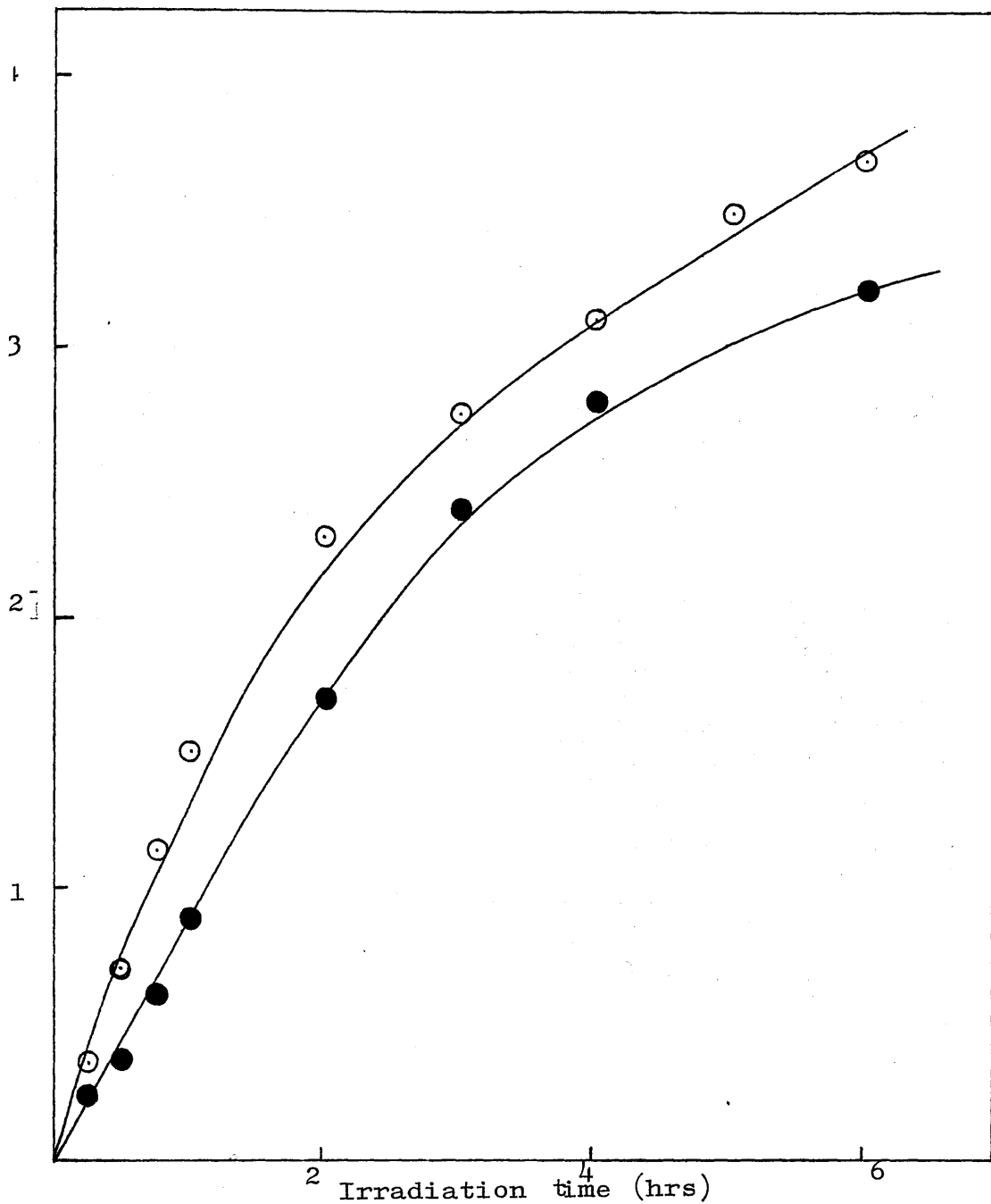


Fig.6.18: Effect of benzoin on the production of carbon dioxide from P(2-EHA) as a function of irradiation time, ○ without benzoin, ● 1% benzoin.

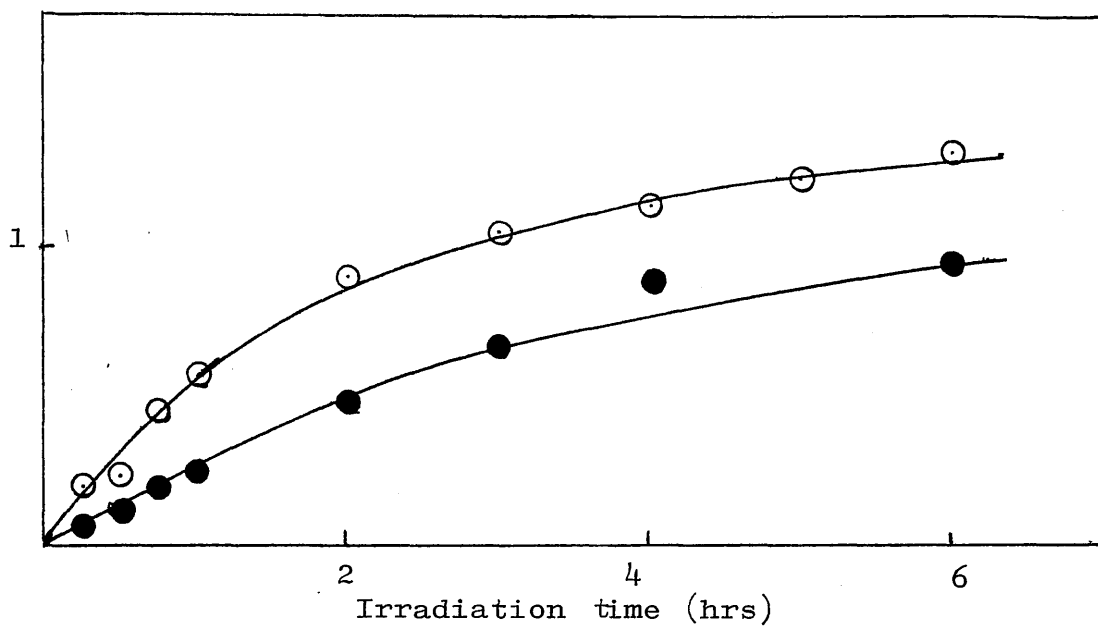


Fig.6.19: Effect of benzoin on the production of 3-methylheptane from P(2-EHA) as a function of irradiation time, \circ without benzoin, \bullet 1% benzoin.

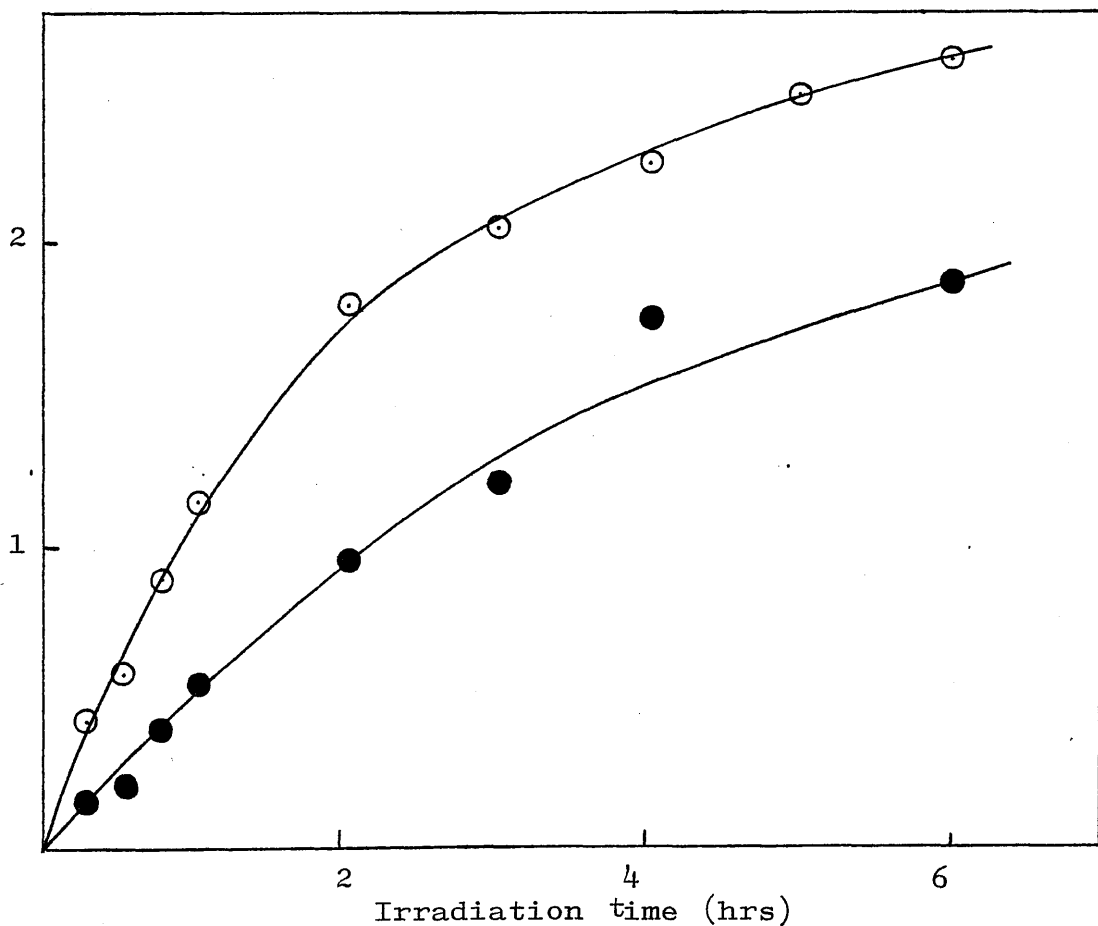


Fig.6.20: Effect of benzoin on the production of 2-ethyl-1-hexene from P(2-EHA) as a function of irradiation time, \circ without benzoin, \bullet 1% benzoin.

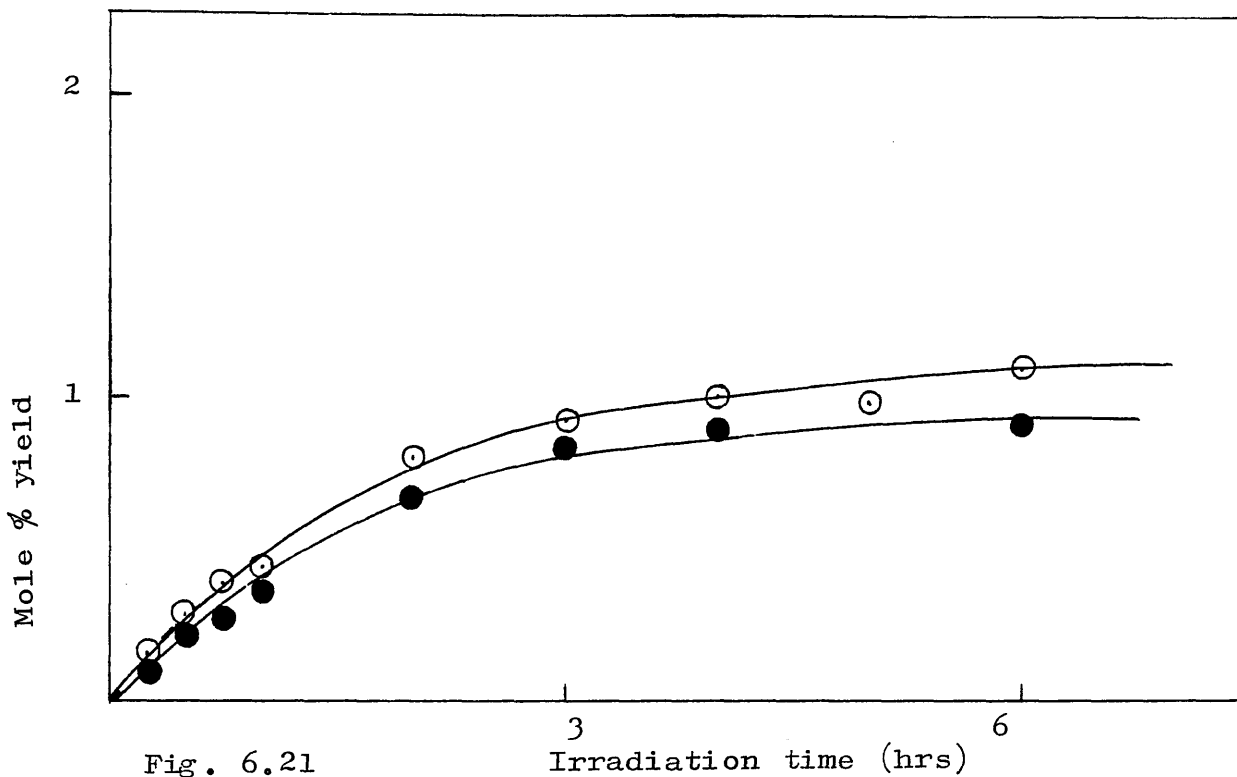


Fig. 6.21

Effect of benzoin on the production of 2-ethyl-1-hexanal from P(2-EHA) as a function of irradiation, ○ without benzoin, ● with 1% benzoin.

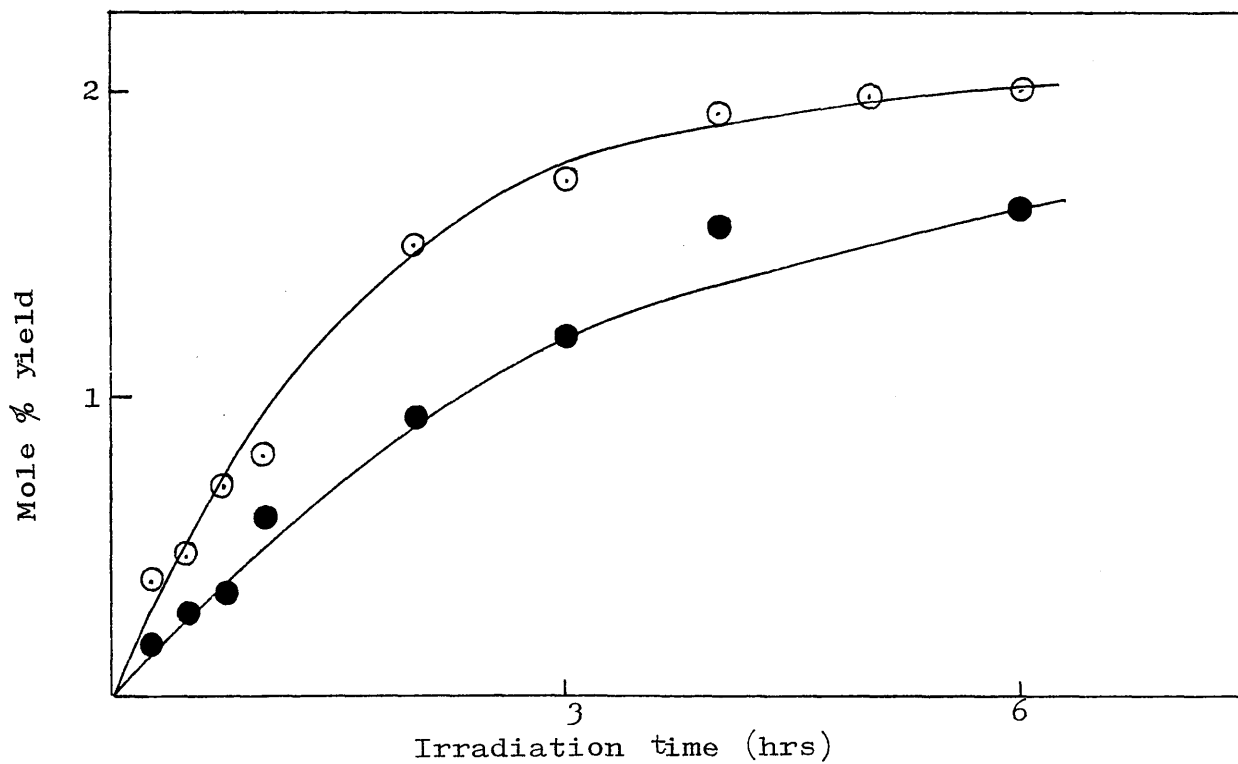


Fig. 6.22

Effect of benzoin on the production of 2-ethylhexyl formate for P(2-EHA) as a function of irradiation time, ○ without benzoin, ● with 1% benzoin.

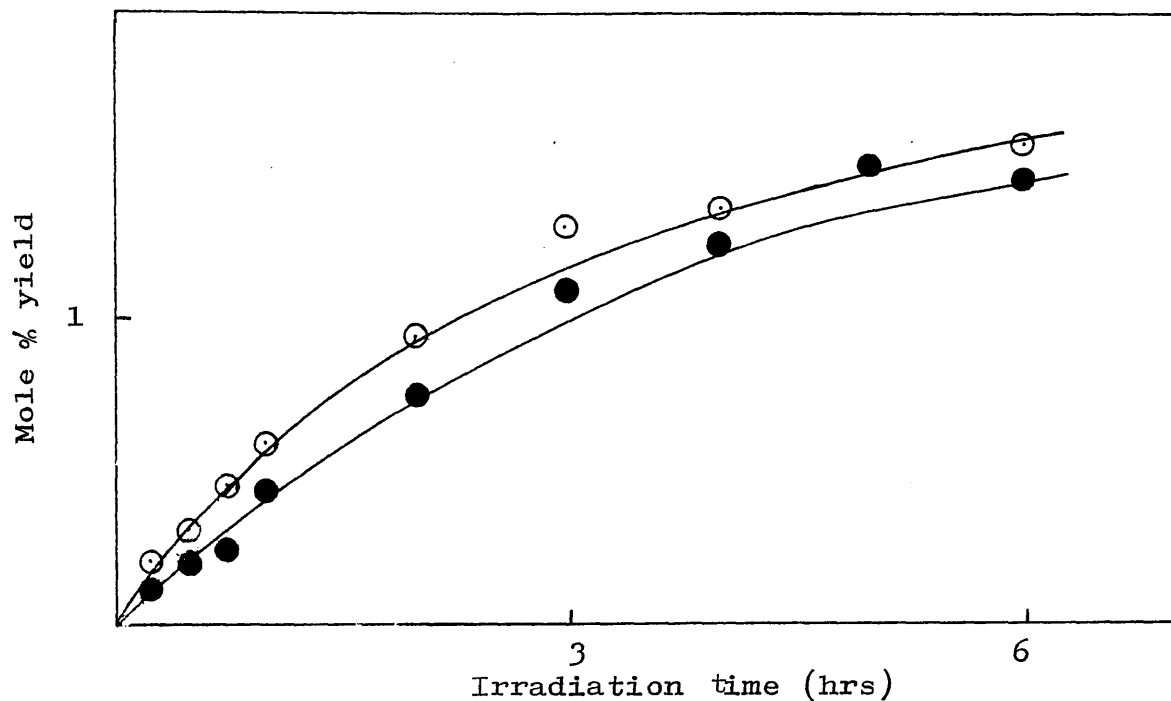


Fig.6.23

Effect of benzoin on the production of 2-ethyl-1-hexanol from P(2-EHA) as a function of irradiation time, ○ without benzoin, ● 1% benzoin

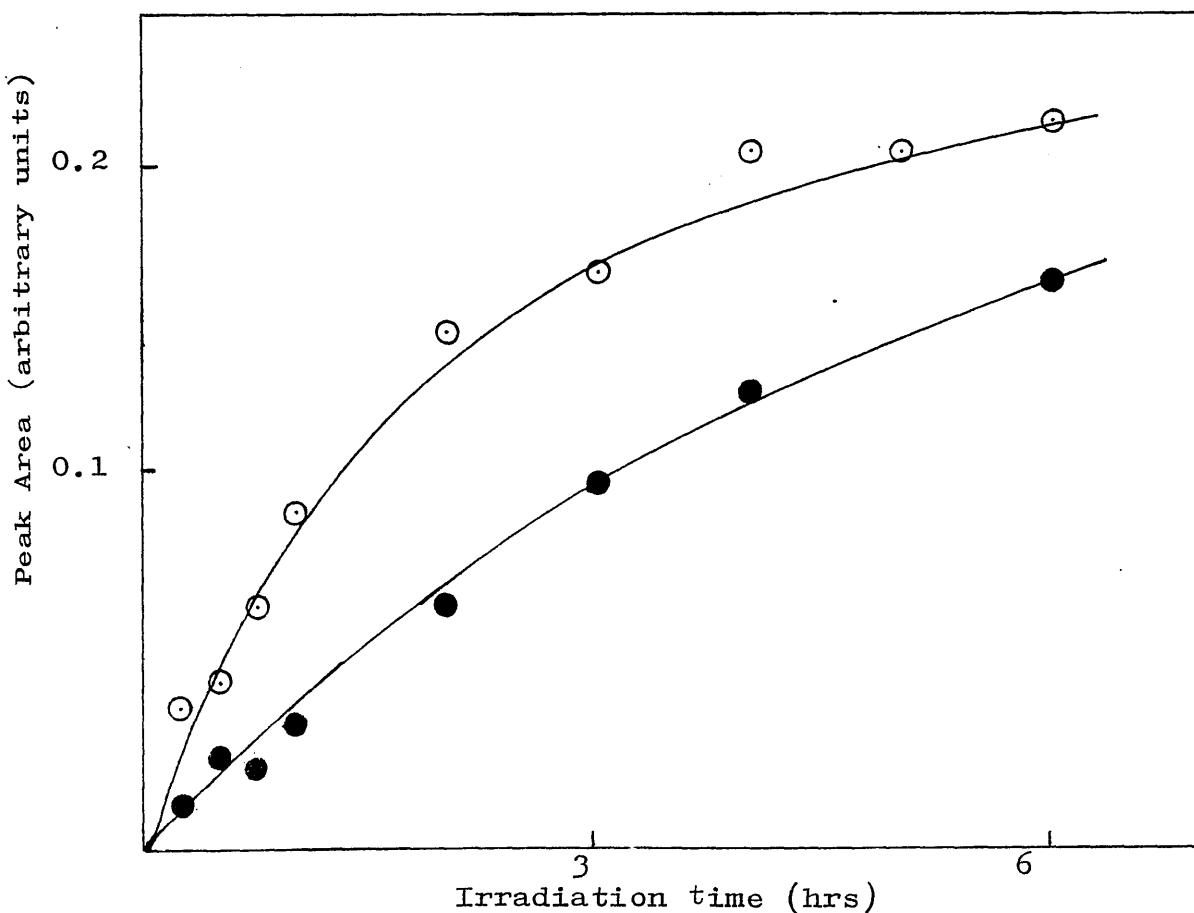


Fig.6.24: Effect of benzoin on the production of short chain fragments from P(2-EHA) as a function of irradiation time, ○ without benzoin, ● 1% benzoin.

Polymer films containing different photosensitizers were irradiated under identical conditions and the molecular mass changes were observed using sorption and counting techniques as described in Chapters Two and Four. It was discussed in Chapter Four in the case of PMA that in the sorption procedure, the count rate is inversely proportional to the molecular mass of the linear polymer and a relationship was assumed to be applicable to the irradiation conditions, so that count rate could be related to the extent of crosslinking.

(a) Effect of benzoin on the molecular mass changes in PMA

Films of PMA (22 μ thick) containing different amounts of benzoin, prepared from methylene chloride as solvent, were irradiated and the extent of crosslinking was investigated. The results obtained are shown in table 6.7, and plotted in fig. 6.25. The data on fig. 6.25 indicate that the presence of 0.25% benzoin in PMA film slightly decreases the extent of crosslinking of PMA as indicated by an increase in count rate.

It is also evident in fig. 6.25 that when 1% or 4% benzoin is incorporated in PMA films, there is an initial increase in the original PMA count rate from 9896 count/min to 11050 count/min. for the former and 12500 count/min for the later, for 30 minutes irradiation time. After half an hour the crosslinking

TABLE 6.7: Effect of irradiation time on the count rate of PMA containing different concentrations of benzoin, 0.25%, 1% and 4% (w/w).

Time (min)	Counts/min for PMA containing benzoin concentration (w/w)		
	0.25%	1%	4%
0	9868	9868	9868
15	8891	11021	11750
30	8100	11065	12096
45	4251	5401	8297
60	1607	2413	4579
90	450	645	956
120	249	325	415
150	290	300	329
180	266	200	255

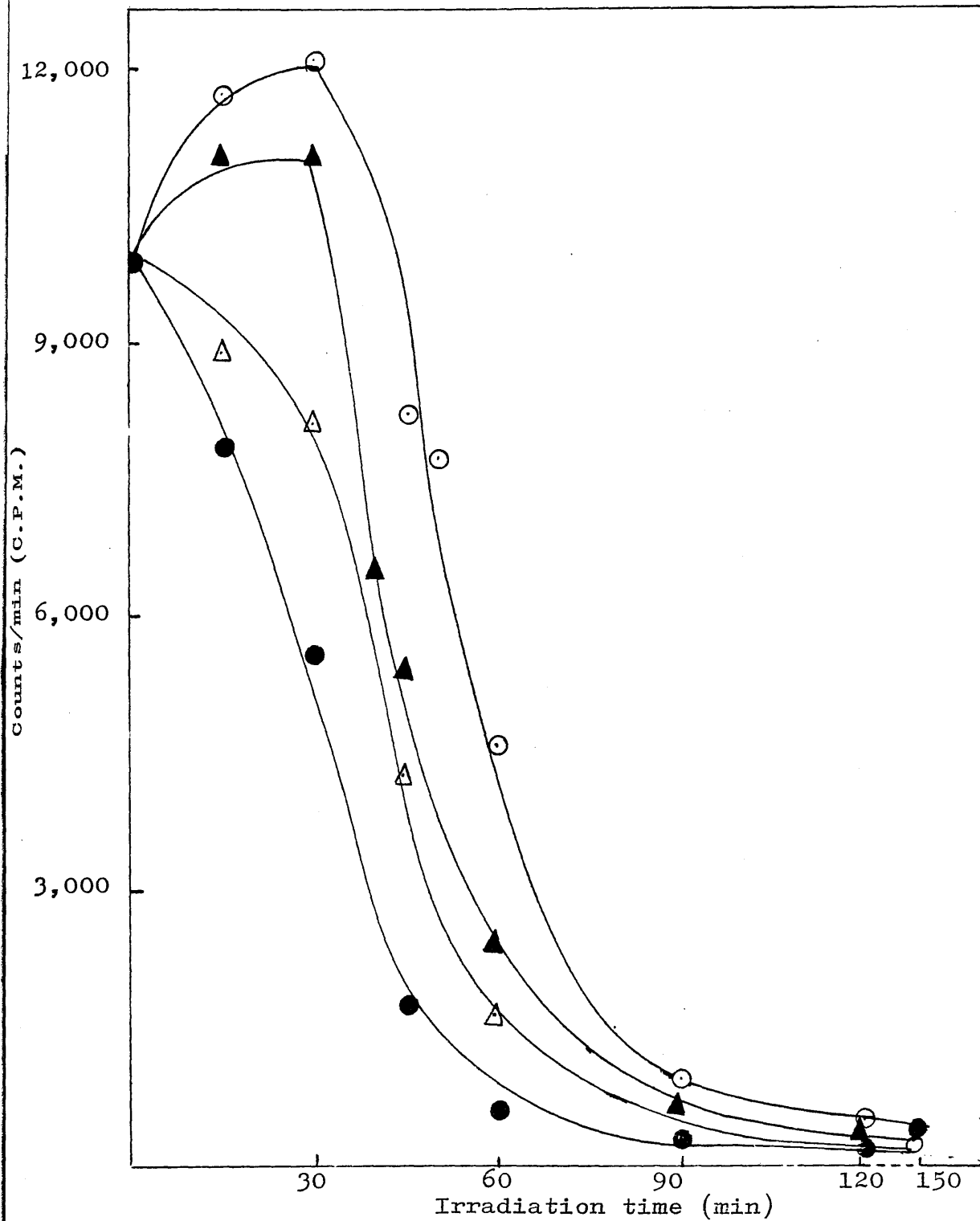


Fig. 6.25: Effect of irradiation time on the count rate of PMA containing different concentrations of benzoin, ● without benzoin, Δ 0.25% benzoin, \blacktriangle 1% benzoin, \odot 4% benzoin (sorption technique)

proceeds with approximately the same rate as for the polymer alone.

(b) Effect of Fluorenone and 2-Chlorothioxanthone on Molecular Mass Changes in PMA

Films of PMA containing 1% of the photosensitizer were prepared and irradiated by standard procedures and count rates were determined following sorption, giving the results shown in fig. 6.26 for fluorenone and fig. 6.27 for 2-chlorothioxanthone. The data are summarised in table 6.8.

In both cases the presence of the photosensitizer leads to an initial increase in count rate for the first 15 minutes and after that the crosslinking starts with a similar rate as without sensitizer. The increase in chain scission in the early stages is in accordance with the increase in short chain fragments formation in the case of the PMA and photosensitizer systems as discussed in the section on product analysis.

(c) Effect of Benzoin on Molecular Mass Changes in P(2-EHA)

P(2-EHA) films(23.5 μ thick) containing 1% benzoin, prepared from methylene chloride were irradiated under identical conditions and the effect on the extent of crosslinking was investigated.

Count rates plotted as a function of irradiation time are shown in fig. 6.28. The data summarised in

TABLE 6.8: Effect of irradiation time on the count rate of PMA containing 1% 2-chlorothioxanthone

Time min	Counts/min	
	1% fluorenone	1% 2-chloro- thioxanthone
0	9868	9868
15	10611	10339
30	10029	9715
45	3989	5750
60	2631	2560
90	664	759
120	270	319
150	301	247
180	179	195

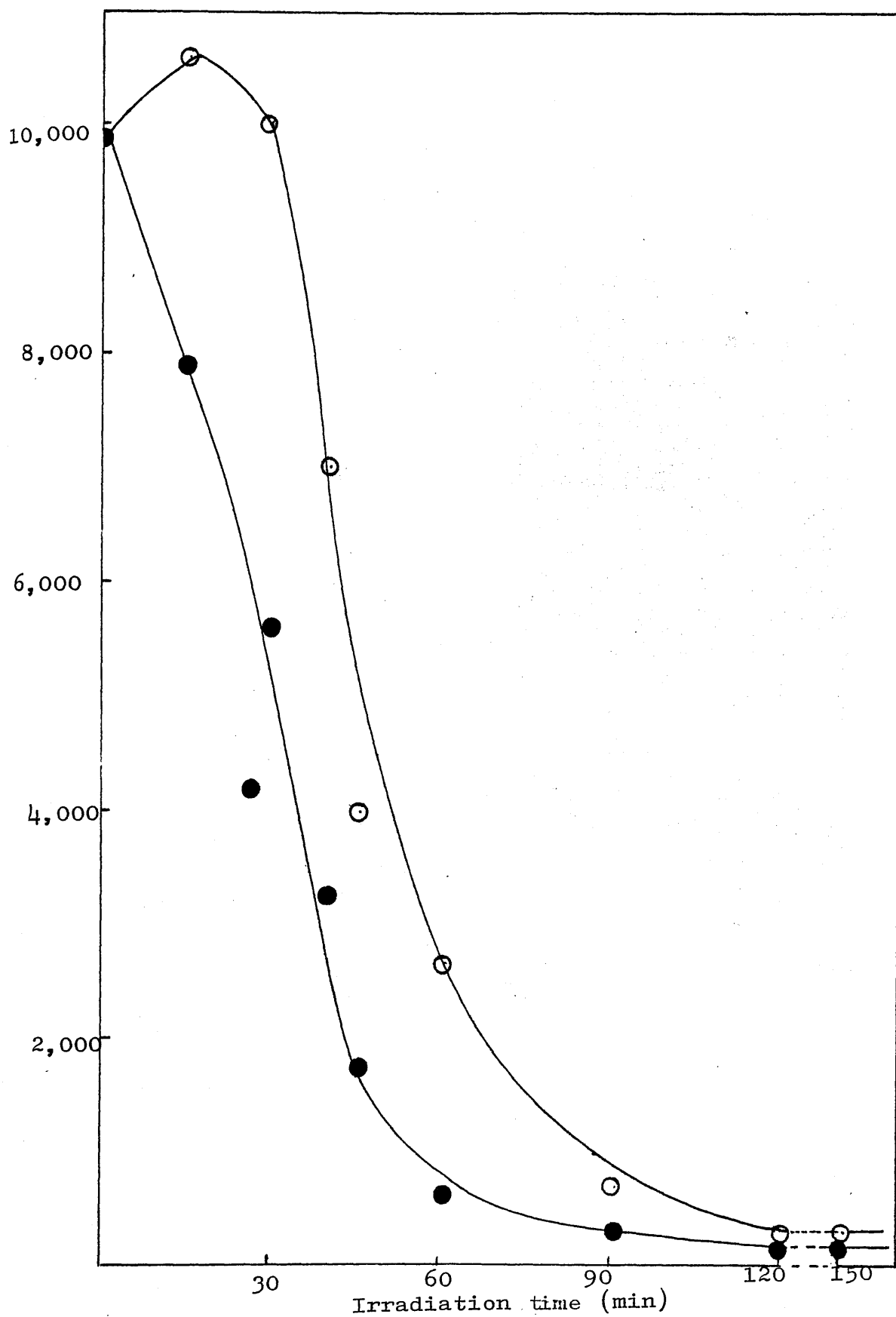


Fig.6.26: Effect of fluorenone on the count rate of PMA as a function of irradiation time, ● without fluorenone, ○ 1% fluorenone (sorption technique)

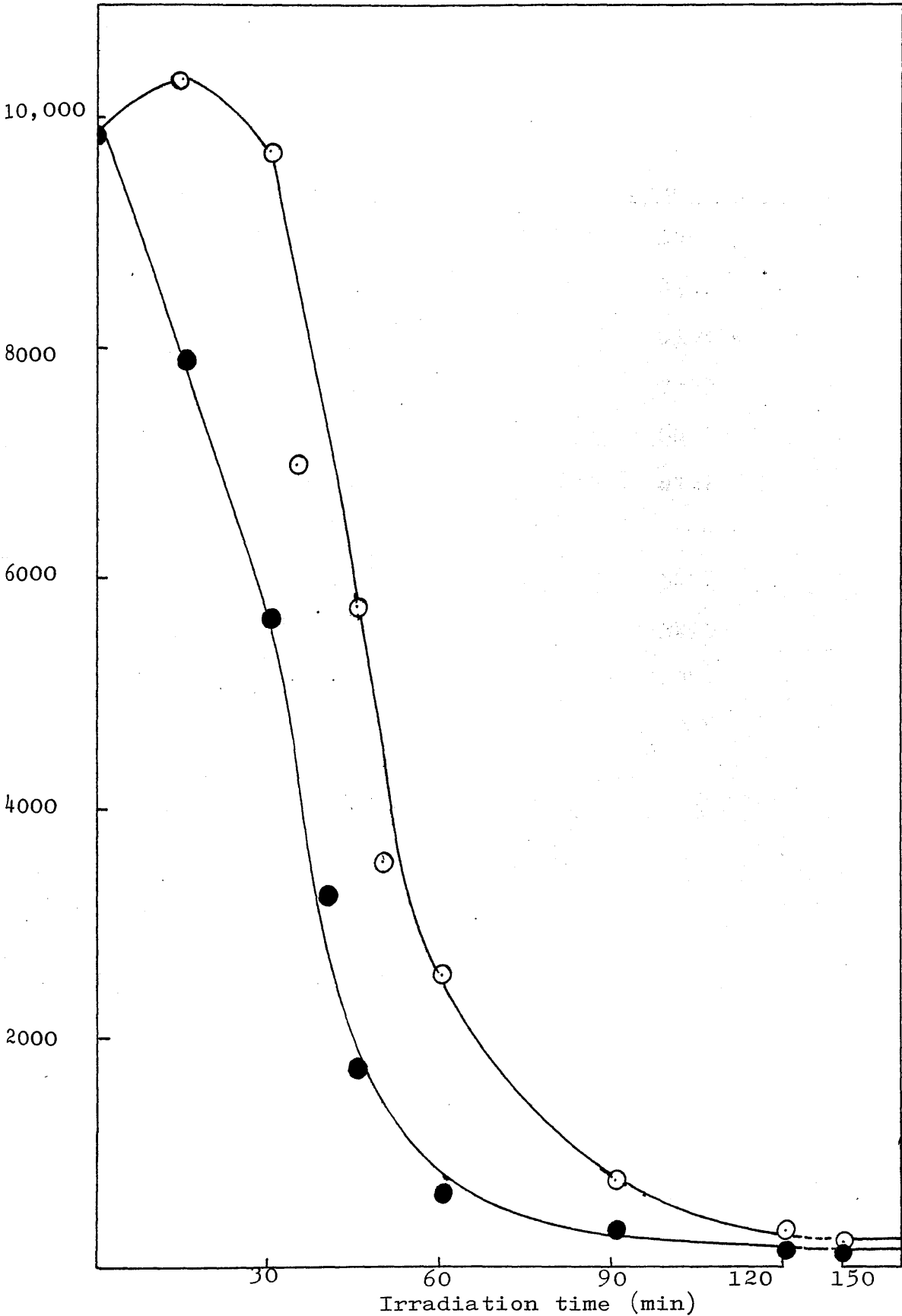


Fig. 6.27: Effect of 2-chlorothioxanthone on the count rate of PMA as a function of irradiation time, ● without 2-chlorothioxanthone, ○ 1% 2-chlorothioxanthone (sorption technique)

TABLE 6.9: Effect of irradiation time on the count rate of P(2-EHA) containing 1% benzoin (w/w).

<u>Time(hours)</u>	<u>Counts/min.</u>
0	8454
0.5	8391
1	8105
2	7239
4	6497
6	4721
8	4608
10	3244
12	3295
15	1997
20	1206

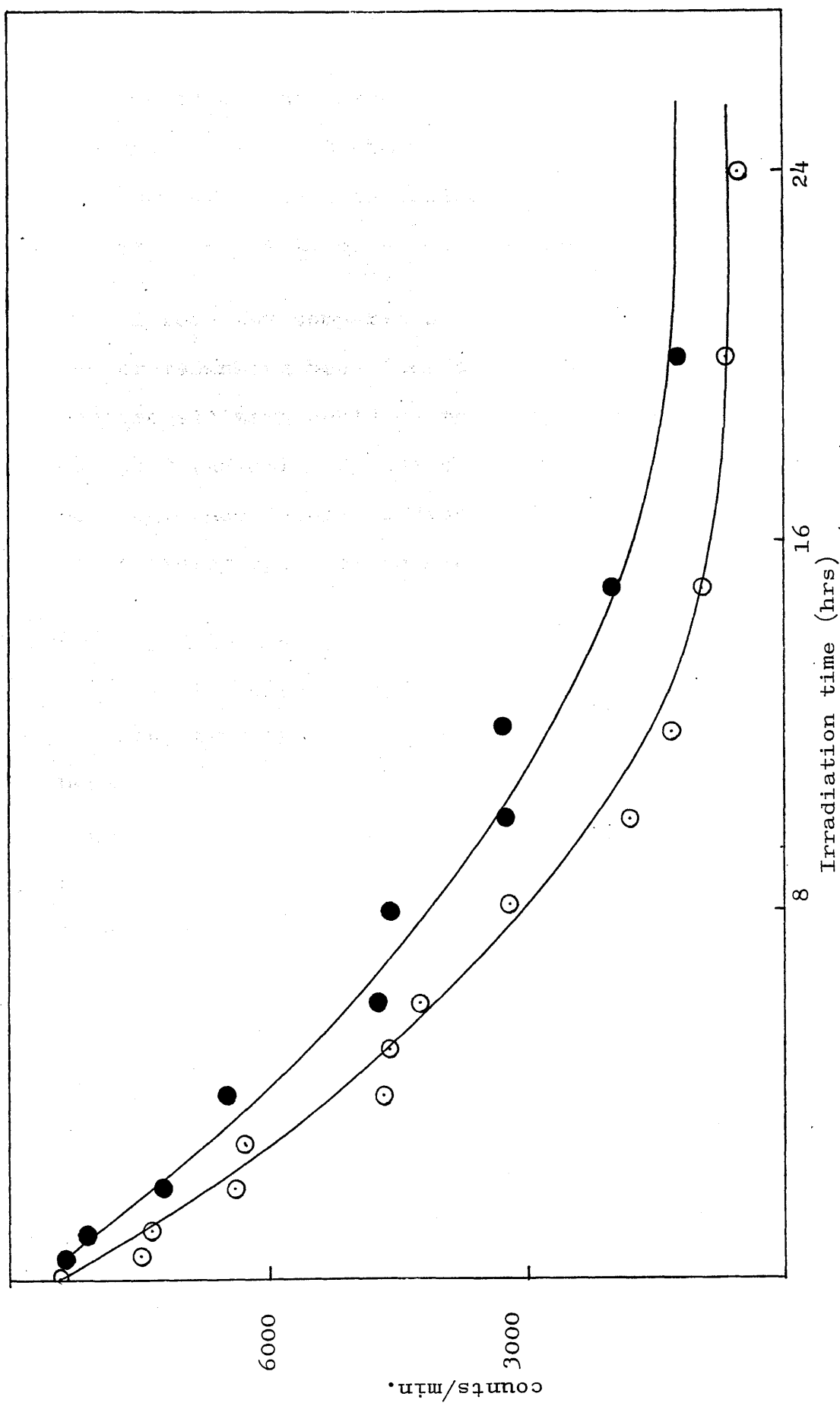


Fig. 6.28: Effect of benzoin on the count rate of P(2-EHA) as a function of irradiation time, ○ without benzoin, ● 1% benzoin.

table 6.9. Fig. 6.28 suggests that although there is a slight increase in count rate, the rate of crosslinking is almost similar to that without sensitizer. This increase in count rate could be related to an increase in chain scission, although the amount of short chain fragments decreases in presence of benzoin as indicated by subambient TVA traces. This will be discussed later.

Before any comparison of the observed changes in the crosslinking behaviour of polymers with different photosensitizers could be made the absorption of incident radiation by the photosensitizers used must be determined. This is discussed in the section on ultra-violet spectral changes.

6.4 Spectral Changes

6.4.1 Infrared Region

Infrared spectra of PMA samples containing 20% benzoin or 33% fluorenone, cast on salt plates, are shown in fig. 6.29 and fig. 6.30, respectively. It was not possible to obtain satisfactory spectra using lower concentrations of photosensitizer. The procedure for casting of the film on the salt plate is described in Chapter Two. After irradiation, the films were washed with methanol in order to remove the photosensitizers and the spectra of washed and dried films were also taken. No changes were observed.

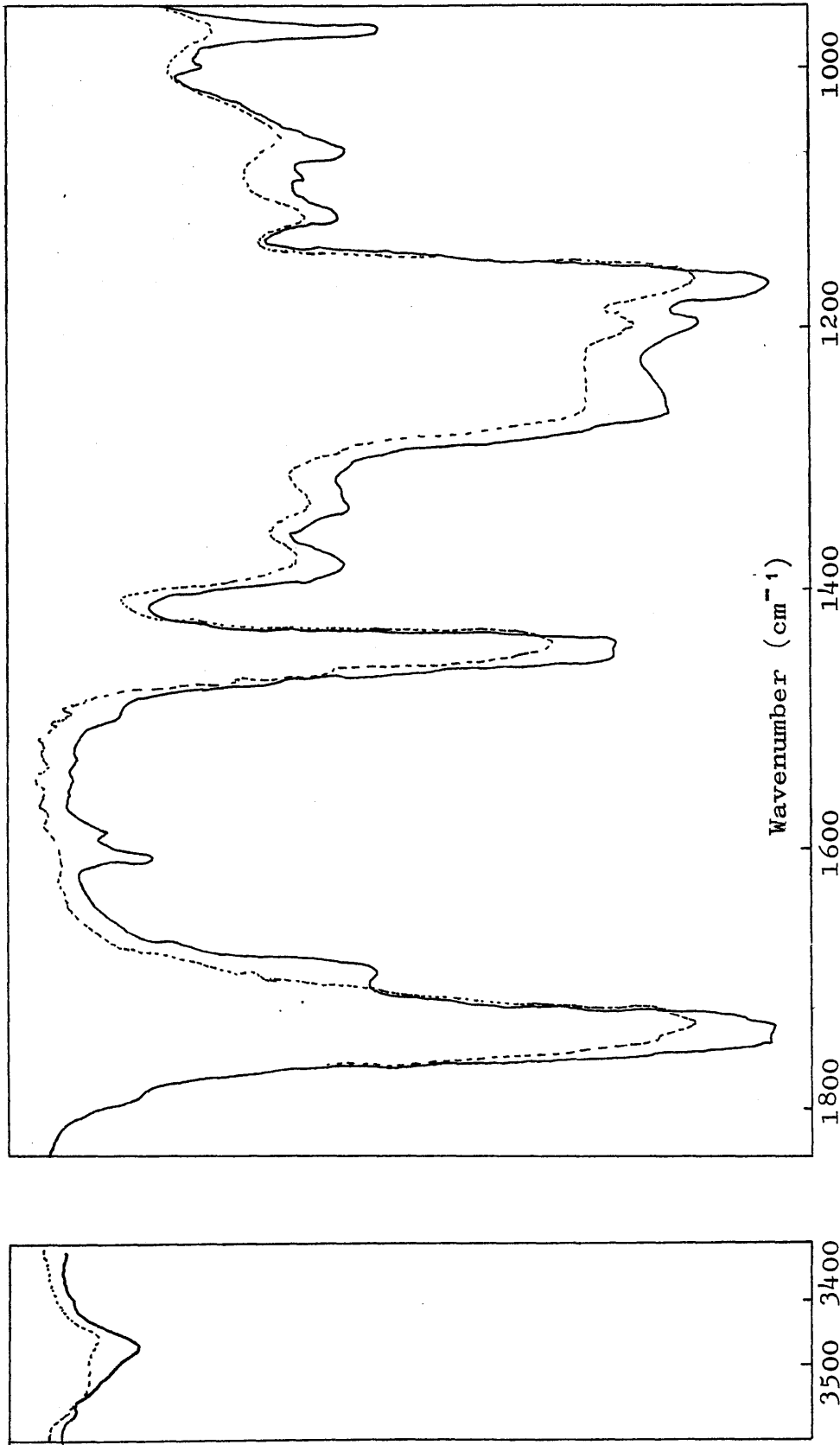


Fig. 6.29: IR absorption spectra of: PMA + 20% benzoin, after 60 min irradiation then washed twice with MeOH

Transmittance

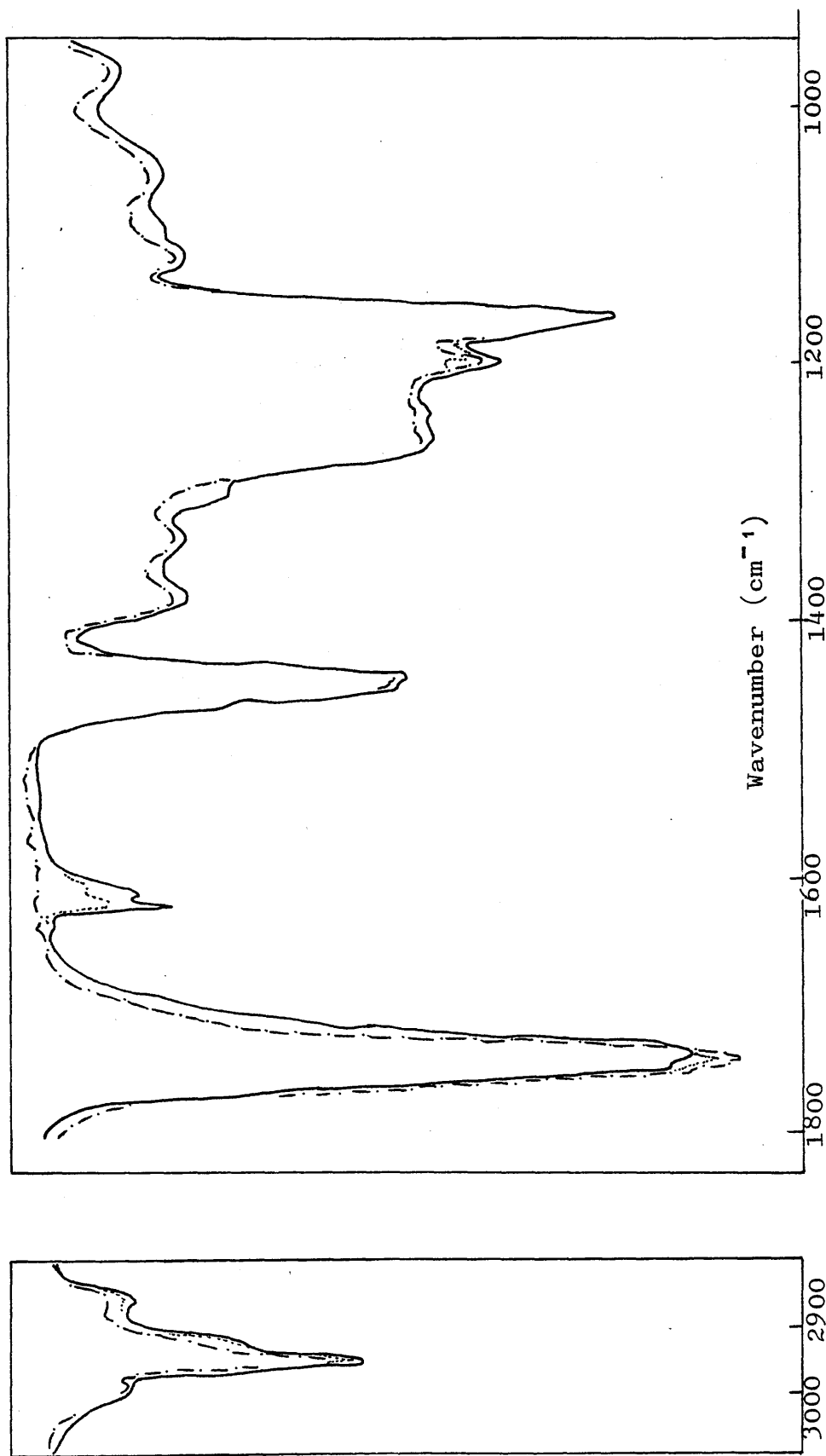


Fig. 6.30: IR absorption spectra of: — PMA + 33.3% fluorenone, after 45 min. irradiation, - - - - - washed with methanol and dried.

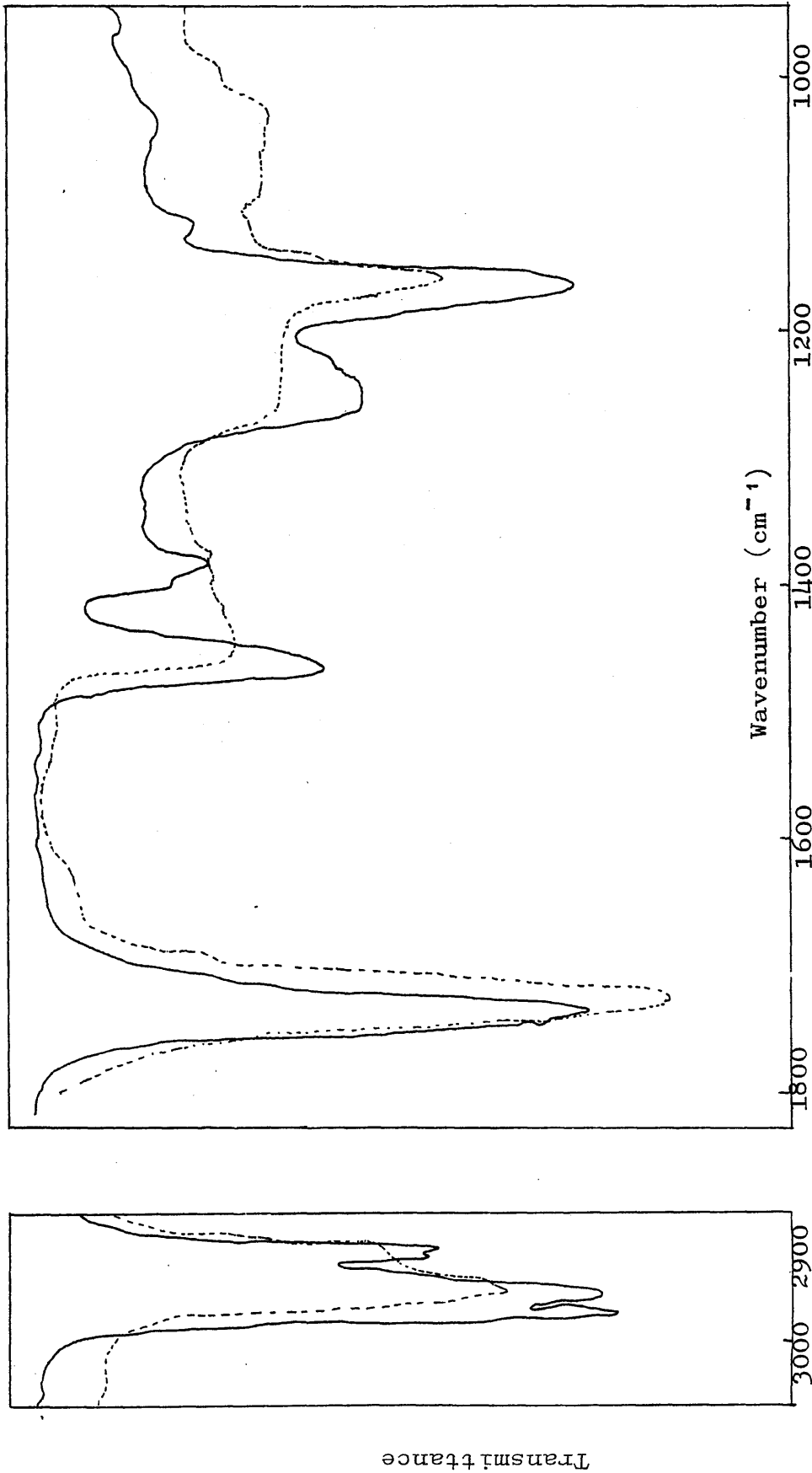


Fig. 6.31: IR absorption spectra of P(2-EHA) film, residual P(2-EHA) in CHCl_3 after 30 min irradiation of 20% benzoin + P(2-EHA) and washing the film with THF in order to remove benzoin.

Fig. 6.31 shows the infrared spectrum of P(2-EHA) containing 20% benzoin before irradiation. After irradiation the benzoin was washed from the film with tetrahydrofuran (THF) and the remaining polymer was dissolved in chloroform. The infrared spectrum did not reveal any new peaks or any changes.

The possibility of the radicals from benzoin becoming attached to the polymer chains cannot be ruled out on this evidence, because it would be difficult to see such a small amount by infrared spectroscopy.

6.4.2 Ultra-Violet Region

The absorbance of polymer films containing photosensitizers, in the ultra-violet region was measured before and after irradiation. Significant changes were observed in all samples. Fig. 6.32 for PMA containing 4% benzoin, after three successive exposure periods, shows that a progressive increase in absorption occurs in the neighbourhood of 230 nm and above 275 nm extending up to 350 nm, while absorption at 250 nm (which is due to benzoin as in the absorption spectrum fig. 6.33 rapidly decreases. It can be reasonably assumed that new chromophores are being formed during degradation. After 30 minutes irradiation time benzoin seems to be completely eliminated (shown by the disappearance of 250 nm band of benzoin in fig. 6.32). Similar changes are observed when fluorenone and

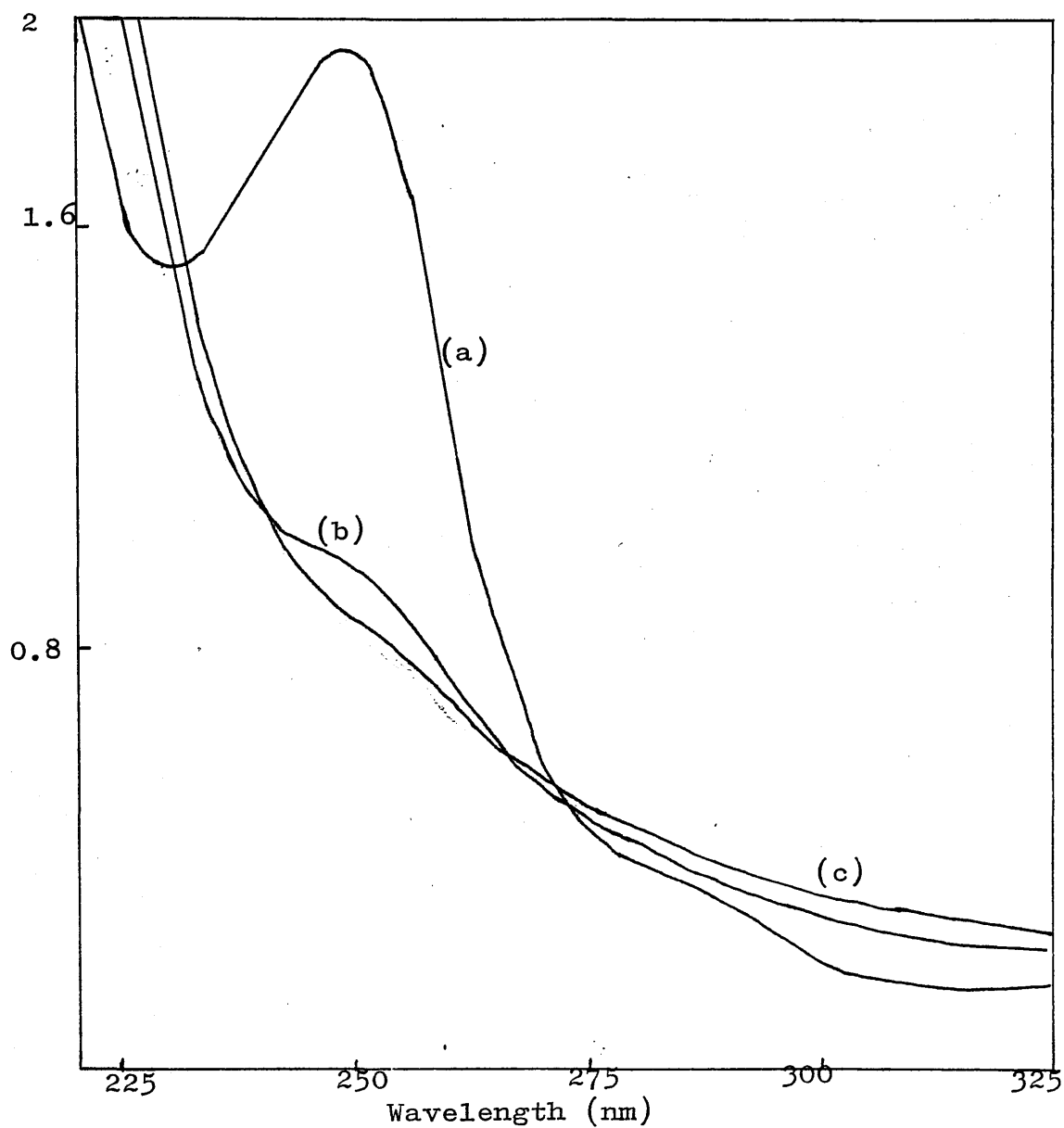


Fig.6.32: Ultra-violet spectra of PMA film containing 4% benzoin.

- (a) before irradiation
- (b) after 15 min. irradiation time
- (c) after 30 min. irradiation time

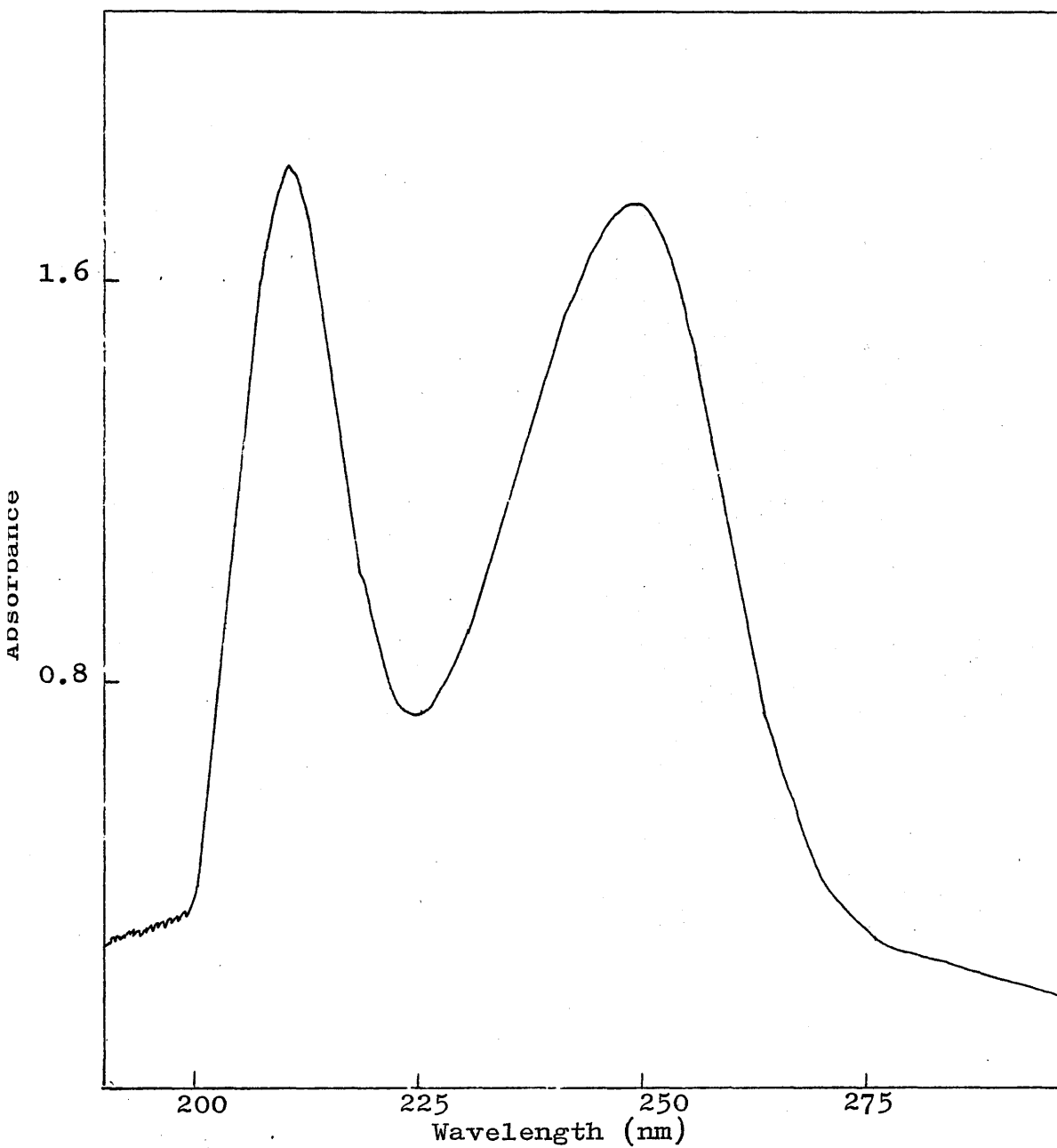


Fig. 6.33

Ultra-violet absorption spectrum of benzoin in chloroform (2.3×10^{-4} M, 10 mm path length).

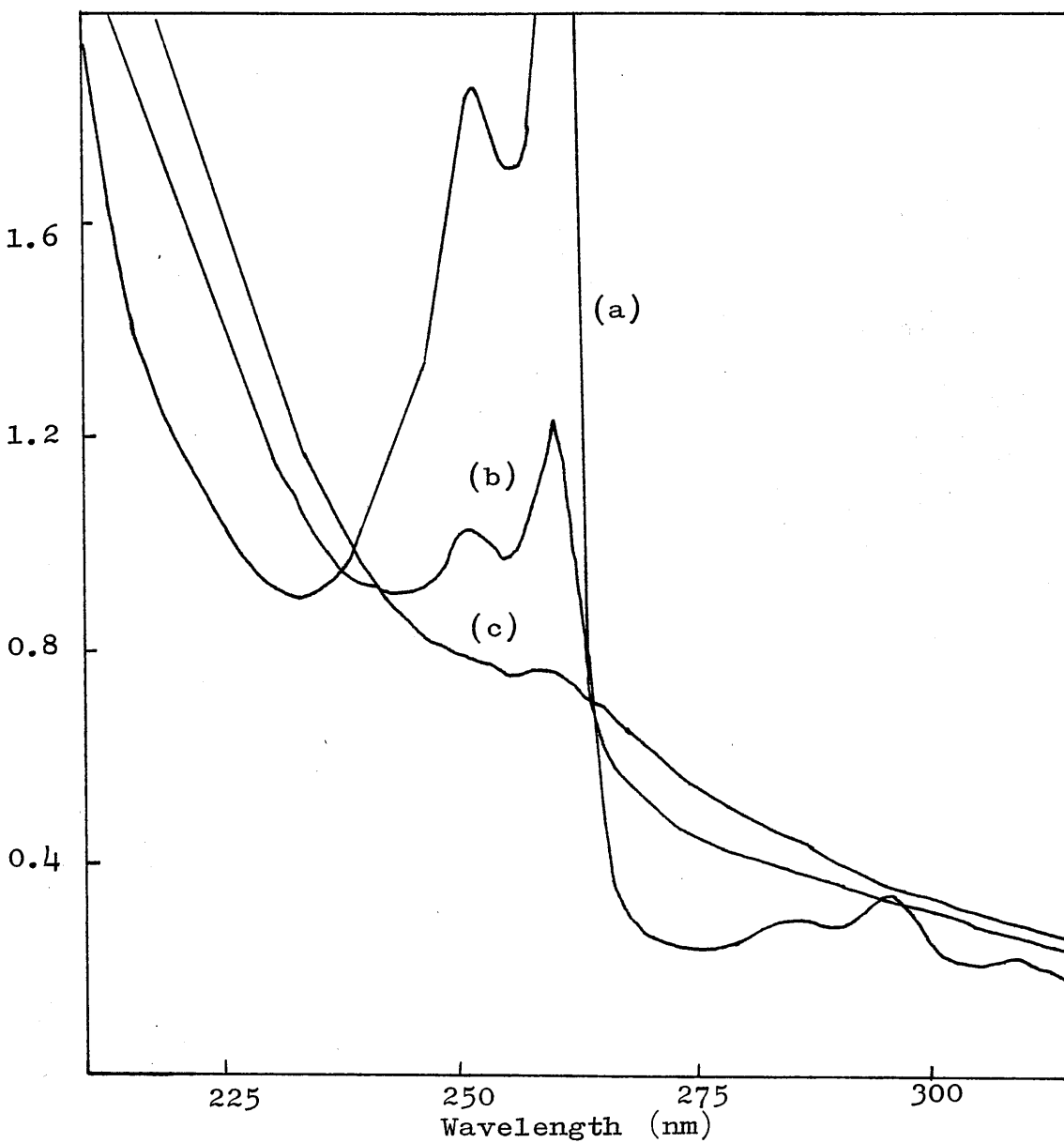


Fig. 6.34: Ultra-violet spectra of PMA film containing 4% fluorenone.

- (a) before irradiation
- (b) after 30 min irradiation time
- (c) after 60 min irradiation time

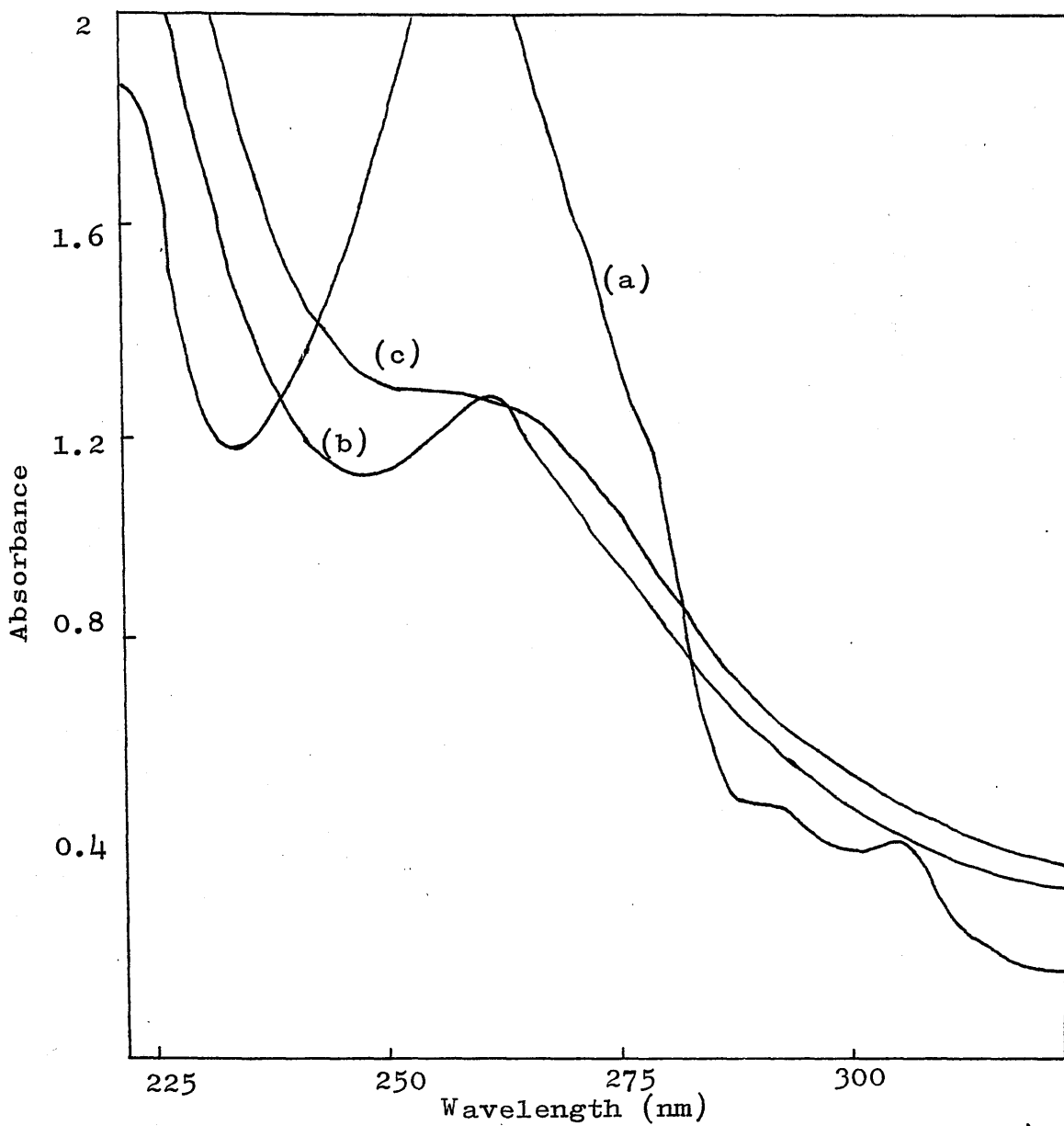


Fig. 6.35: Ultra - violet spectra of PMA film containing 4% 2-chlorothioxanthone

- (a) before irradiation
- (b) after 15 min. irradiation time
- (c) after 60 min. irradiation time

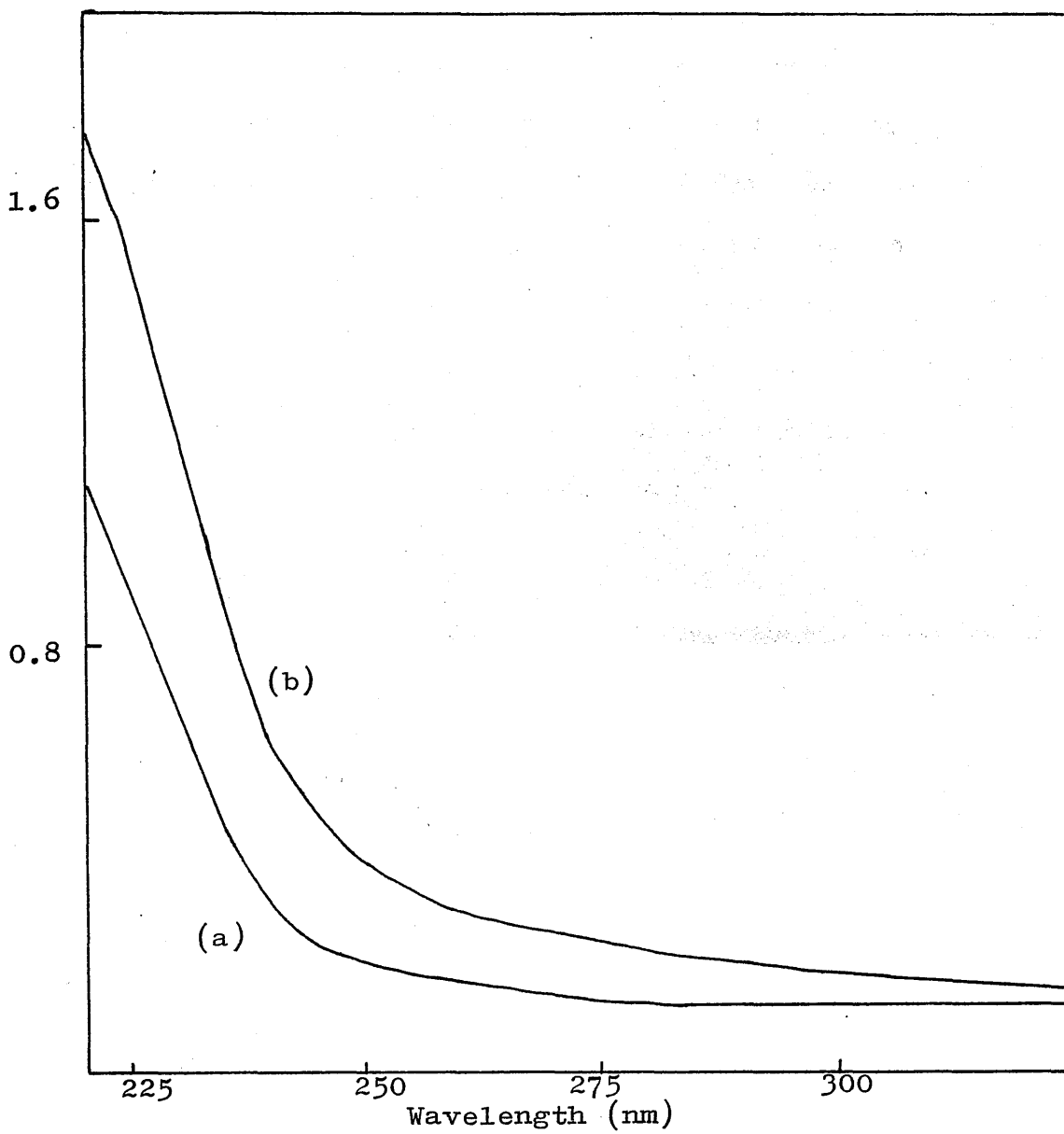


Fig. 6.36: Ultra-violet spectra of PMA

(a) before irradiation

(b) irradiating for 40 min under vacuum

2-chlorothioxanthone were used as photosensitizers for PMA degradation as shown in fig. 6.34 and 6.35 respectively.

An increase in absorbance by PMA during photodegradation has been reported in Chapter Four. However, after irradiation of a PMA film (fig. 6.36) and PMA film containing 4% photosensitizers of the same thickness and under identical conditions, a greater increase in absorbance was observed in the latter case (figs. 6.32, 6.34, 6.35). This increase could possibly be due to the additional number of conjugated double bonds formed during increased chain scission.

6.5 Discussion

From experimental results and observations on the polymer plus photosensitizer system, a general trend began to emerge. The presence of photosensitizer does seem to change the behaviour of the polymer to some extent. This is illustrated by the slight increase in the amount of chain scission reactions, while the crosslinking process seems to be retarded in the early stages of degradation, and by the more rapid development of absorption in the ultra-violet region. The growth in the proportion of short chain fragments, as indicated in the subambient TVA traces, is accompanied by a decline in the production of photolysis products.

Any photolysis mechanism proposed for this photosensitized polymer degradation must satisfy the experimental evidence and account for the trends observed. Any deviation from the well-established photodegradation mechanism of the polymer can be attributed to the effect of photosensitizer.

Photodegradation of polyacrylates is initiated by absorption at the carbonyl group of the ester side chain (around 275 nm) and subsequent scission of the weakest bond. The ester radical gives rise to volatile products. The corresponding polymer radical can undergo chain scission and crosslinking (discussed in Chapters Four and Five).

The aromatic carbonyl compounds used as photosensitizers in vinyl polymerization, have strong absorption in the ultraviolet region between 250-330 nm. Sometimes these sensitizers cause extensive crosslinking in polymers which do not absorb in this region (70,78). It seemed reasonable to expect that incorporation of these sensitizers would lead to either of two possibilities when the polymer was subjected to photolysis. Firstly, the enhanced quantity of absorbed energy could be transferred to the polymer, causing a cleavage of the more labile bonds in the polymer as discussed in Chapter One. If this were the case, the incorporation of photosensitizers into the polymer would be expected to result in an increase in the rate of chain scission and

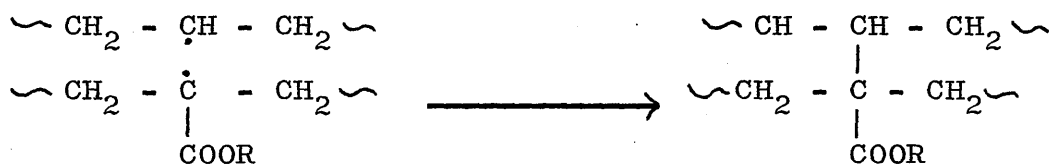
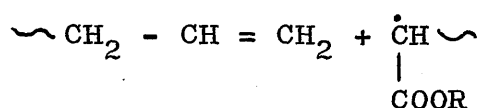
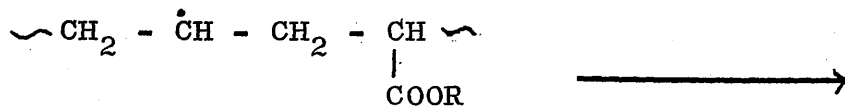
crosslinking of the polymer. On the other hand, if the absorbed energy is not transferred to the polymer but is dissipated as heat or by phosphorescence, fluorescence etc., then the strongly absorbing photosensitizer could act as an optical filter, the overall effect being one of protection of the polymer by preferential absorption on the sensitizer.

Photosensitizers used in this study were benzoin, fluorenone and 2-chlorothioxanthone and their effect on the polyacrylates degradation behaviour is discussed below.

(a) Effect of Benzoin on the Photodegradation Behaviour of PMA

When benzoin is incorporated in PMA films, it causes the absorption to increase from 7% to 23% in the region 275 nm as shown in fig. 6.32. The decrease in the yield of volatiles indicates that this increase in absorption energy due to benzoin is not transferred to the polymer chain, but used up in the fragmentation of benzoin. Photochemical homolysis of benzoin into benzoyl and hydroxybenzyl radicals is well known (73,76). The primary radicals from benzoin do not seem to be participating in the photodegradation mechanism to form benzaldehyde by hydrogen transfer of the hydroxyl proton of the hydroxybenzyl radical to the benzoyl radical [eq.(1)].

Benzoin is almost completely photolysed in 30 minutes under the experimental conditions, as seen by the decrease in absorption in the neighbourhood of 250 nm (fig. 6.32). Molecular mass changes indicate that there is a decrease in the molecular mass for the first 30 minutes indicating a predominance of chain scission. There is a consequent increase in the amount of short chain fragments in the products. It appears as though for the first half an hour, most of the light energy is absorbed by the photosensitizer. The small amount of energy available for the decomposition of the ester side chains is indicated by the decrease in the yield of total volatiles. The radical left on the polymer was suggested as a common precursor for chain scission and crosslinking:



As a consequence of the production of fewer $\dot{\text{C}}\text{OOCH}_3$ radicals, there would be a decrease in tertiary hydrogen abstraction reactions resulting in smaller number of radical sites for crosslinking. Hence the radical left on the polymer chain may only be stabilized by the formation of double bonds, together with the formation of short chain fragments.

The more rapid development of absorption observed in the ultra-violet spectra of polymer films with photosensitizer can be attributed to unsaturation due to conjugation, which supports the fact that chain scission is predominant for the first half an hour.

After 30 minutes irradiation, all the benzoin seems to be photolysed from the film, hence crosslinking of PMA proceeds with a similar rate as in pure polymer.

The effects of fluorenone and 2-chlorothioxanthone on the photodegradation behaviour of PMA were more or less similar to those observed in presence of benzoin, although the yield of volatiles decreases in the order benzoin > fluorenone > 2-chlorothioxanthone. The strong absorption of the last compound in the 275 nm region may be responsible for this decrease in the production of volatiles. The incorporation of these two photosensitizers results in a slight decrease in the molecular mass of PMA in the first 15 minutes of irradiation. The rate of disappearance of these two sensitizers from PMA films under ultra-violet light is slower than in the case of benzoin, as shown in the ultra-violet absorption spectra. Fluorenone contains fused rings which favour rapid internal conversion of electronically excited states to ground states having high vibrational energy (46). A somewhat similar situation could be expected for the other sensitizer.

The amount of short chain fragments seems to be increasing in the presence of these two photosensitizer.

(b) Effect of Benzoin on the Photodegradation
Behaviour of P(2-EHA)

When benzoin was introduced into P(2-EHA) films and these were then irradiated under identical conditions, a decrease in product formation was observed accompanied by a slight increase in the extent of chain scission. Similar changes were observed in case of PMA in presence of photosensitizers with the difference that the amount of short chain fragment was found to decrease in the case of P(2-EHA). This difference might be related to the glass transition temperatures (T_g) of PMA and P(2-EHA), 8°C and -24°C respectively. The latter is in rubbery form. Differences in molecular mobility between these two polymers may influence the 'cage reactions' eg. disproportionation of primary radicals (by formation of benzaldehyde by hydrogen transfer of the hydroxyl proton of the hydroxybenzyl radical to benzoyl radical) would be expected to be more important in PMA system (42). While in a mobile medium in the case of P(2-EHA) these radicals may possibly add to the short chain fragments, making them involatile for distillation. It has not been possible to identify these products in this study as the techniques (IR and UV spectroscopy) used were not sensitive enough to identify the presence of ^{the} small amount of photosensitizer residues attached to the polymer chains.

REFERENCES

1. N. Grassie, "Degradation" in "Polymer Science" edited by A.D. Jenkins, North-Holland Publishing Co. (1972).
2. P.R.E.J. Cowley and H.W. Melville, Proc. Roy. Soc. A210, 461 (1952).
3. R.B. Fox, "Photodegradation of High Polymers" in "Progress in Polymer Science", Vol. 1, edited by A.D. Jenkins, Pergamon, N.Y. (1967).
4. B. Rånby and J.F. Rabek, "Photodegradation, Photoxidation and Photostabilization of Polymers", Wiley Interscience, N.Y. (1975).
5. R.P. Wayne, "Photochemistry", Butterworths, London (1970).
6. J.G. Galvert and N.J. Pitts, Jr., "Photochemistry", Wiley, N.Y. (1966).
7. O. Cicchetti, Advan. Polym. Sci., 7, 70 (1970).
8. K. Tsuji and T. Seiki, J. Polym. Sci., B10, 139 (1972).
9. A.R. Burgess, Chem. Ind. (London), 78, (1952).
10. K. Tsuji, Advan. Polym. Sci., 12, 131 (1973).
11. N. Grassie, "Chemistry of High Polymer Degradation Processes", Interscience, N.Y. (1956).
12. H.H.G. Jellinek, "Degradation of Vinyl Polymers" Academic Press, N.Y. (1955).
13. H.H.G. Jellinek, J. Polym. Sci., 62, 281 (1962).
14. H.H.G. Jellinek, Pure and Applied Chemistry., 4, 419(1962).

15. W.H. Gibb and J.R. MacCallum, Europ. Polym. J., 8, 1223 (1972).
16. N. Grassie and I.C. McNeill, J. Polym. Sci., 33, 171 (1958).
17. N. Grassie and I.C. McNeill, J. Polym. Sci., 39, 211 (1959).
18. F.W. Billmeyer, "Textbook of Polymer Science", John Wiley and Sons, N.Y. (1962).
19. R.B. Fox, L.G. Isaacs, S. Stokes and R.E. Kagarise, J. Polym. Sci., A2, 2085 (1964).
20. L. Ackerman and W.J. McGill, J.S.A. Chem. Inst., 26, 82 (1973).
21. W.J. McGill and L. Ackerman, J. Appl. Polym. Sci., 19, 2773 (1975).
22. A. Charlesby and S.H. Pinner, Proc. Roy. Soc. A 249 367 (1959).
23. W.J. McGill and L. Ackerman, J. Polym. Sci., Polym. Chem. Edition, 12, 1541 (1974).
24. G.G. Cameron and D.R. Kane, Makromol. Chem., 113, 75 (1968).
25. J. Jacob and R. Steele, J. Appl. Polym. Sci., 3, 239, 245 (1960).
26. A.R. Schultz and F.A. Bovey, J. Polym. Sci., 22, 485 (1956).
27. W. Burlant, J. Hinsch and C. Taylor, J. Polym. Sci., A1, 2, 57 (1964).
28. A. Todd, J. Polym. Sci., 42, 223 (1960).

29. A. Rosenberg and H. Heusinger, *Europ. Polym. J.*, 9, 569 (1973).
30. P. Hesse, A. Rosenberg and H. Heusinger, *Europ. Polym. J.*, 9, 581 (1973).
31. R.B. Fox., C.G. Isaacs and S. Stokes, *J. Polym. Sci.*, A1, 1, 1079 (1963).
32. D. Campbell, *Makromol. Rev.*, 4, 91(1970).
33. C.V. Stephenson, J.C. Lacey and W.S. Wilcox, *J. Polym. Sci.*, 55, 451 (1961).
34. P.R.E.J. Cowley and H.W. Melville, *Proc. Roy. Soc.*, A 211, 320 (1952).
35. N. Grassie and J.R. MacCallum, *J. Polym. Sci.*, A2, 983 (1964).
36. L.G. Isaacs and R.B. Fox, *J. Appl. Polym. Sci.*, 9, 3489 (1965).
37. N. Grassie, B.J.D. Torrance and J.B. Colford, *J. Polym. Sci.*, A1, 7, 1425 (1969).
38. N. Grassie and B.J.D. Torrance, *J. Polym. Sci.*, A1, 6, 3303, 3315 (1965).
39. N. Grassie and R.H. Jenkins, *Europ. Polym. J.*, 9, 697 (1973).
40. N. Grassie and J.D. Fortune, *Makromol. Chem*; 168, 1, 13(1973).
41. N. Grassie, A. Scotney and T.I. Davis, *Makromol. Chem.*, 176, 963 (1975).
42. J. Hutchinson and A. Ledwith, *Advan. Polym. Sci.*, 14, 49 (1974).
43. G. Oster in "Encyclopedia of Polymer Science and

- Technology", Vol.9, Editors, H. Mark, N.G. Gaylord and N.M. Bikales, Interscience Publishers, Inc., N.Y. (1968).
44. E.D. Owen and R.J. Bailey, J. Polym. Sci., A1, 10, 113 (1972).
45. Y. Trudelle and J. Neel, C.R. Acad. Sci., Ser. C., 260, 1950 (1965).
46. G. Oster, G.K. Oster and H. Moroson, J. Polym. Sci., 34, 671 (1959).
47. N.K. Funze and A.A. Berlin, Vysokomol. Soedin., 11, 1444 (1969).
48. H.S. Mathieson, E.E. Auer, E.B. Bevilacqua and E.J. Hart, J. Amer. Chem. Soc., 73, 5395 (1951).
49. Polymer Handbook, Ed. J. Brandrup and E.H. Immergut, Interscience Publishers, N.Y. (1975).
50. I.C. McNeill, L. Ackerman, S.N. Gupta, M. Zulfiqar and S. Zulfiqar, J. Polym. Sci. Chem. Edn., 15, 2381 (1977).
51. K. Morimoto and S. Suzuki, J. Appl. Polym. Sci., 19, 2947 (1975).
52. P.J. Flory and J. Rehner, Jr., J. Chem. Phys., 11, 521 (1943).
53. S. Glasstone, "Physical Chemistry", Macmillan and Co., Ltd., London.
54. I.C. McNeill, J. Chem. Soc., 639 (1961).
55. R.A. Faires, B.H. Parks, Radiosotopes Lab. Techniques, Newnes, London (1958).

56. W.A. Noyes, Jr., G.B. Porter and J.E. Jolley,
Chem. Revs., 56, 49 (1956).
57. J.P. Allison, J. Polym.Sci., A1, 4, 1209 (1966).
58. N. Grassie, J.G. Speakman and T.I. Davis, J. Polym.
Sci., A1, 9, 931 (1971).
59. J. Fourie and W.J. McGill, S. Afr. J. Chem., 32(2),
63 (1979).
60. K.J. Bombaugh, C.E. Cook and B.H. Clampitt, Anal.
Chem., 35, 1835 (1963).
61. R.A. Raphael, J. Chem. Soc (London) 1948, 1058 (1948).
62. P. Ausloos, Can. J. Chem., 36, 383 (1958); J. Amer.
Chem. Soc., 80, 1310 (1958).
63. J.C.J. Thynne, Trans. Faraday Soc., 58, 676 (1962).
64. H.W. Anderson and G.K. Rollefson, J. Amer. Chem.
Soc., 63, 816 (1941).
65. G.G. Cameron and D.R. Kane, J. Polym. Sci., B 2,
693 (1964).
66. P. Gray and A. Williams, Chem. Rev., 59, 239 (1959).
67. H.C. McBay and C. Tucker, J. Org. Chem., 19, 869,
1003 (1954).
68. F.E. Rust, F.H. Suebold and W.E. Vaughan, J. Amer.
Chem. Soc., 72, 338 (1950).
69. G. Oster and N.L. Yang, Chem. Rev., 68, 125 (1968).
70. A. Charlesby, C.S. Grace and F.B. Pilkington, Proc.Roy.
Soc. A 268, 205 (1962).
71. G. Oster, J. Polym. Sci., 22, 185 (1956).
72. J.F. Rabek, Photochem. Photobiol., 7, 5 (1968).

73. R.B. Chimmayanandam and H.W. Melville, Trans. Faraday Soc., 50, 73(1954).
74. S.G. Cohen, A. Parola and G.H. Parsons, Chem. Rev., 73, 141 (1973).
75. P.N. Green, J.R.A. Young and M.J. Davis, Paint. Manuf., 48 (3), 32 (1978).
76. G.L. Gloss and D.R. Paulson, J. Amer. Chem. Soc., 92, 7229 (1970).
77. A. Ledwith, P.J. Russell and L.H. Sutcliffe, J. Chem. Soc., Perkin II, 1925 (1972).
78. R.J. Foster, P.H. Whitling, J.M. Mellor and D. Phillips, J. Appl. Polym. Sci., 22, 1129 (1978).